

CERN-PH-EP-2014-158

Submitted to: JHEP

Search for anomalous production of prompt same-sign lepton pairs and pair-produced doubly charged Higgs bosons with $\sqrt{s} = 8$ TeV pp collisions using the ATLAS detector

The ATLAS Collaboration

Abstract

A low-background inclusive search for new physics in events with same-sign dileptons is presented. The search uses proton–proton collisions corresponding to 20.3 fb^{-1} of integrated luminosity taken in 2012 at a centre-of-mass energy of 8 TeV with the ATLAS detector at the LHC. Pairs of isolated leptons with the same electric charge and large transverse momenta of the type $e^\pm e^\pm$, $e^\pm \mu^\pm$, and $\mu^\pm \mu^\pm$ are selected and their invariant mass distribution is examined. No excess of events above the expected level of Standard Model background is found. The results are used to set upper limits on the cross-sections for processes beyond the Standard Model. Limits are placed as a function of the dilepton invariant mass within a fiducial region corresponding to the signal event selection criteria. Exclusion limits are also derived for a specific model of doubly charged Higgs boson production.

Search for anomalous production of prompt same-sign lepton pairs and pair-produced doubly charged Higgs bosons with $\sqrt{s} = 8$ TeV pp collisions using the ATLAS detector

The ATLAS Collaboration

ABSTRACT: A low-background inclusive search for new physics in events with same-sign dileptons is presented. The search uses proton–proton collisions corresponding to 20.3 fb^{-1} of integrated luminosity taken in 2012 at a centre-of-mass energy of 8 TeV with the ATLAS detector at the LHC. Pairs of isolated leptons with the same electric charge and large transverse momenta of the type $e^\pm e^\pm$, $e^\pm \mu^\pm$, and $\mu^\pm \mu^\pm$ are selected and their invariant mass distribution is examined. No excess of events above the expected level of Standard Model background is found. The results are used to set upper limits on the cross-sections for processes beyond the Standard Model. Limits are placed as a function of the dilepton invariant mass within a fiducial region corresponding to the signal event selection criteria. Exclusion limits are also derived for a specific model of doubly charged Higgs boson production.

Contents

1	Introduction	1
2	The ATLAS detector	2
3	Background and signal simulation	3
4	Physics object reconstruction	5
5	Data and event selection	7
6	Background estimation	7
6.1	Background from prompt same-sign lepton pairs	8
6.2	Background from opposite-sign lepton pairs	8
6.3	Background from non-prompt leptons	9
6.3.1	Measurement of f for muons	10
6.3.2	Measurement of f for electrons	10
6.4	Validation of background extraction methods	11
7	Systematic uncertainties	14
8	Results and interpretation	16
8.1	Signal region	16
8.2	Fiducial cross-section limits	18
8.3	Cross-section and mass limits for pair-produced doubly charged Higgs bosons	20
9	Conclusion	26

1 Introduction

In proton–proton (pp) collisions, Standard Model (SM) processes rarely produce two isolated leptons with large transverse momentum (p_T) and the same electric charge (same-sign). However, such signatures frequently occur in models of physics beyond the SM. Supersymmetry [1], universal extra dimensions [2], left-right symmetric models [3–6], see-saw models [7–14], vector-like quarks [15–20], the Zee–Babu neutrino mass model [21–23], and the coloured Zee–Babu model [24] could all give rise to final states with two same-sign leptons.

An inclusive search in events with pairs of isolated same-sign leptons is presented in this paper. The dilepton pairs are selected in the pp collision data corresponding to 20.3 fb^{-1} of integrated luminosity taken in 2012 at a centre-of-mass energy of $\sqrt{s} = 8 \text{ TeV}$

with the ATLAS detector [25] at the Large Hadron Collider (LHC). The same-sign dilepton pairs can be either two electrons ($e^\pm e^\pm$), two muons ($\mu^\pm \mu^\pm$), or one electron and one muon ($e^\pm \mu^\pm$), and must have a transverse momentum (p_T) of at least 25 (20) GeV for the leading (subleading) lepton. After selection of these pairs the resulting invariant mass distributions are examined. The data are found to be consistent with the SM background predictions, and exclusion limits are set on the fiducial cross-section of new physics in the same-sign dilepton final state. Limits are also provided separately for two positively or negatively charged leptons as a function of the dilepton invariant mass. The analysis, using the 8 TeV dataset, provides significantly stronger constraints on new physics models than that presented in earlier ATLAS publications using 4.7 fb^{-1} of pp collision data recorded at $\sqrt{s} = 7 \text{ TeV}$ [26, 27]. Exclusion limits are also presented for the mass of pair-produced doubly charged Higgs bosons ($H^{\pm\pm}$) [27]. The CDF experiment has performed similar inclusive searches [28, 29] without observing any evidence for new physics. This search is more inclusive than other similar searches at ATLAS and CMS in events with same-sign dileptons with additional requirements on missing transverse energy, jets, and charged particles [30–36]. Recently, the ATLAS experiment published limits on doubly charged Higgs production in multi-lepton events [37] based on the $\sqrt{s} = 8 \text{ TeV}$ data.

2 The ATLAS detector

From the inside to the outside, the ATLAS detector comprises an inner tracking detector (ID), electromagnetic and hadronic calorimeters, and a muon spectrometer (MS). The ID is embedded in a 2 T axial magnetic field produced by a superconducting solenoid and provides precision tracking within the pseudorapidity¹ range $|\eta| < 2.5$. It consists of a silicon pixel detector, a semiconductor tracker (SCT) using silicon microstrip detectors, and, in the region $|\eta| < 2$, a transition-radiation straw tube tracker (TRT).

The calorimeter system consists of electromagnetic and hadronic components and covers the pseudorapidity range $|\eta| < 4.9$. The electromagnetic calorimeter is a lead/liquid-argon sampling calorimeter. It covers $|\eta| < 3.2$ with a fine lateral and longitudinal segmentation up to $|\eta| = 2.5$, and is subdivided into a barrel ($|\eta| < 1.4$) and two endcaps ($1.5 < |\eta| < 3.2$). The steel/scintillator-tile hadronic calorimeter provides coverage up to $|\eta| = 1.7$, while the hadronic calorimeter in the endcap ($1.5 < |\eta| < 3.2$) and in the forward region ($3.1 < |\eta| < 4.9$) uses liquid argon technology.

The muon spectrometer uses toroidal magnetic fields generated by three large superconducting magnet systems with eight coils each. The detector is made up of separate trigger and high-precision tracking chambers. The precision chambers cover the region $|\eta| < 2.7$ with three layers of monitored drift tube chambers, complemented by cathode

¹ATLAS uses a right-handed coordinate system with its origin at the nominal interaction point in the centre of the detector and the z -axis along the beam line. The x -axis points from the interaction point to the centre of the LHC ring, and the y -axis points upwards. Cylindrical coordinates (r, ϕ) are used in the transverse plane, ϕ being the azimuthal angle around the beam line. The pseudorapidity is defined in terms of the polar angle θ as $\eta = -\ln \tan(\theta/2)$.

strip chambers in the forward region. The trigger system covers the range $|\eta| < 2.4$ using resistive plate chambers in the barrel and thin-gap chambers in the endcap regions.

A three-level trigger system is used to select events. The first level is implemented in custom electronics, and is followed by two software-based trigger levels. This system selects from the collision rate of around 20 MHz about 400 Hz of events to be recorded for physics analyses.

More details about the detector and the trigger system can be found elsewhere [25].

3 Background and signal simulation

Monte Carlo (MC) simulations are used to estimate the background contributions and also to model hypothetical signal events. The MC background samples used are shown in table 1. For each process the table provides information on the generator, the chosen parton distribution function (PDF) and the order of cross-section calculations used for the normalisation.

The irreducible background in the analysis comes mainly from the purely leptonic decays of WZ and ZZ production processes. A small contribution arises from $W^\pm W^\pm$ production [38], which proceeds via the t-channel exchange of a gluon and results in at least two jets in the final state, in addition to the two W bosons. The small contributions from multiple parton interactions (MPI) for WW , WZ and ZZ are also considered. In these processes two hard scatterings occur in the same pp collision, each producing either a W or Z boson. Other smaller sources of background are the processes in which a W or Z boson is produced in association with a top-quark pair ($t\bar{t}W$ and $t\bar{t}Z$). One of the reducible backgrounds arises from the opposite-sign lepton pairs where the charge for one of the leptons is wrongly reconstructed. In order to estimate the contribution, Drell–Yan (Z/γ^* +jets), $t\bar{t}$, $W^\pm W^\mp$ and Wt simulations are used, and misidentification probabilities derived from data are applied to the MC samples (see section 6.2). The process $W\gamma$, where the photon converts to an e^+e^- pair, is also simulated. The production of $Z\gamma$ is included in the Z/γ^* process.

The MC program SHERPA-1.4.1 [39] is used to model the WZ , ZZ , $W^\pm W^\mp$ and $W\gamma$ processes. These samples use the default SHERPA parameterisation for the renormalisation and factorisation scales. For processes with a Z boson, the contribution from $\gamma^* \rightarrow \ell^+\ell^-$ due to internal or external bremsstrahlung of final-state quarks or leptons is simulated for $m(\ell^+\ell^-) > 0.1$ GeV. The $t\bar{t}W$, $t\bar{t}Z$ and $W^\pm W^\pm$ events are generated using MADGRAPH-5.1.4.8 [40, 41], and for the fragmentation and hadronisation, PYTHIA-6.426 [42] is used for $t\bar{t}W$ and $t\bar{t}Z$ and PYTHIA-8.165 [43] for $W^\pm W^\pm$. The MPI samples are generated by PYTHIA-8.165. The Drell–Yan process is modelled using ALPGEN-2.14 [44], and the top-quark pair production and single top-quark production in association with a W boson are generated with MC@NLO-4.06 [45, 46]. These are interfaced to HERWIG-6.520 [47, 48] for the fragmentation and hadronisation process, and JIMMY-4.31 [49] is used for the underlying-event description.

The CT10 [50] PDF set is used for WZ , ZZ , $W^\pm W^\mp$, $W\gamma$, $t\bar{t}$, and Wt processes and CTEQ6L1 for others. The cross-sections for MPI diboson and $W^\pm W^\pm$ produc-

Process	Generator + fragmentation/ hadronisation	PDF set	Normalisation based on
WZ	SHERPA-1.4.1 [39]	CT10 [50]	NLO QCD with MCFM-6.2[51]
ZZ	SHERPA-1.4.1	CT10	NLO QCD with MCFM-6.2
$W^\pm W^\pm$	MADGRAPH-5.1.4.8 [40] PYTHIA-8.165 [43]	CTEQ6L1 [52]	LO QCD
$t\bar{t}V$, $V = W, Z$	MADGRAPH-5.1.4.8 + PYTHIA-6.426	CTEQ6L1	NLO QCD [53, 54]
MPI VV $V = W, Z$	PYTHIA-8.165[43]	CTEQ6L1	LO QCD
$Z/\gamma^* + \text{jets}$	ALPGEN-2.14 [44] + HERWIG-6.520 [47, 48]	CTEQ6L1	DYNNLO-1.1 [55] with MSTW2008 NNLO [56]
$t\bar{t}$	MC@NLO-4.06 [45, 46] + HERWIG-6.520	CT10	NNLO+NNLL QCD [57–62]
Wt	MC@NLO-4.06 + HERWIG-6.520	CT10	NNLO+NNLL QCD [63, 64]
$W^\pm W^\mp$	SHERPA-1.4.1	CT10	NLO QCD with MCFM-6.2
$W\gamma$	SHERPA-1.4.1	CT10	NLO QCD with MCFM-6.3

Table 1: Generated samples used for background estimates. The generator, PDF set and order of cross-section calculations used for the normalisation are shown for each sample. The upper part of the table shows the MC samples used for the SM background coming from leptons with the same charge (MPI stands for multiple parton interactions), the lower part gives the background sources arising in the $e^\pm e^\pm$ or $e^\pm \mu^\pm$ channel due to electron charge misidentification.

tion are calculated at leading order (LO) in QCD. For diboson samples (WZ , ZZ and WW), the cross-sections are normalised to next-to-leading order (NLO) in QCD using MCFM-6.2 [51]. The QCD next-to-next-to-leading-order (NNLO) and next-to-next-to-leading-logarithm (NNLL) calculations are utilised for top-quark processes [53, 54, 57–64]. The Drell–Yan cross-section is also calculated at NNLO in QCD by DYNNLO-1.1 with MSTW2008 NNLO [55, 56].

Some typical same-sign dilepton signals of physics beyond the SM are simulated to evaluate the efficiency and acceptance of the event selection, which are needed to set the cross-section limits (see section 8.2). Pair production of doubly charged Higgs bosons via a virtual Z/γ^* exchange is generated [65]. Right-handed W bosons (W_R) decaying to a

charged lepton and a right-handed neutrino (N_R) are also used [66]. The production of a fourth-generation heavy $b'\bar{b}'$ pair with the b' quarks decaying into a W boson and either a top quark or an up-type quark is considered [67]. The above processes are generated using PYTHIA-8.165. MADGRAPH is used to simulate the coloured Zee–Babu process, in which a diquark (S_{DQ}) with charge $\pm 2/3$ or $\pm 4/3$ decays into two same-sign leptoquarks (S_{LQ}): $pp \rightarrow S_{DQ} \rightarrow S_{LQ}S_{LQ} \rightarrow \ell\ell qq$ [24]. For this process, PYTHIA-8.165 is utilised for the fragmentation and hadronisation. For all signal samples mentioned above, the MSTW2008LO PDF set is used and cross-sections are calculated at LO in QCD.

The background and some of the signal samples are processed using the GEANT4-based [68] ATLAS detector simulation package [69]. Other signal samples are produced with a fast simulation [70] using a parameterisation of the calorimeter response. Additional inelastic pp interactions (referred to as ‘pile-up’), generated with PYTHIA-6.426, are overlaid on the hard-scatter events to emulate the multiple pp interactions in the current and nearby bunch crossings. The distribution of the number of interactions per bunch crossing in the MC simulation is reweighted to that observed in the data. The simulated response is also corrected for differences in efficiencies, momentum scales, and momentum resolutions observed between data and simulation.

4 Physics object reconstruction

The analysis makes use of muons and electrons and the basic reconstruction and identification is explained in the following. In addition, the jet reconstruction is detailed as jets misidentified as electrons are a main source of background and as electrons and muons in the vicinity of a jet are not considered in this analysis.

Jets are reconstructed in $|\eta| < 4.9$ from topological clusters [71] formed from the energy deposits in the calorimeter, using the anti- k_t algorithm [72] with a radius parameter of 0.4. Jets are calibrated [73] using an energy- and η -dependent simulation-based calibration scheme, with in-situ corrections based on data. The impact of multiple overlapping pp interactions is accounted for using a technique that provides an event-by-event and jet-by-jet pile-up correction [74]. To reduce the effect from pile-up, for jets with $p_T < 50$ GeV, $|\eta| < 2.4$, the p_T of all tracks inside the jet is summed and the fraction belonging to tracks from the primary vertex is required to be larger than 0.5. The primary vertex is defined as the interaction vertex which has the highest squared- p_T sum of associated tracks with $p_T > 0.4$ GeV found in the event. At least three charged-particle tracks must be associated with this vertex.

An electron is formed from a cluster of cells in the electromagnetic calorimeter associated with a track in the ID. The electron p_T is obtained from the calorimeter energy measurement and the direction of the associated track. The electron must be within the range $|\eta| < 2.47$ and not in the transition region between the barrel and endcap calorimeters ($1.37 < |\eta| < 1.52$). In addition, a ‘‘tight’’ [75] set of identification criteria need to be satisfied. One major source of background surviving these selections comes from jets misidentified as electrons. To suppress this background, in particular at low p_T , the electrons are required to be isolated. The sum of the transverse energies in the electro-

magnetic and hadronic calorimeter cells around the electron direction in a cone of size $\Delta R = \sqrt{(\Delta\eta)^2 + (\Delta\phi)^2} = 0.2$ is required to be less than $3 \text{ GeV} + (p_{\text{T}}^e - 20 \text{ GeV}) \times 0.037$, where p_{T}^e is the electron transverse momentum. The core of the electron energy depositions in the electromagnetic calorimeter is excluded and, before the cut, the sum is corrected for lateral shower leakage and pile-up from additional pp collisions. A further isolation cut is applied using the ID information. The sum of the p_{T} of all tracks with $p_{\text{T}} > 0.4 \text{ GeV}$ in a cone of size $\Delta R = 0.3$ surrounding the electron track (the latter being excluded from the sum) is required to be less than 10% of the electron p_{T} . The isolation selections were optimised using electron pairs with a mass compatible with the Z boson in the data, such that the application of both isolation criteria to electrons yields an efficiency that is pile-up independent and more than 99% for electrons with $p_{\text{T}} > 40 \text{ GeV}$. The efficiency slowly decreases with diminishing p_{T} to around 92% at $p_{\text{T}} = 20 \text{ GeV}$. However, these isolation selections help to suppress the background from jets misidentified as electrons, which becomes more prominent as p_{T} decreases. To further suppress leptons from hadron decays, jets in a cone of size $\Delta R = 0.4$ around the electron direction are examined. Since the jet reconstruction algorithm also reconstructs electrons as jets, any jet within $\Delta R = 0.2$ of an electron is not considered to avoid double counting. The electron is rejected if there is a remaining jet in the cone with $p_{\text{T}} > 25 \text{ GeV} + p_{\text{T}}^e \times 0.05$, where p_{T}^e is the electron p_{T} . The non-constant cut value on the jet p_{T} is placed to maintain a high efficiency for very high- p_{T} electrons. The background arising in particular from electrons from heavy-flavour decays is reduced by requiring that the electron track is associated with the primary vertex. The transverse impact parameter significance is required to be $|d_0|/\sigma(d_0) < 3$, where d_0 is the transverse impact parameter and $\sigma(d_0)$ is the uncertainty on the measured d_0 . The longitudinal impact parameter z_0 must fulfil $|z_0 \times \sin\theta| < 1 \text{ mm}$.

Muons are reconstructed independently in both the ID and MS. Subsequently, these two tracks are combined based on a statistical combination of the two independent measurements using the parameters of the reconstructed tracks and their covariance matrices. The combined track is required to be within $|\eta| < 2.5$ and the track in the ID must have at least four hits in the SCT, at least one hit in the pixel detector and one hit in the first pixel layer if an active pixel sensor is traversed. The charge measured in the ID and the MS must match as this reduces the small effect of charge misidentification to a negligible level. To reduce background from heavy-flavour hadron decays, each muon is required to be isolated in the calorimeter and the ID. The calorimeter-based isolation is chosen to be $\sum E_{\text{T}} < 3.5 \text{ GeV} + (p_{\text{T}}^\mu - 20 \text{ GeV}) \times 0.06$ where the $\sum E_{\text{T}}$ is calculated in a cone of size $\Delta R = 0.3$ and p_{T}^μ is the muon transverse momentum. The ID-based isolation is defined as $(\sum p_{\text{T}})/p_{\text{T}}^\mu < 0.07$, where the sum runs over ID tracks with $p_{\text{T}} > 1 \text{ GeV}$ in a cone of size $\Delta R = 0.3$ surrounding the muon track, the latter being excluded from the sum. These isolation cuts result in an efficiency for muons from Z decays in data which is above 99% for muons with $p_{\text{T}}^\mu > 40 \text{ GeV}$ and decreases to around 90% at $p_{\text{T}}^\mu = 20 \text{ GeV}$. As for electrons, with diminishing p_{T} the background becomes more pronounced and these cuts result in a better background rejection. To further reduce the background a nearby jet veto is applied, similar to that for electrons: a muon is rejected if a jet with $p_{\text{T}} > 25 \text{ GeV} + p_{\text{T}}^\mu \times 0.05$ is found in a cone of size $\Delta R = 0.4$ around the muon. The muons are required to be associated

with the primary vertex by requiring $|d_0|/\sigma(d_0) < 3$, $|d_0| < 0.2$ mm and $|z_0 \times \sin \theta| < 1$ mm.

5 Data and event selection

This analysis uses the 2012 pp collision data collected at a centre-of-mass energy of 8 TeV with, on average, 21 interactions per bunch crossing. After requiring that all detector components are operational, the dataset amounts to 20.3 fb^{-1} of integrated luminosity.

The events are selected by electron and muon triggers. Events in the $\mu^\pm\mu^\pm$ channel are selected by a dimuon trigger, which requires one muon with transverse momentum larger than 18 GeV and another muon with $p_T > 8$ GeV. At the trigger level, muons are identified by requiring that the candidate muon tracks are reconstructed in both the MS and the ID. Dielectron events are recorded if the event contains two electrons with a p_T larger than 12 GeV that satisfy the “loose” identification criteria. In the $e^\pm\mu^\pm$ channel events are selected by the trigger if both an electron and a muon ($e\mu$) are found or if a high- p_T electron is identified. For the $e\mu$ trigger the electron must have $p_T > 12$ GeV satisfying the “medium” set of identification criteria, whereas the muon must have $p_T > 8$ GeV. The high- p_T electron trigger selects events containing electrons, which satisfy the “medium” identification criteria and have $p_T > 60$ GeV. These triggers yield a sample of dilepton events with high efficiency over the whole p_T range considered in this analysis.

The selected events must have a reconstructed primary vertex and contain lepton pairs with $p_T > 25$ GeV for the leading lepton and $p_T > 20$ GeV for the subleading one. These leptons must have the same electric charge, meet the above selection requirements, and have an invariant mass $m(\ell\ell') > 15$ GeV. To reduce the background from leptons from Z boson decays, events in which an opposite-sign, same-flavour lepton pair is found to be consistent with the invariant mass of the Z boson ($|m_{\ell\ell} - m_Z| < 10$ GeV) are rejected. In the $e^\pm e^\pm$ channel, electron pairs in the mass range between 70 GeV and 110 GeV are vetoed as this region is used for the background estimates (see section 6.2). Any combination of two leptons with the same charge and with $p_T > 25$ GeV and $p_T > 20$ GeV respectively is included. This allows more than one lepton pair per event to be considered, which happens in fewer than 0.1% of the events.

6 Background estimation

The backgrounds in this search can be subdivided into prompt background, backgrounds from SM processes with two opposite-sign leptons where the charge of one of the leptons is misidentified and non-prompt background. Prompt leptons originate from a decay of a W boson, Z boson, and include any leptonic products of a prompt τ lepton decay. Non-prompt leptons are from decays of long-lived particles and mainly arise from semileptonic decays of heavy-flavour hadrons (containing b or c -quarks). Hadrons or overlapping hadrons within a jet which may be misidentified as an electron are also called non-prompt leptons in the following. The prompt background comes from SM processes producing two same-sign leptons from the primary vertex, and arises mainly from WZ , ZZ , $W^\pm W^\pm$, $t\bar{t}W$, and $t\bar{t}Z$ production (see section 6.1). The method used to estimate the background from lepton

charge misidentification is described in section 6.2. Background from non-prompt leptons can arise from various sources and is discussed in section 6.3. For electrons, the main sources are jets misidentified as electrons and semileptonic decays of hadrons containing b - or c -quarks. For muons, the main contribution arises from semileptonic decays of heavy-flavour hadrons. Small contributions also come from pions and kaons that decay in flight and misidentified muons from hadronic showers in the calorimeter which reach the MS and are incorrectly matched to a reconstructed ID track.

6.1 Background from prompt same-sign lepton pairs

The background from SM processes in which prompt same-sign lepton pairs are produced is determined from MC simulations. Processes other than those listed in table 1 do not contribute significantly to this type of background and are neglected. In all of these samples, only reconstructed leptons are considered that are matched to a lepton at generator level from a decay of a W boson, a Z boson, and include any leptonic products of a prompt τ lepton decay. Leptons from any other sources are discarded to avoid double counting with the background from non-prompt leptons.

6.2 Background from opposite-sign lepton pairs

Monte Carlo samples are also used to simulate the contributions from processes in which opposite-sign lepton pairs are produced and one of the leptons has an incorrect charge assigned. In principle, this charge misidentification can occur for muons as well as electrons. However, a study using muons from Z boson decays shows that this effect is negligible in this analysis. In the case of electrons, the dominant process that leads to charge misidentification is electrons emitting hard bremsstrahlung and subsequently producing electron–positron pairs by photon conversion, with one of these leptons having a high p_T . Typically these conversions would be reconstructed as such, but in some asymmetric conversions only one of the tracks is reconstructed and the charge may be opposite to the charge of the original lepton that radiated the photon. The charge misidentification probability is measured using electrons from Z boson decays. This is done in a data-driven way using the same likelihood method as used in ref. [26]. The electrons are required to pass the same selection cuts as detailed in sections 4 and 5, and are selected by requiring same-sign electron pairs with an invariant mass between 80 GeV and 100 GeV. This results in a very pure sample of electron pairs for which the charge of one of the electrons is incorrectly assigned. A comparison between data and MC events shows that the charge misidentification rate as a function of E_T is well modelled in the simulation. Simulation is used to predict the backgrounds from Drell–Yan, $t\bar{t}$, and $W^\pm W^\mp$ production, correcting the event weights for events with a charge-misidentified electron by an $|\eta|$ -dependent factor derived from these studies. The process $V\gamma \rightarrow \ell\ell'\gamma \rightarrow \ell\ell'ee, V = W, Z$ can also give rise to same-sign lepton pairs when the photon converts. Since this background is closely related to the electron charge misidentification, the same correction factor is applied to the electrons from converted photons in the MC simulation. The contribution of conversions from $Z\gamma$ events is implicitly accounted for in the simulation of the Z/γ process and is included in the charge misidentification category.

The uncertainty in the measurement of the charge misidentification rate is estimated by varying the invariant mass window and by loosening the isolation criteria. The total systematic error varies between 6% and 20% depending on the pseudorapidity. For tracks with very high p_T , the charge can be incorrectly assigned due to the imperfect resolution and alignment of the detector, since the curvature of the tracks is very small. An additional uncertainty of 20% is assigned to the misidentification rate for electrons with $p_T > 100$ GeV, based on the following study. Since the charge misidentification rate is affected by the detector material description in the simulation, simulations with different material descriptions² are compared with the nominal simulation. The largest variation is found in the endcap region and this difference is taken as the overall uncertainty.

6.3 Background from non-prompt leptons

The background from non-prompt and misidentified leptons is determined in a data-driven way as a function of the lepton p_T and $|\eta|$. For both the electrons and the muons (see sections 6.3.1 and 6.3.2) the following method is used to predict the contribution of non-prompt leptons in the signal region. A background region is defined that contains predominantly non-prompt leptons or jets that are kinematically similar to those in the signal region. A factor f is determined, which is the ratio of the number of leptons satisfying a given selection criterion (N_P) to the number of leptons, which do not meet this requirement but satisfy a less stringent criterion (N_F),

$$f = \frac{N_P - N_P^{\text{prompt}}}{N_F - N_F^{\text{prompt}}}. \quad (6.1)$$

This ratio, which is determined as a function of p_T and $|\eta|$, is corrected for the residual contribution of prompt leptons (N_P^{prompt} and N_F^{prompt}) using MC simulations. The factors f are calculated separately for the different pass and fail criteria that apply to the signal and validation regions discussed in sections 4 and 6.4, respectively.

The total number of events with non-prompt leptons, N_{NP} , in a given signal or validation region is predicted to be

$$N_{\text{NP}} = \sum_i^{N_{P_1+F_s}} f_s(p_{T_i}, |\eta_i|) + \sum_i^{N_{F_1+P_s}} f_1(p_{T_i}, |\eta_i|) - \sum_i^{N_{F_1+F_s}} f_1(p_{T_i}, |\eta_i|) \times f_s(p_{T_i}, |\eta_i|). \quad (6.2)$$

The first term is the number of pairs $N_{P_1+F_s}$, where the leading lepton (denoted by l) fulfils the selection requirements (P_1) and the subleading lepton (denoted by s) fails to satisfy its selection criteria (F_s). This is weighted per pair by the factor f_s of the subleading lepton (the lepton which failed). Similarly for the second term, the leading lepton fails its selection (F_1) and the subleading lepton satisfies its respective selection criteria (P_s), hence the weight per pair is given by the factor f_1 for the leading lepton. The last term is included to avoid double counting and represents the case where both the leading and subleading leptons fail to satisfy their respective criteria, and so a weight for each lepton is

²These simulations contain the following additional material: 5% in the whole of the ID, 20% for the pixel and SCT services each, 15% X_0 at the end of the SCT/TRT endcap and 15% X_0 at the ID endplate.

needed. The factors f_1 and f_s are taken to be the same in regions where both leptons fulfil the same selection requirement, as in the signal region and some of the validation regions.

6.3.1 Measurement of f for muons

In the case of muons the factor f is determined using a background region that contains mainly muons from semileptonic decays of b - and c -hadrons. This region is defined by taking advantage of the long lifetimes of b - and c -hadrons. Events are selected containing same-sign muon pairs that fulfil the same selection criteria as for the signal region (see section 4), but requiring that at least one of the leptons has $|d_0|/\sigma(d_0) > 3$ and $|d_0| < 10$ mm. The same dimuon trigger as in the signal region is used here. The number of muons passing these impact parameter cuts is subdivided in two categories: N_P , which are those muons passing the calorimeter and track-based isolation cuts, and N_F , which contain those muons which fail the calorimeter-based isolation cut, the track-based isolation cut or both. The measured factor f is between 0.11 and 0.20 for muons with $p_T > 20$ GeV.

Muons from b - and c -hadron decays tend to have large impact parameters, to be accompanied by other tracks, and to be less isolated than prompt muons, which are associated with the primary vertex. Since the muon isolation can depend on the impact parameter, a correction needs to be applied to the factor f in the signal region. This correction is determined using $b\bar{b}$ and $c\bar{c}$ MC simulations. In both the signal region and background region f is determined and the correction is then given by the ratio of these two quantities. As the correction factor is found to be independent of p_T , the overall value of 1.3 is measured using same-sign muon pairs with $p_T > 20$ GeV and $m_{\mu\mu} > 15$ GeV.

The two main sources of uncertainty in this procedure come from the uncertainty associated with the correction made to f before its use in the signal region, which comes primarily from the statistical error on the MC sample used in its derivation, and from the statistical uncertainties in the background data sample. Further sources of uncertainty arise from the prompt background subtraction and a possible difference between the signal and background region in the fraction of non-prompt muons from heavy-flavour decays and light particles, such as pions and kaons, which decay in flight. The total uncertainty on f is 17% at $p_T \approx 20$ GeV increasing to 23% for $p_T \approx 60$ GeV. A value of 100% is used for $p_T > 100$ GeV due to a lack of statistics to determine f .

6.3.2 Measurement of f for electrons

To measure f for electrons a dijet data sample is selected which contains events with either a jet misidentified as an electron or a non-prompt electron from a semileptonic decay of b - and c -hadrons. The selected region consists of events that contain exactly one electron with $p_T > 20$ GeV and a jet in the opposite azimuthal direction ($\Delta\phi(e, jet) > 2.4$). The electron has to satisfy the “medium” identification criteria, the same impact parameter cuts as for the signal region and is rejected if, after removal of any jet within $\Delta R = 0.2$ of the electron, there is a remaining jet within $\Delta R = 0.4$. These events are selected by a set of prescaled single-electron triggers with different electron p_T thresholds. To ensure that the electron and the jet are well balanced in terms of energy, a $p_T > 30$ GeV requirement is applied to the jet. The different cut value from the electron case accounts for the differences in

the electron and jet energy scale calibrations and for energy depositions from other decay products in the isolation cone around the electron direction. Electron pairs from Z/γ^* or $t\bar{t}$ events do not satisfy the above selection criteria. To suppress electrons from W boson decays, events are rejected if the transverse mass³ exceeds 40 GeV.

The number N_{P} is calculated from events in this background region for which the electron satisfies the same electron selection criteria as applied in the signal region. The value of N_{F} is based on electron candidates satisfying the signal selection criteria but passing less stringent electron identification cuts (“medium”) and failing to meet the calorimeter-based or track-based isolation requirements, or both. The numbers are corrected for the small remaining contribution from prompt electrons (see equation (6.1)). The measured factor f is 0.18 at $p_{\text{T}} = 20$ GeV and increases to around 0.3 for $p_{\text{T}} \approx 100$ GeV. The main systematic uncertainty is due to the jet requirements in the event selection. This effect is estimated by varying the jet p_{T} between 30 GeV and 50 GeV, which leads to an uncertainty ranging between 10% and 30% depending on the electron p_{T} . Other systematic uncertainties arise from a possible difference in the heavy-flavour fraction in the signal and background region, and the prompt background subtraction. The total uncertainty varies between approximately 40% at $p_{\text{T}} \approx 20$ GeV and 13% for $p_{\text{T}} \approx 100$ GeV. Due to a lack of statistics to calculate f for electrons with $p_{\text{T}} > 100$ GeV, the value of f for $60 < p_{\text{T}} < 100$ GeV electrons is used, and the uncertainty is increased to 100%.

6.4 Validation of background extraction methods

The background predictions from the various sources (prompt, non-prompt and charge misidentification) are validated using different methods, as discussed in the following and summarised in table 2.

To test the predictions for the non-prompt background, validation regions (VR) that contain same-sign lepton pairs are defined. In these regions one or both of the leptons fail one of the signal selection cuts but pass a less stringent cut, which is called a “weaker” selection in the following. The dilepton invariant mass, the lepton p_{T} and η distributions are compared between data and predictions.

One of the validation regions selects a leading lepton that satisfies the signal selection criteria and a subleading lepton that passes the “weak” isolation cuts, which means the subleading lepton fails to meet the signal calorimeter or ID-based isolation requirement and instead passes isolation cuts that are loosened by 4 GeV (weak isolation on subleading lepton VR). For this region, the factor f for the subleading lepton is determined according to equation (6.1) using as pass criteria the “weak” isolation requirements and as fail criteria the loose isolation criteria applied in the “weak” selection. The invariant mass distributions for the three final states in this validation region are shown in figure 1 together with one example for the p_{T} distribution. The predictions agree well with the data.

³Transverse mass $m_{\text{T}} = \sqrt{2 \times E_{\text{T}}^{\ell} \times E_{\text{T}}^{\text{miss}} \times (1 - \cos \Delta\phi)}$, where $\Delta\phi$ is the azimuthal angle between the directions of the electron and the missing transverse momentum (with magnitude $E_{\text{T}}^{\text{miss}}$). The missing transverse momentum is defined as the momentum imbalance in the plane transverse to the beam axis and is obtained from the negative vector sum of the momenta of all particles detected in the event [76].

Validation method	Primary background or validation criterion
Weak isolation VR's	Electron and muon non-prompt background
Fail- d_0 VR's	Electron and muon non-prompt background
Medium VR	Electron and muon non-prompt background
Low muon p_T VR	Muon non-prompt background
Opposite-sign VR	Normalisation, efficiencies, lepton p_T scale and resolution
Prompt VR	Prompt MC background predictions
Same-sign dielectron Z peak closure test	Charge misidentification correction applied to opposite-sign MC background samples

Table 2: A summary of the validation methods used and an explanation of the type of background the methods are testing or which data-driven estimates they validate. These tests are carried out using validation regions (VR) or closure tests and are discussed in detail in the text.

In another validation region the “weak” isolation selection is applied to the leading lepton (weak isolation on leading lepton VR). In the $\mu^\pm\mu^\pm$ and $e^\pm\mu^\pm$ channel one validation region (fail- d_0 VR) requires that one muon has an impact parameter significance of $|d_0|/\sigma(d_0) > 3$ and in order to increase the statistics the $|d_0|$ cut is loosened to 10 mm. In the $e^\pm e^\pm$ final state one region (medium VR) contains same-sign electron pairs, in which one of the electrons fails the “tight” identification cuts but passes the looser “medium” selections instead. One region (low muon p_T VR) used in the $e^\pm\mu^\pm$ channel selects same-sign electron–muon pairs, where both leptons satisfy the signal selection criteria but the muon has a transverse momentum between 18 GeV and 20 GeV.

To test the trigger and reconstruction efficiencies, as well as the lepton momentum scale and resolution, an opposite-sign validation region (opposite-sign VR) is defined. This region is populated with prompt lepton pairs that pass the same event selection as for the same-sign signal region, but the leptons have opposite charge. In order to cross-check the normalisation of the dominant WZ and ZZ MC predictions, a prompt validation region (prompt VR) is utilised. Events are selected in which at least three leptons are present. One pair must be from a same-sign lepton pair and another from an opposite-sign same-flavour lepton pair that has an invariant mass ($m_{\ell\ell}$) compatible with the Z boson mass ($|m_{\ell\ell} - m_Z| < 10$ GeV). The data and predictions are compared for different cuts on the invariant mass of the same-sign lepton pair. To test the correction factor for the charge misidentification (see section 6.2), the factor f is applied to simulated Z decays into an electron pair where one electron is reconstructed with the wrong charge. A closure test is carried out in the region around the Z peak. This test shows that the shape of the background from charge misidentification is correctly reproduced.

In all channels and validation regions the agreement between observation and prediction is good, as can be seen in table 3. The agreement between data and predictions is typically better than 1σ and at most 1.7σ .

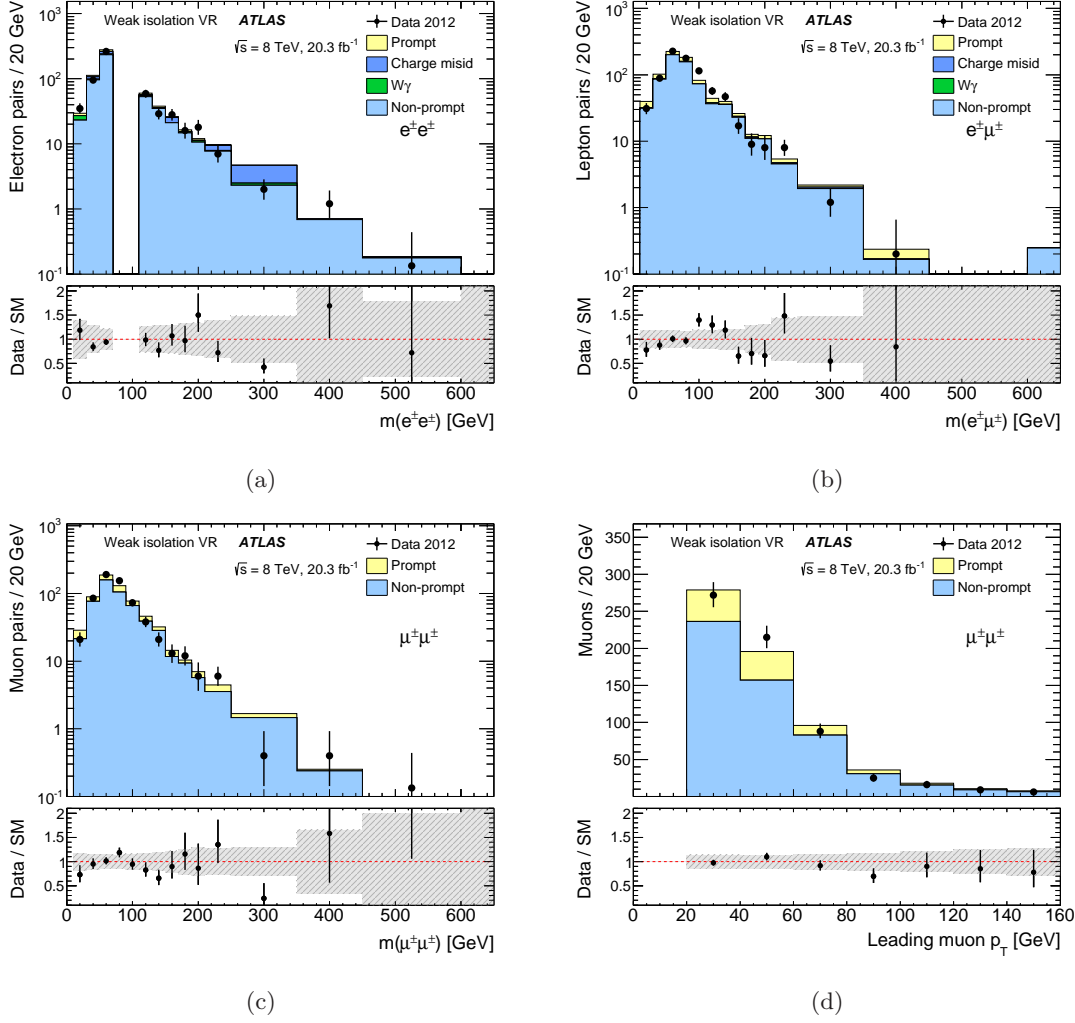


Figure 1: Invariant mass distributions in one of the validation regions (VR) used in the (a) $e^\pm e^\pm$ (b) $e^\pm \mu^\pm$ and (c) $\mu^\pm \mu^\pm$ channels. The p_T distribution for the leading muon in the $\mu^\pm \mu^\pm$ channel is shown in (d). In (a), (c) and (d) the leading lepton of the pair passes the signal isolation cuts while the subleading lepton passes the “weak” isolation cuts (weak isolation on subleading lepton VR). The mass range between 70 GeV and 110 GeV is not included in the $e^\pm e^\pm$ channel as this region is used to estimate the background from charge misidentification. The electron passes the isolation cuts defined for the signal region while the muon passes the “weak” isolation cuts in (b) (weak isolation on muon VR). The data are compared to the background expectations and the lower panels show the ratio of data to the background prediction. The error bars on the data points show the statistical uncertainty and the dashed band shows the total uncertainties of the predictions. The last bin in the histograms includes overflows, and is normalised as though it is 50 GeV wide in (a) - (c) and 20 GeV wide in (d).

Region	Number of electron pairs		
	Predictions	Data	Difference/ σ
Weak isolation on both leptons VR	280 ± 130	285	0.0
Weak isolation on leading lepton VR	190 ± 60	224	-0.6
Weak isolation on subleading lepton VR	620 ± 120	574	+0.4
Medium VR	195 ± 32	217	-0.7
Opposite-sign VR	4740000 ± 330000	4895830	-0.5
Prompt VR with $m_{\ell^\pm\ell^\pm} > 15$ GeV	275 ± 23	268	+0.3
Z peak closure test	12700 ± 1300	11793	+0.7
Region	Number of electron-muon pairs		
	Predictions	Data	Difference/ σ
Weak isolation on muon VR	790 ± 130	800	-0.1
Weak isolation on electron VR	750 ± 150	965	-1.4
Fail- d_0 VR	249 ± 19	216	+1.7
Low muon p_T VR	211 ± 12	201	+0.8
Opposite-sign VR	70400 ± 4700	71771	-0.3
Prompt VR with $m_{\ell^\pm\ell^\pm} > 15$ GeV	950 ± 60	1001	-0.8
Region	Number of muon pairs		
	Predictions	Data	Difference/ σ
Weak isolation on both leptons VR	280 ± 40	283	-0.1
Weak isolation on leading lepton VR	199 ± 25	199	0.0
Weak isolation on subleading lepton VR	697 ± 90	652	+0.5
Fail- d_0 VR	250 ± 31	255	-0.2
Opposite-sign VR	8144000 ± 10000	8216983	-0.7
Prompt VR with $m_{\ell^\pm\ell^\pm} > 15$ GeV	651 ± 43	714	-1.5

Table 3: Expected and observed numbers of lepton pairs for the different validation regions, explained in detail in the text. The uncertainties on the predictions include the statistical and systematic uncertainties. The column 'Difference/ σ ' is calculated by dividing the difference between the predictions and the data by the uncertainty (σ) of the prediction.

7 Systematic uncertainties

The systematic uncertainties considered in this analysis are summarised in table 4. Experimental systematic uncertainties arise from the trigger selection and the lepton reconstruction and identification. These include the effects of the energy scale and resolution uncertainties. Also shown is the overall uncertainty in the $e^\pm e^\pm$ and $e^\pm \mu^\pm$ channels from electron charge misidentification (discussed in section 6.2) and the non-prompt background estimation (presented in section 6.3).

The uncertainty on the integrated luminosity is 2.8%. It is derived following the same methodology as that detailed in ref. [77]. Another systematic uncertainty is due to the

Source	Process	Uncertainty		
		$e^\pm e^\pm$	$e^\pm \mu^\pm$	$\mu^\pm \mu^\pm$
Trigger	Signal and background from MC simulations	2.1-2.6%	2.1-2.6%	2.1-2.6%
Electron reconstruction and identification	Signal, prompt background	1.9-2.7%	1.4%	
Muon reconstruction and identification	Signal, prompt background		0.28%	0.6%
Electron charge misidentification	Opposite-sign backgrounds	9%	1.2%	
Determination of factor f for e/μ	Non-prompt backgrounds	22%	24%	17%
Luminosity	Signal and background from MC simulations	2.8%	2.8%	2.8%
MC statistics	Backgrounds from MC simulations	5%	1.6%	1.3%
Photon misidentification as electron	$W\gamma$	13%	11%	
MC cross-sections	Prompt, opposite-sign backgrounds	4%	2.5%	4%

Table 4: Sources of systematic uncertainty (in %) on the signal yield and the expected background predictions, described in the second column, for the mass range $m_{\ell\ell} > 15$ GeV.

limited number of events available in the MC samples and also the data control samples used for the background predictions. The overall effect from the MC samples used per channel is shown in table 4. Systematic uncertainties on different physics processes from the same source are assumed to be 100% correlated. An example is the charge misidentification rate uncertainty for the Z/γ^* , $t\bar{t}$, WW and $W\gamma$ samples.

Theoretical uncertainties on the production cross-section arise from the choice of renormalisation and factorisation scales in the fixed-order calculations as well as the uncertainties on the PDF sets and the value of the strong coupling constant α_s used in the perturbative expansion. The uncertainties due to the renormalisation and factorisation scales are found by varying the scales by a factor of two relative to their nominal values. The PDF and α_s uncertainties are determined using different PDF sets and PDF error sets following the recommendations documented in ref. [78]. The uncertainties on the MC modelling of background processes are estimated by testing different generators as well as parton shower and hadronisation models. The resulting total cross-section uncertainties are 7% for WZ [79], 5% for ZZ [79], and 22% for $t\bar{t}V$ [54, 80]. The uncertainties on $W^\pm W^\pm$ cross-sections and diboson production in MPI processes are taken to be 50% and 100% respectively, but their contributions to the final results are small.

8 Results and interpretation

8.1 Signal region

The invariant mass distributions for the data and the expected SM background are shown in figure 2, separately for the $e^\pm e^\pm$, $e^\pm \mu^\pm$ and $\mu^\pm \mu^\pm$ final states. In general, good agreement is seen in both the total normalisation and shapes for all channels within the uncertainties. The last bin in the figures contains the overflow bin. There is no event in the overflow in the $\mu^\pm \mu^\pm$ channel, while the mass distribution extends up to around 1300 (1100) GeV in the $e^\pm e^\pm$ ($e^\pm \mu^\pm$) channel. The expected and observed numbers of events for several cuts on the dilepton mass for each final state are given in table 5, which also shows the contributions from the different background types. In the $e^\pm e^\pm$ channel the dominant background contribution comes from charge misidentification of electrons from the Drell–Yan process. In the $e^\pm \mu^\pm$ and $\mu^\pm \mu^\pm$ channel the prompt production dominates the background. The prompt background predominantly arises from WZ boson production, which amounts to around 70% of the prompt background. This fraction slightly decreases for high-mass dilepton pairs. Other contributions are from ZZ and $W^\pm W^\pm$ production and a very small fraction comes from the $t\bar{t}W$ and $t\bar{t}Z$ production or from diboson production in MPI processes. For dilepton masses $m_{\ell\ell} > 500$ GeV, the contribution from $W^\pm W^\pm$ and ZZ to the prompt background becomes more pronounced with $W^\pm W^\pm$ being the largest contribution to the prompt background for $m_{\ell\ell} > 600$ GeV in the $\mu^\pm \mu^\pm$ channel.

Table 6 shows a similar comparison of the data with the SM expectation separately for $\ell^+ \ell^+$ and $\ell^- \ell^-$ pairs. Due to the contribution of the valence quarks in the proton, more W^+ than W^- bosons are produced in pp collisions resulting in a higher background for the $\ell^+ \ell^+$ final state. For all final states no significant excesses or deficits are observed between the data and the SM background predictions.

Based on the above findings, upper limits are computed at the 95% confidence level (CL) using the CL_S [81] prescription. Limits are given on the number of same-sign lepton pairs (N_{95}) contributed by new physics beyond the SM for various invariant mass thresholds. In this procedure the number of pairs in each mass bin is described using a Poisson probability density function. The systematic uncertainties (as discussed in section 7) are incorporated into the limit calculation as nuisance parameters with Gaussian priors with the correlations between uncertainties taken into account. The limits can be translated into an upper limit on the fiducial cross-section using: $\sigma_{95}^{\text{fid}} = N_{95}/(\epsilon_{\text{fid}} \times \int L dt)$, where ϵ_{fid} is the efficiency for finding a lepton pair from a possible signal from new physics in the fiducial region at particle level, and $\int L dt$ is the integrated luminosity. The efficiency ϵ_{fid} is discussed in detail in the next section.

The fiducial volume at particle level, as summarised in table 7, is chosen to be very similar to the one used in the object and event selections (see sections 4 and 5). The leptons must be isolated and fulfil the same kinematic requirements on transverse momentum and pseudorapidity as imposed at reconstruction level. Lepton isolation is implemented by requiring that the sum of the p_T of the stable charged particles with $p_T > 1$ (0.4) GeV in a cone of size $\Delta R = 0.3$ around the lepton is required to be less than 7% (10%) of the lepton p_T for muons (electrons). In addition, the two leptons must have the same

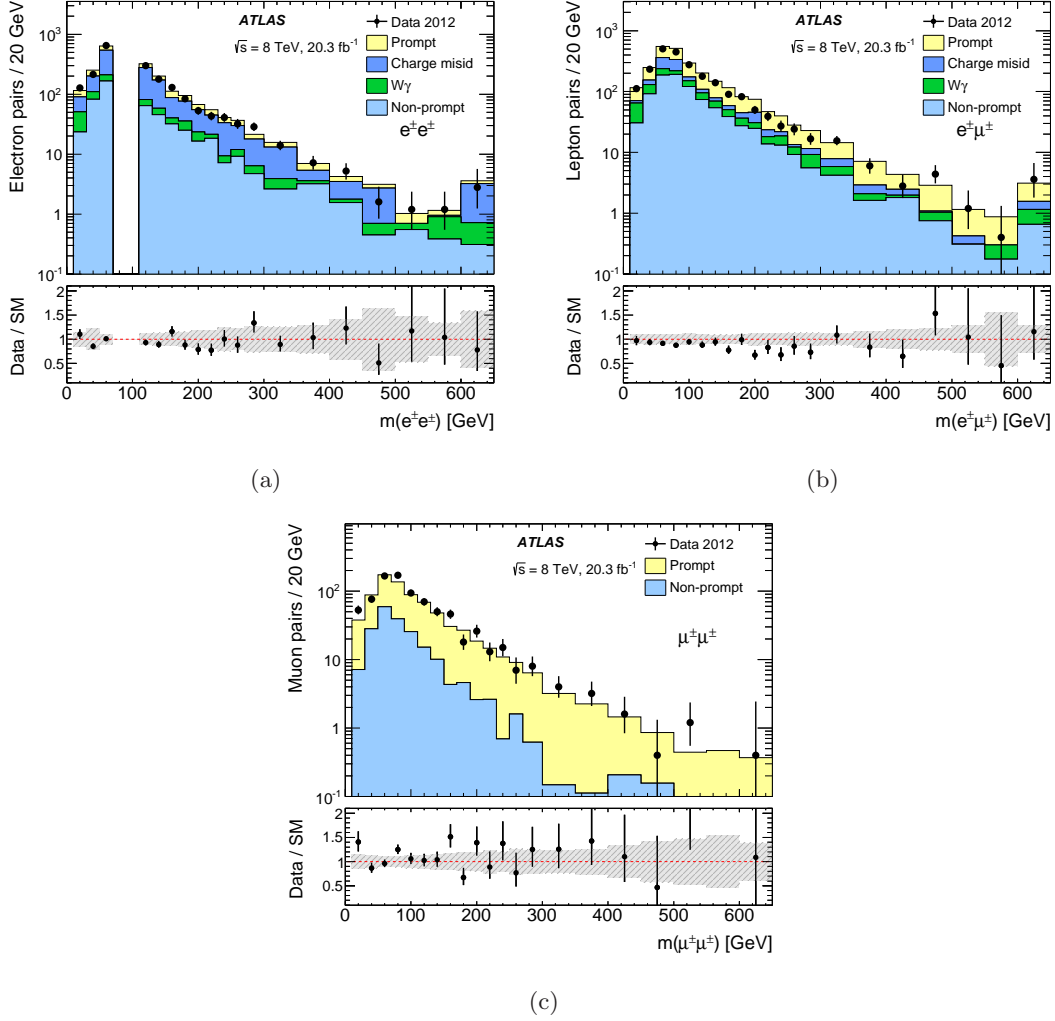


Figure 2: Invariant mass distribution of (a) $e^\pm e^\pm$ (b) $e^\pm \mu^\pm$ and (c) $\mu^\pm \mu^\pm$ pairs as a function of a threshold on the dilepton mass in the same-sign signal region. The mass range between 70 GeV and 110 GeV is not included in the $e^\pm e^\pm$ channel as this region is used to estimate the background from charge misidentification. The data are compared to the SM expectations and the lower panels show the ratio of data to the background prediction. The error bars on the data points show the statistical uncertainty and the dashed band shows the total uncertainties of the predictions. The last bin in the histograms includes overflows, and is normalised as though it is 50 GeV wide.

charge and pass the same invariant mass cut, $m_{\ell\ell} > 15$ GeV, as required at reconstruction level. In addition, in the $e^\pm e^\pm$ channel the mass range $70 < m_{\ell\ell} < 110$ GeV is vetoed. Finally, events are rejected in which an opposite-sign, same-flavour lepton pair is found with $|m_{\ell\ell} - m_Z| < 10$ GeV.

$m(e^\pm e^\pm)$ [GeV]	Number of electron pairs					Data
	Prompt	Non-Prompt	e^\pm charge misid.	$W\gamma \rightarrow Wee$	Total SM	
> 15	347 ± 25	520 ± 120	1020 ± 150	180 ± 40	2060 ± 190	1976
> 100	174 ± 14	250 ± 50	550 ± 80	75 ± 16	1050 ± 100	987
> 200	51.5 ± 4.9	72 ± 13	150 ± 27	22 ± 5	296 ± 31	265
> 300	15.7 ± 1.9	23 ± 5	43 ± 12	8.0 ± 2.3	89 ± 14	83
> 400	5.3 ± 0.9	8.1 ± 2.4	16 ± 8	3.8 ± 1.3	33 ± 8	30
> 500	2.3 ± 0.5	3.1 ± 1.5	6 ± 5	2.7 ± 1.0	14 ± 5	13
> 600	0.91 ± 0.28	$0.8^{+1.0}_{-0.8}$	6 ± 5	1.0 ± 0.6	9 ± 5	7

$m(e^\pm \mu^\pm)$ [GeV]	Number of electron–muon pairs					Data
	Prompt	Non-Prompt	e^\pm charge misid.	$W\gamma \rightarrow Wee$	Total SM	
> 15	1030 ± 50	910 ± 220	370 ± 40	270 ± 50	2580 ± 240	2315
> 100	458 ± 26	340 ± 80	87 ± 11	104 ± 20	990 ± 90	859
> 200	130 ± 9	79 ± 17	29 ± 4	28 ± 6	265 ± 22	226
> 300	43 ± 5	24 ± 6	9.5 ± 1.9	8.1 ± 2.4	84 ± 8	85
> 400	16.0 ± 2.1	9.2 ± 3.0	2.5 ± 0.8	2.7 ± 1.1	31 ± 4	31
> 500	6.8 ± 1.1	2.8 ± 1.5	1.5 ± 0.4	1.6 ± 0.8	12.6 ± 2.1	13
> 600	3.5 ± 0.7	1.6 ± 1.0	0.9 ± 0.4	1.2 ± 0.7	7.4 ± 1.5	9

$m(\mu^\pm \mu^\pm)$ [GeV]	Number of muon pairs			
	Prompt	Non-Prompt	Total SM	Data
> 15	580 ± 40	203 ± 34	780 ± 50	843
> 100	245 ± 21	56 ± 11	301 ± 24	330
> 200	67 ± 7	8.7 ± 2.3	76 ± 8	87
> 300	20.7 ± 2.9	1.9 ± 1.0	22.6 ± 3.1	27
> 400	7.7 ± 1.5	1.2 ± 0.9	9.0 ± 1.7	9
> 500	2.9 ± 0.8	$0.32^{+0.41}_{-0.32}$	3.2 ± 0.9	4
> 600	0.9 ± 0.4	$0.0^{+0.2}_{-0.0}$	0.9 ± 0.4	1

Table 5: Expected and observed numbers of isolated same-sign lepton pairs in the $e^\pm e^\pm$, $e^\pm \mu^\pm$ and $\mu^\pm \mu^\pm$ channel for various cuts on the dilepton invariant mass, $m(\ell^\pm \ell^\pm)$. The uncertainties shown are the systematic uncertainties.

8.2 Fiducial cross-section limits

To derive upper limits on the cross-section due to physics beyond the SM, the fiducial efficiency, ϵ_{fid} , is calculated. The quantity ϵ_{fid} is the ratio, for leptons from the signal processes, of the number of selected lepton pairs to the number of true same-sign lepton pairs satisfying the fiducial selection at particle level. The value of ϵ_{fid} generally depends on the new physics process, e.g. the number of leptons in the final state passing the kinematic

$m(\ell\ell)$ [GeV]	e^+e^+ pairs		$e^+\mu^+$ pairs		$\mu^+\mu^+$ pairs	
	Total SM	Data	Total SM	Data	Total SM	Data
> 15	1120 ± 100	1124	1440 ± 130	1327	454 ± 32	502
> 100	610 ± 60	593	570 ± 50	523	184 ± 16	198
> 200	187 ± 22	167	146 ± 13	143	48 ± 6	62
> 300	61 ± 11	48	50 ± 5	56	15.3 ± 2.2	18
> 400	19 ± 6	18	18.4 ± 2.6	21	6.2 ± 1.2	6
> 500	9 ± 5	9	7.8 ± 1.4	8	2.6 ± 0.8	1
> 600	7 ± 5	5	4.8 ± 1.1	6	0.8 ± 0.4	0

$m(\ell\ell)$ [GeV]	e^-e^- pairs		$e^-\mu^-$ pairs		$\mu^-\mu^-$ pairs	
	Total SM	Data	Total SM	Data	Total SM	Data
> 15	940 ± 100	852	1140 ± 110	988	328 ± 23	341
> 100	440 ± 50	394	417 ± 40	336	117 ± 9	132
> 200	109 ± 16	98	119 ± 11	83	27.6 ± 2.8	25
> 300	29 ± 7	35	35 ± 4	29	7.3 ± 1.2	9
> 400	14 ± 5	12	12.1 ± 2.3	10	2.7 ± 0.7	3
> 500	5.0 ± 1.3	4	4.9 ± 1.5	5	$0.64^{+0.33}_{-0.26}$	3
> 600	2.7 ± 0.9	2	2.5 ± 1.0	3	$0.09^{+0.23}_{-0.09}$	1

Table 6: Expected and observed numbers of positively or negatively charged lepton pairs for various cuts on the dilepton invariant mass, $m(\ell\ell)$. The uncertainties shown are the systematic uncertainties.

Selection	Electron requirement	Muon requirement
Leading lepton p_T	$p_T > 25$ GeV	$p_T > 25$ GeV
Subleading lepton p_T	$p_T > 20$ GeV	$p_T > 20$ GeV
Lepton η	$ \eta < 1.37$ or $1.52 < \eta < 2.47$	$ \eta < 2.5$
Isolation	$\sum p_T(\Delta R = 0.3)/p_T^e < 0.1$	$\sum p_T(\Delta R = 0.3)/p_T^\mu < 0.07$

Selection	Event selection
Lepton pair	Same-sign pair with $m_{\ell\ell} > 15$ GeV
Electron pair	Veto pairs with $70 < m_{\ell\ell} < 110$ GeV
Event	No opposite-sign same-flavour pair with $ m_{\ell\ell} - m_Z < 10$ GeV

Table 7: Summary of requirements on generated leptons and lepton pairs in the fiducial region at particle level. More information on the calculation of the isolation p_T is given in the text.

selection criteria or the number of jets that may affect the lepton isolation. To minimise this dependence, the definition of the fiducial region is closely related to the analysis selection. The limits are quoted using the lowest fiducial efficiency obtained for the following beyond-the-SM processes.

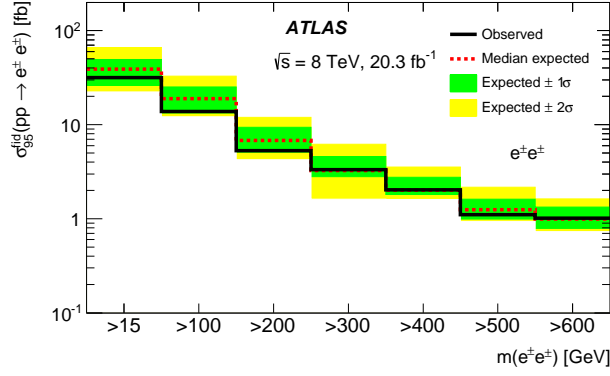
Firstly, production of doubly charged Higgs boson pairs with masses ranging between 100 GeV and 1 TeV is considered. Another process is production of a diquark (S_{DQ}) with charge $\pm 2/3$ or $\pm 4/3$ in the Zee–Babu model, which decays into two same-sign leptoquarks (S_{LQ}), decaying subsequently into a same-sign lepton pair. This model is considered for diquark masses between 2.5 TeV and 3.5 TeV and leptoquark masses between 1 TeV and 1.4 TeV. The third process is a production of a right-handed W_R boson decaying into a lepton and a Majorana neutrino N_R , with N_R subsequently decaying into a lepton and two jets, for W_R masses between 1 TeV and 2 TeV, and N_R masses between 250 GeV and 1.5 TeV. The last process is pair production of b' chiral quarks, decaying either exclusively into Wt or decaying into Wq , q being an up-type quark, with a 33% branching ratio in each quark channel, for b' masses between 400 GeV and 1 TeV.

The fiducial efficiencies vary between 46% and 74% with similar values for the $e^\pm e^\pm$, $e^\pm \mu^\pm$ and $\mu^\pm \mu^\pm$ final states. The lowest values of ϵ_{fid} are found in the case of the fourth-generation down-type chiral quark model, and the highest for the production of W_R bosons and N_R neutrinos. The primary reason for this dependence is that the electron identification efficiency varies by about 15% over the relevant p_T range [75]. For muons differences in the efficiencies arise due to the detector acceptances [82], which are populated differently depending on the kinematics of the leptons produced in the new physics process. Further differences of the order of 1% arise since the calorimeter-based isolation criterion is not emulated because the isolation energy has a poor resolution in the calorimeter. The fiducial efficiencies are also derived separately for $\ell^+ \ell^+$ and $\ell^- \ell^-$ pairs and found to be charge independent.

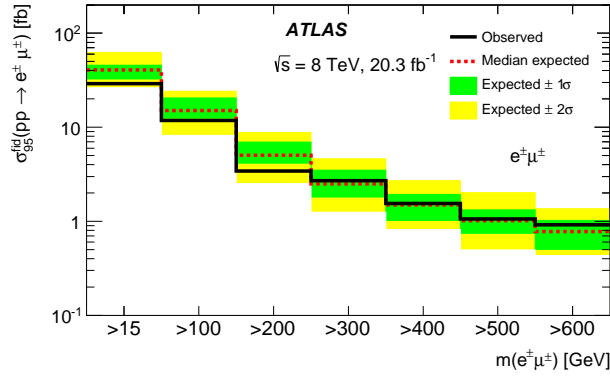
In the following, cross-section limits are presented for the case which yields the lowest fiducial efficiency, that is 48%, 50% and 46% in the $e^\pm e^\pm$, $e^\pm \mu^\pm$ and $\mu^\pm \mu^\pm$ channel respectively. The 95% CL upper limits on the fiducial cross-section are shown in figure 3 and in table 8 separately for each final state. The cross-section limits are statistical combinations of the $\ell^+ \ell^+$ and $\ell^- \ell^-$ limits and observed limits vary between 0.48 fb and 32 fb depending on the mass cut and the final state for the inclusive analysis. The limits obtained for $\ell^+ \ell^+$ and $\ell^- \ell^-$ pairs are also shown in table 8 and range between 0.32 fb to 28 fb. Since the total limits are the limits on the sum of $\ell^+ \ell^+$ and $\ell^- \ell^-$, they are, in general, larger than charge separated limits. For all final states the observed limits are generally within 1σ of the expected limits, which are obtained using simulated pseudo-experiments using only SM processes.

8.3 Cross-section and mass limits for pair-produced doubly charged Higgs bosons

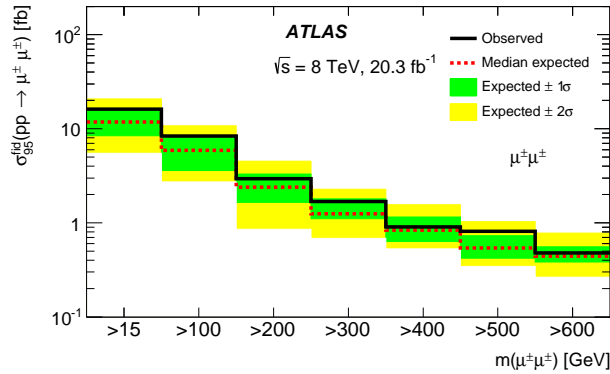
As an example of the models producing same-sign lepton pairs, mass limits are obtained for doubly charged Higgs bosons, which are pair produced via s -channel Z boson or photon exchange in the framework of the left-right symmetric models [3–6]. In this framework, left-handed states, $H_L^{\pm\pm}$, and right-handed states $H_R^{\pm\pm}$ are predicted. These Higgs bosons have identical kinematic properties, but their production rate differs due to the different couplings to Z bosons [7]. The cross-section, which is known at NLO, is around 2.5 times higher for $H_L^{++} H_L^{--}$ pair production compared to $H_R^{++} H_R^{--}$. In this analysis the decay



(a)



(b)



(c)

Figure 3: Fiducial cross-section limits at 95% CL for (a) $e^\pm e^\pm$, (b) $e^\pm \mu^\pm$ and (c) $\mu^\pm \mu^\pm$ pairs, as a function of the lower bound on the lepton pair mass. The green and yellow bands show the 1σ and 2σ bands on the expected limits. The mass range between 70 GeV and 110 GeV is not included in the $e^\pm e^\pm$ channel as this region is used to estimate the background from charge misidentification.

Mass range	95% CL upper limit [fb]					
	$e^\pm e^\pm$		$e^\pm \mu^\pm$		$\mu^\pm \mu^\pm$	
	Expected	Observed	Expected	Observed	Expected	Observed
> 15 GeV	39_{-13}^{+10}	32	41_{-8}^{+5}	29	12_{-3}^{+4}	16
> 100 GeV	19_{-6}^{+6}	14	$15.1_{-2.6}^{+5.5}$	11.8	$5.9_{-2.3}^{+2.2}$	8.4
> 200 GeV	$6.8_{-1.7}^{+2.6}$	5.3	$5.0_{-0.9}^{+1.9}$	3.4	$2.4_{-0.8}^{+0.9}$	2.9
> 300 GeV	$3.3_{-0.4}^{+1.3}$	3.3	$2.5_{-0.7}^{+1.0}$	2.7	$1.25_{-0.15}^{+0.55}$	1.69
> 400 GeV	$2.02_{-0.21}^{+0.74}$	2.03	$1.5_{-0.5}^{+0.4}$	1.6	$0.83_{-0.20}^{+0.32}$	0.91
> 500 GeV	$1.25_{-0.26}^{+0.36}$	1.10	$1.02_{-0.27}^{+0.30}$	1.06	$0.54_{-0.12}^{+0.19}$	0.82
> 600 GeV	$0.99_{-0.20}^{+0.34}$	1.02	$0.78_{-0.28}^{+0.24}$	0.92	$0.44_{-0.06}^{+0.11}$	0.48
Mass range	$e^+ e^+$		$e^+ \mu^+$		$\mu^+ \mu^+$	
	Expected	Observed	Expected	Observed	Expected	Observed
	> 15 GeV	27_{-6}^{+11}	28	25_{-4}^{+10}	23	$9.5_{-3.1}^{+3.3}$
> 100 GeV	$14.3_{-2.8}^{+5.4}$	13.5	$11_{-2.1}^{+4}$	9	$5.0_{-1.3}^{+1.6}$	6.3
> 200 GeV	$5.4_{-1.4}^{+2.0}$	4.6	$3.6_{-0.7}^{+1.3}$	3.6	$2.2_{-0.5}^{+0.8}$	3.6
> 300 GeV	$2.5_{-0.6}^{+0.9}$	2.0	$1.9_{-0.5}^{+0.8}$	2.6	$1.11_{-0.29}^{+0.46}$	1.42
> 400 GeV	$1.59_{-0.34}^{+0.47}$	1.64	$1.10_{-0.23}^{+0.46}$	1.39	$0.74_{-0.17}^{+0.27}$	0.74
> 500 GeV	$1.44_{-0.36}^{+0.34}$	1.55	$0.79_{-0.22}^{+0.21}$	0.89	$0.42_{-0.10}^{+0.24}$	0.38
> 600 GeV	$1.27_{-0.26}^{+0.37}$	1.10	$0.65_{-0.16}^{+0.14}$	0.77	$0.37_{-0.05}^{+0.09}$	0.32
Mass range	$e^- e^-$		$e^- \mu^-$		$\mu^- \mu^-$	
	Expected	Observed	Expected	Observed	Expected	Observed
	> 15 GeV	23_{-5}^{+8}	19	$19.0_{-2.8}^{+8.0}$	16.0	$6.8_{-1.5}^{+2.7}$
> 100 GeV	$10.8_{-2.4}^{+4.4}$	9.0	$8.2_{-2.1}^{+2.2}$	5.6	$3.5_{-0.9}^{+1.4}$	5.1
> 200 GeV	$3.9_{-1.2}^{+1.4}$	3.5	$2.8_{-0.9}^{+1.2}$	1.5	$1.41_{-0.33}^{+0.54}$	1.29
> 300 GeV	$2.1_{-0.5}^{+0.7}$	2.6	$1.6_{-0.4}^{+0.6}$	1.3	$0.79_{-0.16}^{+0.30}$	1.0
> 400 GeV	$1.56_{-0.31}^{+0.41}$	1.35	$0.91_{-0.26}^{+0.34}$	0.77	$0.52_{-0.13}^{+0.20}$	0.59
> 500 GeV	$0.69_{-0.17}^{+0.27}$	0.64	$0.62_{-0.12}^{+0.12}$	0.65	$0.355_{-0.013}^{+0.139}$	0.683
> 600 GeV	$0.58_{-0.08}^{+0.21}$	0.61	$0.49_{-0.10}^{+0.16}$	0.59	$0.332_{-0.011}^{+0.014}$	0.454

Table 8: Upper limit at 95% CL on the fiducial cross-section for $\ell^\pm \ell^\pm$ pairs from non-SM signals. The expected limits and their 1σ uncertainties are given together with the observed limits derived from the data. Limits are given separately for the $e^\pm e^\pm$, $e^\pm \mu^\pm$ and $\mu^\pm \mu^\pm$ channel inclusively and separated by charge.

of the two $H^{\pm\pm}$ bosons into leptons ($H^{\pm\pm}H^{\mp\mp} \rightarrow \ell_1^\pm \ell_2^\pm \ell_3^\mp \ell_4^\mp$) is considered. This is done using the same search strategy as for the fiducial cross-section limits, which looks for signs of new physics in events containing same-sign lepton pairs. Alternatively this search could be carried out looking for events with two same-sign lepton pairs (four-lepton final states). However, the four-lepton channel has a low efficiency due to the cases where at least one of the leptons falls outside the acceptance.

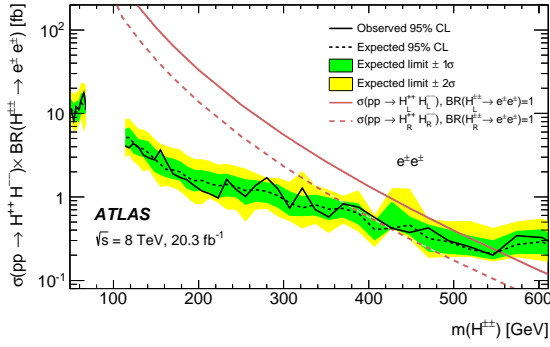
In the following, $H^{\pm\pm}$ boson mass values in the range 50 GeV to 1 TeV are considered. The cross-section is determined using $\sigma_{HH} \times BR = N_H^{\text{rec}} / (2 \times A \times \epsilon \times \int L dt)$, where BR is the branching ratio of the decay into a lepton pair ($H^{\pm\pm} \rightarrow \ell^\pm \ell'^\pm$), N_H^{rec} is the number of reconstructed Higgs boson candidates, $A \times \epsilon$ is the acceptance times efficiency to find a lepton pair from the $H^{\pm\pm}$ decay, and the factor of two accounts for the two same-sign lepton pairs from the H^{++} and H^{--} bosons. The $A \times \epsilon$ is calculated for the simulated mass points and masses in between are interpolated via an empirical fit function. In the mass range considered in this analysis, the width of the $H^{\pm\pm}$ resonance is much smaller than the detector resolution of the lepton pairs. To extract the cross-section limits of $H^{\pm\pm}$ bosons the size of the mass bins used is optimised for each final state, such that in each mass bin the Higgs selection efficiency is very similar. Limits on the cross-section for pair production of $H^{\pm\pm}$ and $H^{\mp\mp}$ bosons times the branching ratio in each of the three final states are extracted using the CL_S technique.

The results at 95% CL are shown in figure 4. The scatter between adjacent mass bins in the observed limits is due to fluctuations in the background yields derived from limited statistics. In general, good agreement is seen between observed and expected limits with maximum deviations of 2σ . In the three final states, the cross-section limits vary between 11 fb for a $H^{\pm\pm}$ mass of 50 GeV to around 0.3 fb for a $H^{\pm\pm}$ mass of 600 GeV. The expected cross-section curves for the pair production of H_L and H_R are also shown in figure 4. The

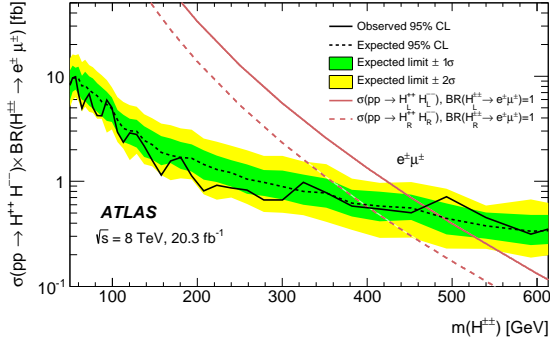
Signal	95% CL lower limit [GeV]					
	$e^\pm e^\pm$		$e^\pm \mu^\pm$		$\mu^\pm \mu^\pm$	
	Expected	Observed	Expected	Observed	Expected	Observed
$H_L^{\pm\pm}$	553 ± 30	551	487 ± 41	468	543 ± 40	516
$H_R^{\pm\pm}$	425 ± 30	374	396 ± 34	402	435 ± 33	438

Table 9: Lower limits at 95% CL on the mass of $H_L^{\pm\pm}$ and $H_R^{\pm\pm}$ bosons, assuming a 100% branching ratio to $e^\pm e^\pm$, $e^\pm \mu^\pm$ and $\mu^\pm \mu^\pm$ pairs. The 1σ variations are also shown for the expected limits.

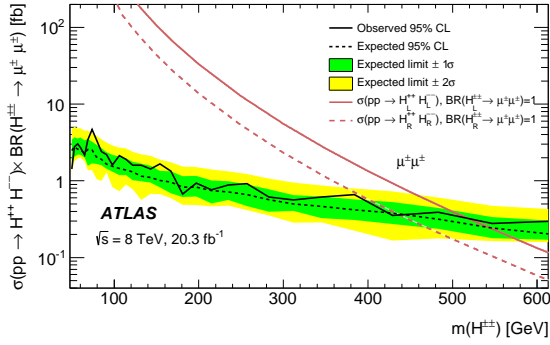
lower mass limits are given by the crossing point of the cross-section limit curve and the expected curve, and are summarised in table 9. The 1σ errors on the expected limits are symmetrised to reduce the effect from bin by bin statistical fluctuations. For this scenario the best limits are obtained for $H_L^{\pm\pm}$ in the $e^\pm e^\pm$ channel with a limit around 550 GeV and for $H_R^{\pm\pm}$ in the $\mu^\pm \mu^\pm$ channel with a limit around 430 GeV. The limits are 10–20% worse in the $e^\pm \mu^\pm$ channel due to the larger background at high invariant masses from



(a)



(b)



(c)

Figure 4: Upper limits at 95% CL on the cross-section as a function of the dilepton invariant mass for the production of a doubly charged Higgs boson decaying into (a) $e^\pm e^\pm$, (b) $e^\pm \mu^\pm$, and (c) $\mu^\pm \mu^\pm$ pairs with a branching ratio of 100%. The green and yellow bands correspond to the 1σ and 2σ bands on the expected limits respectively. Also shown are the expected cross-sections as a function of mass for left- and right-handed $H^{\pm\pm}$. The mass range between 70 GeV and 110 GeV is not included in the $e^\pm e^\pm$ channel as this region is used to estimate the background from charge misidentification.

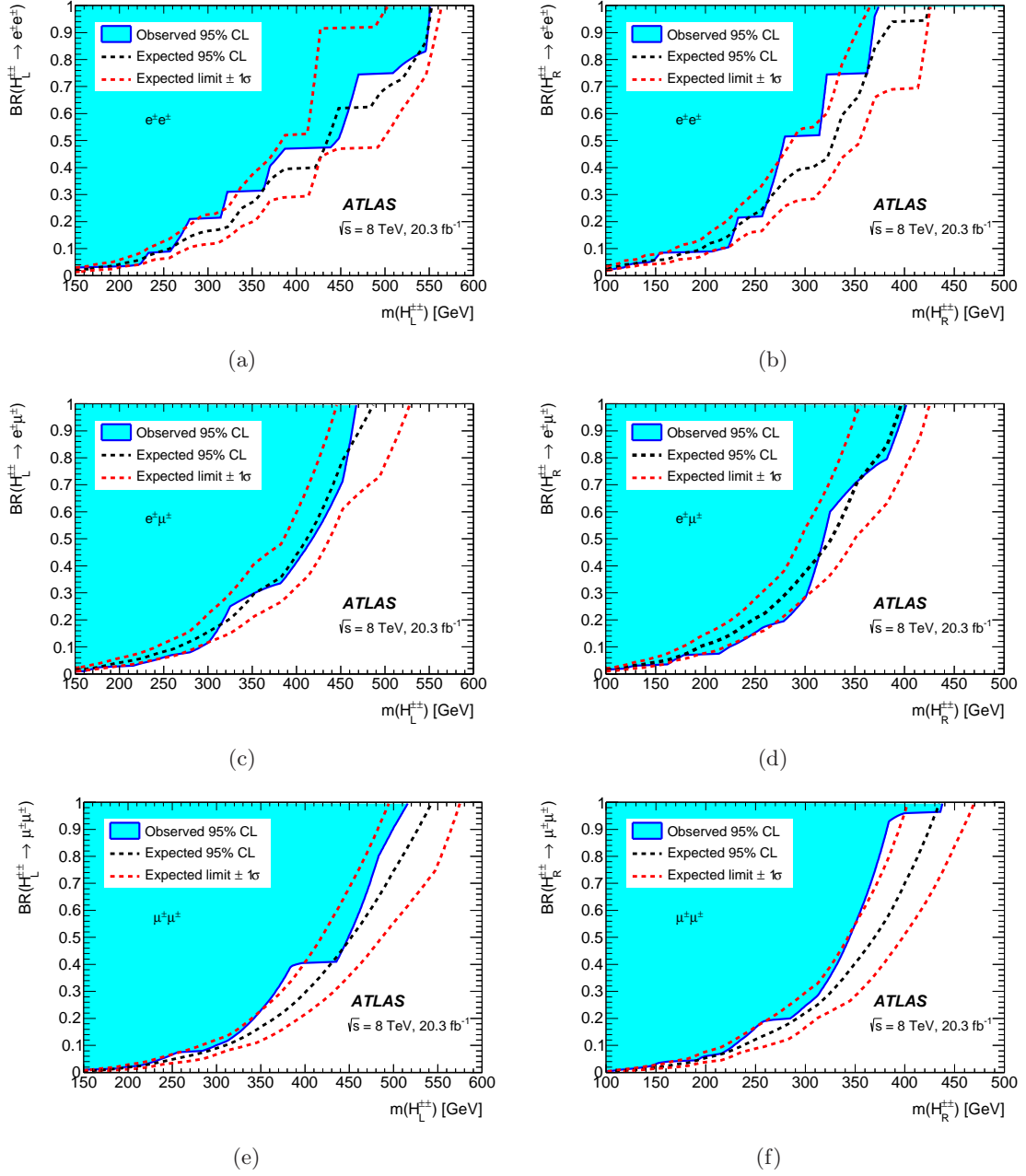


Figure 5: Observed and expected 95% CL limits on $H_L^{\pm\pm} \rightarrow \ell^{\pm}\ell^{\pm}$ (left column) and $H_R^{\pm\pm} \rightarrow \ell^{\pm}\ell^{\pm}$ production (right column) in the branching ratio versus $H^{\pm\pm}$ mass plane for the $e^{\pm}e^{\pm}$ (top), $e^{\pm}\mu^{\pm}$ (middle) and $\mu^{\pm}\mu^{\pm}$ (bottom) channel. The blue shaded area is excluded.

WZ production. The WZ gives approximately twice as many events in the $e^\pm\mu^\pm$ channel than in the $e^\pm e^\pm$ or $\mu^\pm\mu^\pm$ channel whereas the signal contributions are similar in all three channels. The mass limit on the singlet $H^{\pm\pm}$ predicted in the Zee–Babu model [23] is the same as the one obtained for $H_L^{\pm\pm}$ as the cross-sections and decay kinematics are identical. Compared to the results based on the 2011 data [27], the limits on the doubly charged Higgs mass are increased by 30–40%. The mass limits vary with the branching ratio of the $H^{\pm\pm}$ decay into lepton pairs. Figure 5 shows the mass limits as a function of the branching ratio for $H_L^{\pm\pm}$ and $H_R^{\pm\pm}$ in the three final states.

9 Conclusion

In this paper a search for anomalous production of same-sign $e^\pm e^\pm$, $e^\pm\mu^\pm$, and $\mu^\pm\mu^\pm$ pairs is presented using 20.3 fb^{-1} of $\sqrt{s} = 8 \text{ TeV}$ pp collision data recorded with the ATLAS detector at the LHC. To make this search as inclusive as possible, there are no additional requirements on missing transverse momentum, jets, or other final-state particles. The data agree with the SM expectation and no significant deviations are observed. Fiducial cross-section limits are derived for contributions from new physics beyond the SM, which give rise to final states with two same-sign isolated leptons. The 95% CL upper limits on the cross-section are given as functions of a threshold on the invariant mass of the lepton pair. For invariant mass cuts ranging between 15 GeV and 600 GeV, the observed fiducial cross-section upper limit varies between 0.48 fb and 32 fb depending on the dilepton invariant mass and flavour combination. Limits are also set for a model of doubly charged Higgs bosons, in which doubly charged Higgs bosons are pair produced. Assuming these Higgs bosons decay exclusively into $e^\pm e^\pm$, $e^\pm\mu^\pm$ or $\mu^\pm\mu^\pm$ pairs, 95% CL lower mass limits for left-handed Higgs bosons between 465 GeV and 550 GeV are obtained depending on the flavour of the lepton pair. The mass limits for right-handed Higgs bosons range between 370 GeV and 435 GeV. These results represent a significant improvement compared to the previous ATLAS results based on $\sqrt{s} = 7 \text{ TeV}$ data.

Acknowledgments

We thank CERN for the very successful operation of the LHC, as well as the support staff from our institutions without whom ATLAS could not be operated efficiently.

We acknowledge the support of ANPCyT, Argentina; YerPhI, Armenia; ARC, Australia; BMWF and FWF, Austria; ANAS, Azerbaijan; SSTC, Belarus; CNPq and FAPESP, Brazil; NSERC, NRC and CFI, Canada; CERN; CONICYT, Chile; CAS, MOST and NSFC, China; COLCIENCIAS, Colombia; MSMT CR, MPO CR and VSC CR, Czech Republic; DNRF, DNSRC and Lundbeck Foundation, Denmark; EPLANET, ERC and NSRF, European Union; IN2P3-CNRS, CEA-DSM/IRFU, France; GNSF, Georgia; BMBF, DFG, HGF, MPG and AvH Foundation, Germany; GSRT and NSRF, Greece; ISF, MINERVA, GIF, I-CORE and Benozziyo Center, Israel; INFN, Italy; MEXT and JSPS, Japan; CNRST, Morocco; FOM and NWO, Netherlands; BRF and RCN, Norway; MNiSW and NCN, Poland; GRICES and FCT, Portugal; MNE/IFA, Romania; MES of Russia and ROSATOM,

Russian Federation; JINR; MSTD, Serbia; MSSR, Slovakia; ARRS and MIZŠ, Slovenia; DST/NRF, South Africa; MINECO, Spain; SRC and Wallenberg Foundation, Sweden; SER, SNSF and Cantons of Bern and Geneva, Switzerland; NSC, Taiwan; TAEK, Turkey; STFC, the Royal Society and Leverhulme Trust, United Kingdom; DOE and NSF, United States of America.

The crucial computing support from all WLCG partners is acknowledged gratefully, in particular from CERN and the ATLAS Tier-1 facilities at TRIUMF (Canada), NDGF (Denmark, Norway, Sweden), CC-IN2P3 (France), KIT/GridKA (Germany), INFN/CNAF (Italy), NL-T1 (Netherlands), PIC (Spain), ASGC (Taiwan), RAL (UK) and BNL (USA) and in the Tier-2 facilities worldwide.

References

- [1] R. M. Barnett, J. F. Gunion, and H. E. Haber, *Discovering Supersymmetry with Like-sign Dileptons*, *Phys. Lett.* **B 315** (1993) 349, [[hep-ph/9306204](#)].
- [2] J. Alwall, P. Schuster, and N. Toro, *Simplified Models for a First Characterization of New Physics at the LHC*, *Phys. Rev.* **D 79** (2009) 075020, [[arXiv:0810.3921](#)].
- [3] J. C. Pati and A. Salam, *Lepton number as the fourth “color”*, *Phys. Rev.* **D 10** (1974) 275; erratum *ibid.* **D11** (1975) 703.
- [4] R. N. Mohapatra and J. C. Pati, *Left-right gauge symmetry and an “isoconjugate” model of CP violation*, *Phys. Rev.* **D 11** (1975) 566.
- [5] G. Senjanovic and R. N. Mohapatra, *Exact left-right symmetry and spontaneous violation of parity*, *Phys. Rev.* **D 12** (1975) 1502.
- [6] T. G. Rizzo, *Doubly charged Higgs bosons and lepton number violating processes*, *Phys. Rev.* **D 25** (1982) 1355; addendum *ibid.* **27** (1983) 657.
- [7] M. Mühlleitner and M. Spira, *A Note on Doubly-Charged Higgs Pair Production at Hadron Colliders*, *Phys. Rev.* **D 68** (2003) 117701, [[hep-ph/0305288](#)].
- [8] A. G. Akeroyd and M. Aoki, *Single and Pair Production of Doubly Charged Higgs Bosons at Hadron Colliders*, *Phys. Rev.* **D 72** (2005) 035011, [[hep-ph/0506176](#)].
- [9] A. Hektor, M. Kadastik, M. Muntel, M. Raidal, and L. Rebane, *Testing neutrino masses in little Higgs models via discovery of doubly charged Higgs at LHC*, *Nucl. Phys.* **B 787** (2007) 198, [[arXiv:0705.1495](#)].
- [10] P. F. Perez, T. Han, G. Huang, T. Li, and K. Wang, *Testing a Neutrino Mass Generation Mechanism at the LHC*, *Phys. Rev.* **D 78** (2008) 071301, [[arXiv:0803.3450](#)].
- [11] W. Chao, Z. Si, Z. Xing, and S. Zhou, *Correlative signatures of heavy Majorana neutrinos and doubly-charged Higgs bosons at the Large Hadron Collider*, *Phys. Lett.* **B 666** (2008) 451, [[arXiv:0804.1265](#)].
- [12] R. Foot, H. Lew, X.-G. He, and G. C. Joshi, *See-saw neutrino masses induced by a triplet of leptons*, *Z. Phys.* **C 44** (1989) 441.
- [13] R. Franceschini, T. Hambye, and A. Strumia, *Type-III see-saw at LHC*, *Phys. Rev.* **D 78** (2008) 033002, [[arXiv:0805.1613](#)].

- [14] F. del Aguila and J. A. Aguilar-Saavedra, *Distinguishing seesaw models at LHC with multi-lepton signals*, *Nucl.Phys.* **B 813** (2009) 22, [[arXiv:0808.2468](#)].
- [15] R. S. Chivukula, B. A. Dobrescu, H. Georgi, and C. T. Hill, *Top quark seesaw theory of electroweak symmetry breaking*, *Phys. Rev.* **D 59** (1999) 075003, [[hep-ph/9809470](#)].
- [16] C. Anastasiou, E. Furlan, and J. Santiago, *Realistic Composite Higgs Models*, *Phys. Rev.* **D 79** (2009) 075003, [[arXiv:0901.2117](#)].
- [17] K. Kong, M. McCaskey, and G. W. Wilson, *Multi-lepton signals from the top-prime quark at the LHC*, *JHEP* **04** (2012) 079, [[arXiv:1112.3041](#)].
- [18] K. S. Babu and R. N. Mohapatra, *Solution to the strong CP problem without an axion*, *Phys. Rev.* **D 41** (1990) 1286.
- [19] B. Grinstein, M. Redi, and G. Villadoro, *Low scale flavor gauge symmetry*, *JHEP* **11** (2010) 067, [[arXiv:1009.2049](#)].
- [20] M. S. Carena, J. Hubisz, M. Perelstein, and P. Verdier, *Collider signature of T-quarks*, *Phys. Rev.* **D 75** (2007) 091701, [[hep-ph/0610156](#)].
- [21] A. Zee, *Quantum Numbers of Majorana Neutrino Masses*, *Nucl. Phys.* **B 264** (1986) 99.
- [22] K. S. Babu, *Model of ‘Calculable’ Majorana Neutrino Masses*, *Phys. Lett.* **B 203** (1988) 132.
- [23] M. Nebot, J. F. Oliver, D. Palao, and A. Santamaria, *Prospects for the Zee-Babu model at the CERN LHC and low energy experiments*, *Phys. Rev.* **D 77** (2008) 093013, [[arXiv:0711.0483](#)].
- [24] M. Kohda, H. Sugiyama, and K. Tsumura, *Lepton number violation at the LHC with leptiquark and diquark*, *Phys. Lett.* **B 718** (2013) 1436, [[arXiv:1210.5622](#)].
- [25] ATLAS Collaboration, *The ATLAS Experiment at the CERN Large Hadron Collider*, *JINST* **3** (2008) S08003.
- [26] ATLAS Collaboration, *Search for anomalous production of prompt like-sign lepton pairs at $\sqrt{s} = 7$ TeV with the ATLAS detector*, *JHEP* **12** (2012) 007, [[arXiv:1210.4538](#)].
- [27] ATLAS Collaboration, *Search for doubly-charged Higgs bosons in like-sign dilepton final states at $\sqrt{s} = 7$ TeV with the ATLAS detector*, *Eur. Phys. J.* **C 72** (2012) 2244, [[arXiv:1210.5070](#)].
- [28] CDF Collaboration, A. Abulencia et al., *Inclusive Search for New Physics with Like-Sign Dilepton Events in $p\bar{p}$ Collisions at $\sqrt{s} = 1.96$ TeV*, *Phys. Rev. Lett.* **98** (2007) 221803, [[hep-ex/0702051](#)].
- [29] CDF Collaboration, T. Aaltonen et al., *Search for New Physics in High p_T Like-Sign Dilepton Events at CDF II*, *Phys. Rev. Lett.* **107** (2011) 181801, [[arXiv:1108.0101](#)].
- [30] CMS Collaboration, *Search for new physics in events with same-sign dileptons and b jets in pp collisions at $\sqrt{s} = 8$ TeV*, *JHEP* **03** (2013) 037, [[arXiv:1212.6194](#)].
- [31] CMS Collaboration, *Search for new physics in events with same-sign dileptons and jets in pp collisions at $\sqrt{s} = 8$ TeV*, *JHEP* **01** (2014) 163, [[arXiv:1311.6736](#)].
- [32] CMS Collaboration, *Search for heavy Majorana neutrinos in $\mu^+\mu^+[\mu^-\mu^-]+jets$ and $e^+e^+[e^-e^-]+jets$ events in pp collisions at $\sqrt{s} = 7$ TeV*, *Phys. Lett.* **B 717** (2012) 109, [[arXiv:1207.6079](#)].

- [33] ATLAS Collaboration, *Search for supersymmetry at $\sqrt{s} = 8$ TeV in final states with jets and two same-sign leptons or three leptons with the ATLAS detector*, *JHEP* **06** (2014) 035, [[arXiv:1404.2500](#)].
- [34] ATLAS Collaboration, *Search for same-sign top-quark production and fourth-generation down-type quarks in pp collisions at $\sqrt{s} = 7$ TeV with the ATLAS detector*, *JHEP* **04** (2012) 069, [[arXiv:1202.5520](#)].
- [35] ATLAS Collaboration, *Search for strong gravity signatures in same-sign dimuon final states using the ATLAS detector at the LHC*, *Phys. Lett. B* **709** (2012) 322, [[arXiv:1111.0080](#)].
- [36] CMS Collaboration, *A search for a doubly-charged Higgs boson in pp collisions at $\sqrt{s} = 7$ TeV*, *Eur. Phys. J. C* **72** (2012) 2189, [[arXiv:1207.2666](#)].
- [37] ATLAS Collaboration, *Search for new phenomena in events with three or more charged leptons in pp collisions at $\sqrt{s} = 8$ TeV with the ATLAS detector*, [[arXiv:1411.2921](#)].
- [38] B. Jäger, C. Oleari, and D. Zeppenfeld, *Next-to-leading order QCD corrections to W^+W^+jj and W^-W^-jj production via weak-boson fusion*, *Phys. Rev. D* **80** (2009) 034022, [[arXiv:0907.0580](#)].
- [39] T. Gleisberg et al., *Event generation with SHERPA 1.1*, *JHEP* **02** (2009) 007, [[arXiv:0811.4622](#)].
- [40] J. Alwall, M. Herquet, F. Maltoni, O. Mattelaer, and T. Stelzer, *MadGraph/MadEvent v4: The New Web Generation*, *JHEP* **09** (2007) 028, [[arXiv:0706.2334](#)].
- [41] J. Alwall, M. Herquet, F. Maltoni, O. Mattelaer, and T. Stelzer, *MadGraph 5 : Going Beyond*, *JHEP* **06** (2011) 128, [[arXiv:1106.0522](#)].
- [42] T. Sjöstrand, S. Mrenna, and P. Skands, *PYTHIA 6.4 physics and manual*, *JHEP* **05** (2006) 026, [[hep-ph/0603175](#)].
- [43] T. Sjöstrand, S. Mrenna, and P. Skands, *A Brief Introduction to PYTHIA 8.1*, *Comput. Phys. Commun.* **178** (2008) 852, [[arXiv:0710.3820](#)].
- [44] M. L. Mangano et al., *ALPGEN, a generator for hard multiparton processes in hadronic collisions*, *JHEP* **07** (2003) 001, [[hep-ph/0206293](#)].
- [45] S. Frixione, and B. R. Webber, *Matching NLO QCD computations and parton shower simulations*, *JHEP* **06** (2002) 029, [[hep-ph/0204244](#)].
- [46] S. Frixione, F. Stoeckli, P. Torrielli, B. R. Webber, and C. D. White, *The MC@NLO 4.0 Event Generator*, [[arXiv:1010.0819](#)].
- [47] G. Marchesini et al., *HERWIG: a Monte Carlo event generator for simulating hadron emission reactions with interfering gluons. Version 5.1 - april 1991*, *Comput. Phys. Commun.* **67** (1992) 465.
- [48] G. Corcella et al., *HERWIG 6: An Event generator for hadron emission reactions with interfering gluons (including supersymmetric processes)*, *JHEP* **01** (2001) 010, [[hep-ph/0011363](#); [hep-ph/0210213](#)].
- [49] J. M. Butterworth, J. R. Forshaw, and M. H. Seymour, *Multiparton interactions in photoproduction at HERA*, *Z. Phys. C* **72** (1996) 637, [[hep-ph/9601371](#)].
- [50] H. L. Lai et al., *New parton distributions for collider physics*, *Phys. Rev. D* **82** (2010) 074024, [[arXiv:1007.2241](#)].

- [51] J. M. Campbell and R. K. Ellis, *MCFM for the Tevatron and the LHC*, *Nucl. Phys. Proc. Suppl.* (2010) 205, [[arXiv:1007.3492](#)].
- [52] J. Pumplin et al., *New Generation of Parton Distributions with Uncertainties from Global QCD Analysis*, *JHEP* **07** (2002) 012, [[hep-ph/0201195](#)].
- [53] A. Kardos et al., *Top quark pair production in association with a Z-boson at NLO accuracy*, *Phys. Rev. D* **85** (2012) 054015, [[arXiv:1111.0610](#)].
- [54] J. M. Campbell, and R. K. Ellis, *$t\bar{t}W^\pm$ production and decay at NLO*, *JHEP* **07** (2012) 052, [[arXiv:1204.5678](#)].
- [55] S. Catani et al., *Vector boson production at hadron colliders: A fully exclusive QCD calculation at NNLO*, *Phys. Rev. Lett.* **103** (2009) 082001, [[arXiv:0903.2120](#)].
- [56] A. D. Martin, W. J. Stirling, R. S. Thorne, and G. Watt, *Parton distributions for the LHC*, *Eur. Phys. J. C* **63** (2009) 189, [[arXiv:0901.0002](#)].
- [57] M. Cacciari et al., *Top-pair production at hadron colliders with next-to-next-to-leading logarithmic soft-gluon resummation*, *Phys. Lett. B* **710** (2012) 612, [[arXiv:1111.5869](#)].
- [58] P. Bärnreuther, M. Czakon, and A. Mitov, *Percent Level Precision Physics at the Tevatron: First Genuine NNLO QCD Corrections to $q\bar{q} \rightarrow t\bar{t} + X$* , *Phys. Rev. Lett.* **109** (2012) 132001, [[arXiv:1204.5201](#)].
- [59] M. Czakon and A. Mitov, *NNLO corrections to top-pair production at hadron colliders: the all-fermionic scattering channels*, *JHEP* **12** (2012) 054, [[arXiv:1207.0236](#)].
- [60] M. Czakon and A. Mitov, *NNLO corrections to top pair production at hadron colliders: the quark-gluon reaction*, *JHEP* **01** (2013) 080, [[arXiv:1210.6832](#)].
- [61] M. Czakon, P. Fiedler, and A. Mitov, *The total top quark pair production cross-section at hadron colliders through $O(\alpha_s^4)$* , *Phys. Rev. Lett.* **110** (2013) 252004, [[arXiv:1303.6254](#)].
- [62] M. Czakon and A. Mitov, *Top++: A Program for the Calculation of the Top-Pair Cross-Section at Hadron Colliders*, *Comput. Phys. Commun.* **185** (2014) 2930, [[arXiv:1112.5675](#)].
- [63] N. Kidonakis, *NNLL resummation for s-channel single top quark production*, *Phys. Rev. D* **81** (2010) 054028, [[arXiv:1001.5034](#)].
- [64] N. Kidonakis, *Two-loop soft anomalous dimensions for single top quark associated production with a W^- or H^-* , *Phys. Rev. D* **82** (2010) 054018, [[arXiv:1005.4451](#)].
- [65] K. Huitu, J. Maalampi, A. Pietilä and M. Raidal, *Doubly charged Higgs at LHC*, *Nucl. Phys. B* **487** (1997) 27, [[hep-ph/9606311](#)].
- [66] G. Barenboim, *Electroweak precision data and right-handed gauge bosons*, *Eur. Phys. J. C* **1** (1998) 369.
- [67] S. Bar-Shalom, M. Geller, S. Nandi, and A. Soni, *Two Higgs doublets, a 4th generation and a 125 GeV Higgs: a review*, *Adv. High Energy Phys.* **2013** (2013) 672972, [[arXiv:1208.3195](#)].
- [68] S. Agostinelli et al. (GEANT4 Collaboration), *GEANT4: A simulation toolkit*, *Nucl. Instrum. Meth. A* **506** (2003) 250.
- [69] ATLAS Collaboration, *The ATLAS Simulation Infrastructure*, *Eur. Phys. J. C* **70** (2010) 823, [[arXiv:1005.4568](#)].

- [70] ATLAS Collaboration, *The simulation principle and performance of the ATLAS fast calorimeter simulation FastCaloSim*, ATL-PHYS-PUB-2010-013, <http://cds.cern.ch/record/1300517>.
- [71] W. Lampl et al., *Calorimeter Clustering Algorithms: Description and Performance*, ATL-LARG-PUB-2008-002, <http://cdsweb.cern.ch/record/1099735>.
- [72] M. Cacciari, G. P. Salam, and G. Soyez, *The anti- k_t jet clustering algorithm*, *JHEP* **04** (2008) 063, [[arXiv:0802.1189](https://arxiv.org/abs/0802.1189)].
- [73] ATLAS Collaboration, *Jet energy measurement with the ATLAS detector in proton-proton collisions at $\sqrt{s} = 7$ TeV*, *Eur. Phys. J. C* **73** (2013) 2304, [[arXiv:1112.6426](https://arxiv.org/abs/1112.6426)].
- [74] M. Cacciari and G. P. Salam, *Pileup subtraction using jet areas*, *Phys. Lett. B* **659** (2008) 119, [[arXiv:0707.1378](https://arxiv.org/abs/0707.1378)].
- [75] ATLAS Collaboration, *Electron reconstruction and identification efficiency measurements with the ATLAS detector using the 2011 LHC proton-proton collision data*, *Eur. Phys. J. C* **74** (2014) 2941, [[arXiv:1404.2240](https://arxiv.org/abs/1404.2240)].
- [76] ATLAS Collaboration, *Performance of missing transverse momentum reconstruction in proton-proton collisions at 7 TeV with ATLAS*, *Eur. Phys. J. C* **72** (2012) 1844, [[arXiv:1108.5602](https://arxiv.org/abs/1108.5602)].
- [77] ATLAS Collaboration, *Improved luminosity determination in pp collisions at $\sqrt{s} = 7$ TeV using the ATLAS detector at the LHC*, *Eur. Phys. J. C* **73** (2013) 2518, [[arXiv:1302.4393](https://arxiv.org/abs/1302.4393)].
- [78] M. Botje et al., *The PDF4LHC Working Group Interim Recommendations*, [arXiv:1101.0538](https://arxiv.org/abs/1101.0538).
- [79] J. M. Campbell, R. K. Ellis, and C. Williams, *Vector boson pair production at the LHC*, *JHEP* **07** (2011) 018, [[arXiv:1105.0020](https://arxiv.org/abs/1105.0020)].
- [80] M. Garzelli, A. Kardos, C. Papadopoulos, and Z. Trocsanyi, *$t\bar{t}W^\pm$ and $t\bar{t}Z^\pm$ Hadroproduction at NLO accuracy in QCD with Parton Shower and Hadronization effects*, *JHEP* **11** (2012) 056, [[arXiv:1208.2665](https://arxiv.org/abs/1208.2665)].
- [81] A. L. Read, *Presentation of search results: The $CL(s)$ technique*, *J. Phys. G* **28** (2002) 2693.
- [82] ATLAS Collaboration, *Muon reconstruction efficiency and momentum resolution of the ATLAS experiment in proton-proton collisions at $\sqrt{s} = 7$ TeV in 2010*, *Eur. Phys. J. C* **74** (2014) 3034, [[arXiv:1404.4562](https://arxiv.org/abs/1404.4562)].

The ATLAS Collaboration

G. Aad⁸⁴, B. Abbott¹¹², J. Abdallah¹⁵², S. Abdel Khalek¹¹⁶, O. Abdinov¹¹, R. Aben¹⁰⁶, B. Abi¹¹³, M. Abolins⁸⁹, O.S. AbouZeid¹⁵⁹, H. Abramowicz¹⁵⁴, H. Abreu¹⁵³, R. Abreu³⁰, Y. Abulaiti^{147a,147b}, B.S. Acharya^{165a,165b,a}, L. Adamczyk^{38a}, D.L. Adams²⁵, J. Adelman¹⁷⁷, S. Adomeit⁹⁹, T. Adye¹³⁰, T. Agatonovic-Jovin^{13a}, J.A. Aguilar-Saavedra^{125a,125f}, M. Agustoni¹⁷, S.P. Ahlen²², F. Ahmadov^{64,b}, G. Aielli^{134a,134b}, H. Akerstedt^{147a,147b}, T.P.A. Åkesson⁸⁰, G. Akimoto¹⁵⁶, A.V. Akimov⁹⁵, G.L. Alberghi^{20a,20b}, J. Albert¹⁷⁰, S. Albrand⁵⁵, M.J. Alconada Verzini⁷⁰, M. Aleksa³⁰, I.N. Aleksandrov⁶⁴, C. Alexa^{26a}, G. Alexander¹⁵⁴, G. Alexandre⁴⁹, T. Alexopoulos¹⁰, M. Alhroob^{165a,165c}, G. Alimonti^{90a}, L. Alio⁸⁴, J. Alison³¹, B.M.M. Allbrooke¹⁸, L.J. Allison⁷¹, P.P. Allport⁷³, J. Almond⁸³, A. Aloisio^{103a,103b}, A. Alonso³⁶, F. Alonso⁷⁰, C. Alpigiani⁷⁵, A. Altheimer³⁵, B. Alvarez Gonzalez⁸⁹, M.G. Alviggi^{103a,103b}, K. Amako⁶⁵, Y. Amaral Coutinho^{24a}, C. Amelung²³, D. Amidei⁸⁸, S.P. Amor Dos Santos^{125a,125c}, A. Amorim^{125a,125b}, S. Amoroso⁴⁸, N. Amram¹⁵⁴, G. Amundsen²³, C. Anastopoulos¹⁴⁰, L.S. Ancu⁴⁹, N. Andari³⁰, T. Andeen³⁵, C.F. Anders^{58b}, G. Anders³⁰, K.J. Anderson³¹, A. Andreazza^{90a,90b}, V. Andrei^{58a}, X.S. Anduaga⁷⁰, S. Angelidakis⁹, I. Angelozzi¹⁰⁶, P. Anger⁴⁴, A. Angerami³⁵, F. Anghinolfi³⁰, A.V. Anisenkov¹⁰⁸, N. Anjos^{125a}, A. Annovi⁴⁷, A. Antonaki⁹, M. Antonelli⁴⁷, A. Antonov⁹⁷, J. Antos^{145b}, F. Anulli^{133a}, M. Aoki⁶⁵, L. Aperio Bella¹⁸, R. Apolle^{119,c}, G. Arabidze⁸⁹, I. Aracena¹⁴⁴, Y. Arai⁶⁵, J.P. Araque^{125a}, A.T.H. Arce⁴⁵, J-F. Arguin⁹⁴, S. Argyropoulos⁴², M. Arik^{19a}, A.J. Armbruster³⁰, O. Arnaez³⁰, V. Arnal⁸¹, H. Arnold⁴⁸, M. Arratia²⁸, O. Arslan²¹, A. Artamonov⁹⁶, G. Artoni²³, S. Asai¹⁵⁶, N. Asbah⁴², A. Ashkenazi¹⁵⁴, B. Åsman^{147a,147b}, L. Asquith⁶, K. Assamagan²⁵, R. Astalos^{145a}, M. Atkinson¹⁶⁶, N.B. Atlay¹⁴², B. Auerbach⁶, K. Augsten¹²⁷, M. Auresseau^{146b}, G. Avolio³⁰, G. Azuelos^{94,d}, Y. Azuma¹⁵⁶, M.A. Baak³⁰, A. Baas^{58a}, C. Bacci^{135a,135b}, H. Bachacou¹³⁷, K. Bachas¹⁵⁵, M. Backes³⁰, M. Backhaus³⁰, J. Backus Mayes¹⁴⁴, E. Badescu^{26a}, P. Bagiacchi^{133a,133b}, P. Bagnaia^{133a,133b}, Y. Bai^{33a}, T. Bain³⁵, J.T. Baines¹³⁰, O.K. Baker¹⁷⁷, P. Balek¹²⁸, F. Balli¹³⁷, E. Banas³⁹, Sw. Banerjee¹⁷⁴, A.A.E. Bannoura¹⁷⁶, V. Bansal¹⁷⁰, H.S. Bansil¹⁸, L. Barak¹⁷³, S.P. Baranov⁹⁵, E.L. Barberio⁸⁷, D. Barberis^{50a,50b}, M. Barbero⁸⁴, T. Barillari¹⁰⁰, M. Barisonzi¹⁷⁶, T. Barklow¹⁴⁴, N. Barlow²⁸, B.M. Barnett¹³⁰, R.M. Barnett¹⁵, Z. Barnovska⁵, A. Baroncelli^{135a}, G. Barone⁴⁹, A.J. Barr¹¹⁹, F. Barreiro⁸¹, J. Barreiro Guimarães da Costa⁵⁷, R. Bartoldus¹⁴⁴, A.E. Barton⁷¹, P. Bartos^{145a}, V. Bartsch¹⁵⁰, A. Bassalat¹¹⁶, A. Basye¹⁶⁶, R.L. Bates⁵³, J.R. Batley²⁸, M. Battaglia¹³⁸, M. Battistin³⁰, F. Bauer¹³⁷, H.S. Bawa^{144,e}, M.D. Beattie⁷¹, T. Beau⁷⁹, P.H. Beauchemin¹⁶², R. Beccherle^{123a,123b}, P. Bechtel²¹, H.P. Beck¹⁷, K. Becker¹⁷⁶, S. Becker⁹⁹, M. Beckingham¹⁷¹, C. Becot¹¹⁶, A.J. Beddall^{19c}, A. Beddall^{19c}, S. Bedikian¹⁷⁷, V.A. Bednyakov⁶⁴, C.P. Bee¹⁴⁹, L.J. Beemster¹⁰⁶, T.A. Beermann¹⁷⁶, M. Begel²⁵, K. Behr¹¹⁹, C. Belanger-Champagne⁸⁶, P.J. Bell⁴⁹, W.H. Bell⁴⁹, G. Bella¹⁵⁴, L. Bellagamba^{20a}, A. Bellerive²⁹, M. Bellomo⁸⁵, K. Belotskiy⁹⁷, O. Beltramello³⁰, O. Benary¹⁵⁴, D. Bencheikroun^{136a}, K. Bendtz^{147a,147b}, N. Benekos¹⁶⁶, Y. Benhammou¹⁵⁴, E. Benhar Nocchioli⁴⁹, J.A. Benitez Garcia^{160b}, D.P. Benjamin⁴⁵, J.R. Bensinger²³, K. Benslama¹³¹, S. Bentvelsen¹⁰⁶, D. Berge¹⁰⁶,

E. Bergeaas Kuutmann¹⁶, N. Berger⁵, F. Berghaus¹⁷⁰, J. Beringer¹⁵, C. Bernard²²,
 P. Bernat⁷⁷, C. Bernius⁷⁸, F.U. Bernlochner¹⁷⁰, T. Berry⁷⁶, P. Berta¹²⁸, C. Bertella⁸⁴,
 G. Bertoli^{147a,147b}, F. Bertolucci^{123a,123b}, C. Bertsche¹¹², D. Bertsche¹¹², M.I. Besana^{90a},
 G.J. Besjes¹⁰⁵, O. Bessidskaia Bylund^{147a,147b}, M. Bessner⁴², N. Besson¹³⁷,
 C. Betancourt⁴⁸, S. Bethke¹⁰⁰, W. Bhimji⁴⁶, R.M. Bianchi¹²⁴, L. Bianchini²³,
 M. Bianco³⁰, O. Biebel⁹⁹, S.P. Bieniek⁷⁷, K. Bierwagen⁵⁴, J. Biesiada¹⁵, M. Biglietti^{135a},
 J. Bilbao De Mendizabal⁴⁹, H. Bilokon⁴⁷, M. Bindi⁵⁴, S. Binet¹¹⁶, A. Bingul^{19c},
 C. Bini^{133a,133b}, C.W. Black¹⁵¹, J.E. Black¹⁴⁴, K.M. Black²², D. Blackburn¹³⁹,
 R.E. Blair⁶, J.-B. Blanchard¹³⁷, T. Blazek^{145a}, I. Bloch⁴², C. Blocker²³, W. Blum^{82,*},
 U. Blumenschein⁵⁴, G.J. Bobbink¹⁰⁶, V.S. Bobrovnikov¹⁰⁸, S.S. Bocchetta⁸⁰, A. Bocci⁴⁵,
 C. Bock⁹⁹, C.R. Boddy¹¹⁹, M. Boehler⁴⁸, T.T. Boek¹⁷⁶, J.A. Bogaerts³⁰,
 A.G. Bogdanchikov¹⁰⁸, A. Bogouch^{91,*}, C. Bohm^{147a}, J. Bohm¹²⁶, V. Boisvert⁷⁶,
 T. Bold^{38a}, V. Boldea^{26a}, A.S. Boldyrev⁹⁸, M. Bomben⁷⁹, M. Bona⁷⁵, M. Boonekamp¹³⁷,
 A. Borisov¹²⁹, G. Borissov⁷¹, M. Borri⁸³, S. Borroni⁴², J. Bortfeldt⁹⁹,
 V. Bortolotto^{135a,135b}, K. Bos¹⁰⁶, D. Boscherini^{20a}, M. Bosman¹², H. Boterenbrood¹⁰⁶,
 J. Boudreau¹²⁴, J. Bouffard², E.V. Bouhova-Thacker⁷¹, D. Boumediene³⁴,
 C. Bourdarios¹¹⁶, N. Bousson¹¹³, S. Boutouil^{136d}, A. Boveia³¹, J. Boyd³⁰, I.R. Boyko⁶⁴,
 J. Bracinik¹⁸, A. Brandt⁸, G. Brandt¹⁵, O. Brandt^{58a}, U. Bratzler¹⁵⁷, B. Brau⁸⁵,
 J.E. Brau¹¹⁵, H.M. Braun^{176,*}, S.F. Brazzale^{165a,165c}, B. Brelief¹⁵⁹, K. Brendlinger¹²¹,
 A.J. Brennan⁸⁷, R. Brenner¹⁶⁷, S. Bressler¹⁷³, K. Bristow^{146c}, T.M. Bristow⁴⁶,
 D. Britton⁵³, F.M. Brochu²⁸, I. Brock²¹, R. Brock⁸⁹, C. Bromberg⁸⁹, J. Bronner¹⁰⁰,
 G. Brooijmans³⁵, T. Brooks⁷⁶, W.K. Brooks^{32b}, J. Brosamer¹⁵, E. Brost¹¹⁵, J. Brown⁵⁵,
 P.A. Bruckman de Renstrom³⁹, D. Bruncko^{145b}, R. Bruneliere⁴⁸, S. Brunet⁶⁰, A. Bruni^{20a},
 G. Bruni^{20a}, M. Bruschi^{20a}, L. Bryngemark⁸⁰, T. Buanes¹⁴, Q. Buat¹⁴³, F. Bucci⁴⁹,
 P. Buchholz¹⁴², R.M. Buckingham¹¹⁹, A.G. Buckley⁵³, S.I. Buda^{26a}, I.A. Budagov⁶⁴,
 F. Buehrer⁴⁸, L. Bugge¹¹⁸, M.K. Bugge¹¹⁸, O. Bulekov⁹⁷, A.C. Bundock⁷³,
 H. Burckhart³⁰, S. Burdin⁷³, B. Burghgrave¹⁰⁷, S. Burke¹³⁰, I. Burmeister⁴³, E. Busato³⁴,
 D. B"uscher⁴⁸, V. B"uscher⁸², P. Bussey⁵³, C.P. Buszello¹⁶⁷, B. Butler⁵⁷, J.M. Butler²²,
 A.I. Butt³, C.M. Buttar⁵³, J.M. Butterworth⁷⁷, P. Butti¹⁰⁶, W. Buttinger²⁸, A. Buzatu⁵³,
 M. Byszewski¹⁰, S. Cabrera Urb"an¹⁶⁸, D. Caforio^{20a,20b}, O. Cakir^{4a}, P. Calafiura¹⁵,
 A. Calandri¹³⁷, G. Calderini⁷⁹, P. Calfayan⁹⁹, R. Calkins¹⁰⁷, L.P. Caloba^{24a}, D. Calvet³⁴,
 S. Calvet³⁴, R. Camacho Toro⁴⁹, S. Camarda⁴², D. Cameron¹¹⁸, L.M. Caminada¹⁵,
 R. Caminal Armadans¹², S. Campana³⁰, M. Campanelli⁷⁷, A. Campoverde¹⁴⁹,
 V. Canale^{103a,103b}, A. Canepa^{160a}, M. Cano Bret⁷⁵, J. Cantero⁸¹, R. Cantrill^{125a},
 T. Cao⁴⁰, M.D.M. Capeans Garrido³⁰, I. Caprini^{26a}, M. Caprini^{26a}, M. Capua^{37a,37b},
 R. Caputo⁸², R. Cardarelli^{134a}, T. Carli³⁰, G. Carlino^{103a}, L. Carminati^{90a,90b},
 S. Caron¹⁰⁵, E. Carquin^{32a}, G.D. Carrillo-Montoya^{146c}, J.R. Carter²⁸, J. Carvalho^{125a,125c},
 D. Casadei⁷⁷, M.P. Casado¹², M. Casolino¹², E. Castaneda-Miranda^{146b}, A. Castelli¹⁰⁶,
 V. Castillo Gimenez¹⁶⁸, N.F. Castro^{125a}, P. Catastini⁵⁷, A. Catinaccio³⁰,
 J.R. Catmore¹¹⁸, A. Cattai³⁰, G. Cattani^{134a,134b}, S. Caughron⁸⁹, V. Cavaliere¹⁶⁶,
 D. Cavalli^{90a}, M. Cavalli-Sforza¹², V. Cavasinni^{123a,123b}, F. Ceradini^{135a,135b}, B. Cerio⁴⁵,
 K. Cerny¹²⁸, A.S. Cerqueira^{24b}, A. Cerri¹⁵⁰, L. Cerrito⁷⁵, F. Cerutti¹⁵, M. Cerv³⁰,
 A. Cervelli¹⁷, S.A. Cetin^{19b}, A. Chafaq^{136a}, D. Chakraborty¹⁰⁷, I. Chalupkova¹²⁸,

P. Chang¹⁶⁶, B. Chapleau⁸⁶, J.D. Chapman²⁸, D. Charfeddine¹¹⁶, D.G. Charlton¹⁸,
 C.C. Chau¹⁵⁹, C.A. Chavez Barajas¹⁵⁰, S. Cheatham⁸⁶, A. Chegwidan⁸⁹, S. Chekanov⁶,
 S.V. Chekulaev^{160a}, G.A. Chelkov^{64,f}, M.A. Chelstowska⁸⁸, C. Chen⁶³, H. Chen²⁵,
 K. Chen¹⁴⁹, L. Chen^{33d,g}, S. Chen^{33c}, X. Chen^{146c}, Y. Chen⁶⁶, Y. Chen³⁵, H.C. Cheng⁸⁸,
 Y. Cheng³¹, A. Cheplakov⁶⁴, R. Cherkaoui El Moursli^{136e}, V. Chernyatin^{25,*}, E. Cheu⁷,
 L. Chevalier¹³⁷, V. Chiarella⁴⁷, G. Chiefari^{103a,103b}, J.T. Childers⁶, A. Chilingarov⁷¹,
 G. Chiodini^{72a}, A.S. Chisholm¹⁸, R.T. Chislett⁷⁷, A. Chitan^{26a}, M.V. Chizhov⁶⁴,
 S. Chouridou⁹, B.K.B. Chow⁹⁹, D. Chromek-Burckhart³⁰, M.L. Chu¹⁵², J. Chudoba¹²⁶,
 J.J. Chwastowski³⁹, L. Chytka¹¹⁴, G. Ciapetti^{133a,133b}, A.K. Ciftci^{4a}, R. Ciftci^{4a},
 D. Cinca⁵³, V. Cindro⁷⁴, A. Ciocio¹⁵, P. Cirkovic^{13b}, Z.H. Citron¹⁷³, M. Citterio^{90a},
 M. Ciubancan^{26a}, A. Clark⁴⁹, P.J. Clark⁴⁶, R.N. Clarke¹⁵, W. Cleland¹²⁴, J.C. Clemens⁸⁴,
 C. Clement^{147a,147b}, Y. Coadou⁸⁴, M. Cobal^{165a,165c}, A. Coccaro¹³⁹, J. Cochran⁶³,
 L. Coffey²³, J.G. Cogan¹⁴⁴, J. Coggeshall¹⁶⁶, B. Cole³⁵, S. Cole¹⁰⁷, A.P. Colijn¹⁰⁶,
 J. Collot⁵⁵, T. Colombo^{58c}, G. Colon⁸⁵, G. Compostella¹⁰⁰, P. Conde Muiño^{125a,125b},
 E. Coniavitis⁴⁸, M.C. Conidi¹², S.H. Connell^{146b}, I.A. Connelly⁷⁶, S.M. Consonni^{90a,90b},
 V. Consorti⁴⁸, S. Constantinescu^{26a}, C. Conta^{120a,120b}, G. Conti⁵⁷, F. Conventi^{103a,h},
 M. Cooke¹⁵, B.D. Cooper⁷⁷, A.M. Cooper-Sarkar¹¹⁹, N.J. Cooper-Smith⁷⁶, K. Copic¹⁵,
 T. Cornelissen¹⁷⁶, M. Corradi^{20a}, F. Corriveau^{86,i}, A. Corso-Radu¹⁶⁴,
 A. Cortes-Gonzalez¹², G. Cortiana¹⁰⁰, G. Costa^{90a}, M.J. Costa¹⁶⁸, D. Costanzo¹⁴⁰,
 D. Côté⁸, G. Cottin²⁸, G. Cowan⁷⁶, B.E. Cox⁸³, K. Cranmer¹⁰⁹, G. Cree²⁹,
 S. Crépe-Renaudin⁵⁵, F. Crescioli⁷⁹, W.A. Cribbs^{147a,147b}, M. Crispin Ortuzar¹¹⁹,
 M. Cristinziani²¹, V. Croft¹⁰⁵, G. Crosetti^{37a,37b}, C.-M. Cuciuc^{26a},
 T. Cuhadar Donszelmann¹⁴⁰, J. Cummings¹⁷⁷, M. Curatolo⁴⁷, C. Cuthbert¹⁵¹,
 H. Czirr¹⁴², P. Czodrowski³, Z. Czyczula¹⁷⁷, S. D'Auria⁵³, M. D'Onofrio⁷³,
 M.J. Da Cunha Sargedas De Sousa^{125a,125b}, C. Da Via⁸³, W. Dabrowski^{38a}, A. Dafinca¹¹⁹,
 T. Dai⁸⁸, O. Dale¹⁴, F. Dallaire⁹⁴, C. Dallapiccola⁸⁵, M. Dam³⁶, A.C. Daniells¹⁸,
 M. Dano Hoffmann¹³⁷, V. Dao⁴⁸, G. Darbo^{50a}, S. Darmora⁸, J.A. Dassoulas⁴²,
 A. Dattagupta⁶⁰, W. Davey²¹, C. David¹⁷⁰, T. Davidek¹²⁸, E. Davies^{119,c}, M. Davies¹⁵⁴,
 O. Davignon⁷⁹, A.R. Davison⁷⁷, P. Davison⁷⁷, Y. Davygora^{58a}, E. Dawe¹⁴³, I. Dawson¹⁴⁰,
 R.K. Daya-Ishmukhametova⁸⁵, K. De⁸, R. de Asmundis^{103a}, S. De Castro^{20a,20b},
 S. De Cecco⁷⁹, N. De Groot¹⁰⁵, P. de Jong¹⁰⁶, H. De la Torre⁸¹, F. De Lorenzi⁶³,
 L. De Nooij¹⁰⁶, D. De Pedis^{133a}, A. De Salvo^{133a}, U. De Sanctis^{165a,165b}, A. De Santo¹⁵⁰,
 J.B. De Vivie De Regie¹¹⁶, W.J. Dearnaley⁷¹, R. Debbé²⁵, C. Debenedetti¹³⁸,
 B. Dechenaux⁵⁵, D.V. Dedovich⁶⁴, I. Deigaard¹⁰⁶, J. Del Peso⁸¹, T. Del Prete^{123a,123b},
 F. Deliot¹³⁷, C.M. Delitzsch⁴⁹, M. Deliyergiyev⁷⁴, A. Dell'Acqua³⁰, L. Dell'Asta²²,
 M. Dell'Orso^{123a,123b}, M. Della Pietra^{103a,h}, D. della Volpe⁴⁹, M. Delmastro⁵,
 P.A. Delsart⁵⁵, C. Deluca¹⁰⁶, S. Demers¹⁷⁷, M. Demichev⁶⁴, A. Demilly⁷⁹, S.P. Denisov¹²⁹,
 D. Derendarz³⁹, J.E. Derkaoui^{136d}, F. Derue⁷⁹, P. Dervan⁷³, K. Desch²¹, C. Deterre⁴²,
 P.O. Deviveiros¹⁰⁶, A. Dewhurst¹³⁰, S. Dhaliwal¹⁰⁶, A. Di Ciaccio^{134a,134b}, L. Di Ciaccio⁵,
 A. Di Domenico^{133a,133b}, C. Di Donato^{103a,103b}, A. Di Girolamo³⁰, B. Di Girolamo³⁰,
 A. Di Mattia¹⁵³, B. Di Micco^{135a,135b}, R. Di Nardo⁴⁷, A. Di Simone⁴⁸, R. Di Sipio^{20a,20b},
 D. Di Valentino²⁹, F.A. Dias⁴⁶, M.A. Diaz^{32a}, E.B. Diehl⁸⁸, J. Dietrich⁴²,
 T.A. Dietzsch^{58a}, S. Diglio⁸⁴, A. Dimitrievska^{13a}, J. Dingfelder²¹, C. Dionisi^{133a,133b},

P. Dita^{26a}, S. Dita^{26a}, F. Dittus³⁰, F. Djama⁸⁴, T. Djobava^{51b}, M.A.B. do Vale^{24c},
 A. Do Valle Wemans^{125a,125g}, T.K.O. Doan⁵, D. Dobos³⁰, C. Doglioni⁴⁹, T. Doherty⁵³,
 T. Dohmae¹⁵⁶, J. Dolejsi¹²⁸, Z. Dolezal¹²⁸, B.A. Dolgoshein^{97,*}, M. Donadelli^{24d},
 S. Donati^{123a,123b}, P. Dondero^{120a,120b}, J. Donini³⁴, J. Dopke¹³⁰, A. Doria^{103a},
 M.T. Dova⁷⁰, A.T. Doyle⁵³, M. Dris¹⁰, J. Dubbert⁸⁸, S. Dube¹⁵, E. Dubreuil³⁴,
 E. Duchovni¹⁷³, G. Duckeck⁹⁹, O.A. Ducu^{26a}, D. Duda¹⁷⁶, A. Dudarev³⁰, F. Dudziak⁶³,
 L. Duflot¹¹⁶, L. Duguid⁷⁶, M. Dührssen³⁰, M. Dunford^{58a}, H. Duran Yildiz^{4a}, M. Düren⁵²,
 A. Durglishvili^{51b}, M. Dwuznik^{38a}, M. Dyndal^{38a}, J. Ebke⁹⁹, W. Edson², N.C. Edwards⁴⁶,
 W. Ehrenfeld²¹, T. Eifert¹⁴⁴, G. Eigen¹⁴, K. Einsweiler¹⁵, T. Ekelof¹⁶⁷, M. El Kacimi^{136c},
 M. Ellert¹⁶⁷, S. Elles⁵, F. Ellinghaus⁸², N. Ellis³⁰, J. Elmsheuser⁹⁹, M. Elsing³⁰,
 D. Emelianov¹³⁰, Y. Enari¹⁵⁶, O.C. Endner⁸², M. Endo¹¹⁷, R. Engelmann¹⁴⁹,
 J. Erdmann¹⁷⁷, A. Ereditato¹⁷, D. Eriksson^{147a}, G. Ernis¹⁷⁶, J. Ernst², M. Ernst²⁵,
 J. Ernwein¹³⁷, D. Errede¹⁶⁶, S. Errede¹⁶⁶, E. Ertel⁸², M. Escalier¹¹⁶, H. Esch⁴³,
 C. Escobar¹²⁴, B. Esposito⁴⁷, A.I. Etienvre¹³⁷, E. Etzion¹⁵⁴, H. Evans⁶⁰, A. Ezhilov¹²²,
 L. Fabbri^{20a,20b}, G. Facini³¹, R.M. Fakhrutdinov¹²⁹, S. Falciano^{133a}, R.J. Falla⁷⁷,
 J. Faltova¹²⁸, Y. Fang^{33a}, M. Fanti^{90a,90b}, A. Farbin⁸, A. Farilla^{135a}, T. Farooque¹²,
 S. Farrell¹⁵, S.M. Farrington¹⁷¹, P. Farthouat³⁰, F. Fassi^{136e}, P. Fassnacht³⁰,
 D. Fassouliotis⁹, A. Favareto^{50a,50b}, L. Fayard¹¹⁶, P. Federic^{145a}, O.L. Fedin^{122,j},
 W. Fedorko¹⁶⁹, M. Fehling-Kaschek⁴⁸, S. Feigl³⁰, L. Feligioni⁸⁴, C. Feng^{33d}, E.J. Feng⁶,
 H. Feng⁸⁸, A.B. Fenyuk¹²⁹, S. Fernandez Perez³⁰, S. Ferrag⁵³, J. Ferrando⁵³,
 A. Ferrari¹⁶⁷, P. Ferrari¹⁰⁶, R. Ferrari^{120a}, D.E. Ferreira de Lima⁵³, A. Ferrer¹⁶⁸,
 D. Ferrere⁴⁹, C. Ferretti⁸⁸, A. Ferretto Parodi^{50a,50b}, M. Fiascaris³¹, F. Fiedler⁸²,
 A. Filipčić⁷⁴, M. Filipuzzi⁴², F. Filthaut¹⁰⁵, M. Fincke-Keeler¹⁷⁰, K.D. Finelli¹⁵¹,
 M.C.N. Fiolhais^{125a,125c}, L. Fiorini¹⁶⁸, A. Firan⁴⁰, A. Fischer², J. Fischer¹⁷⁶,
 W.C. Fisher⁸⁹, E.A. Fitzgerald²³, M. Flechl⁴⁸, I. Fleck¹⁴², P. Fleischmann⁸⁸,
 S. Fleischmann¹⁷⁶, G.T. Fletcher¹⁴⁰, G. Fletcher⁷⁵, T. Flick¹⁷⁶, A. Floderus⁸⁰,
 L.R. Flores Castillo^{174,k}, A.C. Florez Bustos^{160b}, M.J. Flowerdew¹⁰⁰, A. Formica¹³⁷,
 A. Forti⁸³, D. Fortin^{160a}, D. Fournier¹¹⁶, H. Fox⁷¹, S. Fracchia¹², P. Francavilla⁷⁹,
 M. Franchini^{20a,20b}, S. Franchino³⁰, D. Francis³⁰, L. Franconi¹¹⁸, M. Franklin⁵⁷,
 S. Franz⁶¹, M. Fraternali^{120a,120b}, S.T. French²⁸, C. Friedrich⁴², F. Friedrich⁴⁴,
 D. Froidevaux³⁰, J.A. Frost²⁸, C. Fukunaga¹⁵⁷, E. Fullana Torregrosa⁸², B.G. Fulson¹⁴⁴,
 J. Fuster¹⁶⁸, C. Gabaldon⁵⁵, O. Gabizon¹⁷³, A. Gabrielli^{20a,20b}, A. Gabrielli^{133a,133b},
 S. Gadatsch¹⁰⁶, S. Gadomski⁴⁹, G. Gagliardi^{50a,50b}, P. Gagnon⁶⁰, C. Galea¹⁰⁵,
 B. Galhardo^{125a,125c}, E.J. Gallas¹¹⁹, V. Gallo¹⁷, B.J. Gallop¹³⁰, P. Gallus¹²⁷, G. Galster³⁶,
 K.K. Gan¹¹⁰, J. Gao^{33b,g}, Y.S. Gao^{144,e}, F.M. Garay Walls⁴⁶, F. Garbersson¹⁷⁷,
 C. García¹⁶⁸, J.E. García Navarro¹⁶⁸, M. Garcia-Sciveres¹⁵, R.W. Gardner³¹,
 N. Garelli¹⁴⁴, V. Garonne³⁰, C. Gatti⁴⁷, G. Gaudio^{120a}, B. Gaur¹⁴², L. Gauthier⁹⁴,
 P. Gauzzi^{133a,133b}, I.L. Gavrilenko⁹⁵, C. Gay¹⁶⁹, G. Gaycken²¹, E.N. Gazis¹⁰, P. Ge^{33d},
 Z. Gece¹⁶⁹, C.N.P. Gee¹³⁰, D.A.A. Geerts¹⁰⁶, Ch. Geich-Gimbel²¹,
 K. Gellerstedt^{147a,147b}, C. Gemme^{50a}, A. Gemmell⁵³, M.H. Genest⁵⁵, S. Gentile^{133a,133b},
 M. George⁵⁴, S. George⁷⁶, D. Gerbaudo¹⁶⁴, A. Gershon¹⁵⁴, H. Ghazlane^{136b},
 N. Ghodbane³⁴, B. Giacobbe^{20a}, S. Giagu^{133a,133b}, V. Giangiobbe¹², P. Giannetti^{123a,123b},
 F. Gianotti³⁰, B. Gibbard²⁵, S.M. Gibson⁷⁶, M. Gilchriese¹⁵, T.P.S. Gillam²⁸,

D. Gillberg³⁰, G. Gilles³⁴, D.M. Gingrich^{3,d}, N. Giokaris⁹, M.P. Giordani^{165a,165c},
 R. Giordano^{103a,103b}, F.M. Giorgi^{20a}, F.M. Giorgi¹⁶, P.F. Giraud¹³⁷, D. Giugni^{90a},
 C. Giuliani⁴⁸, M. Giuliani^{58b}, B.K. Gjelsten¹¹⁸, S. Gkaitatzis¹⁵⁵, I. Gkialas^{155,l},
 L.K. Gladilin⁹⁸, C. Glasman⁸¹, J. Glatzer³⁰, P.C.F. Glaysher⁴⁶, A. Glazov⁴²,
 G.L. Glonti⁶⁴, M. Goblirsch-Kolb¹⁰⁰, J.R. Goddard⁷⁵, J. Godfrey¹⁴³, J. Godlewski³⁰,
 C. Goeringer⁸², S. Goldfarb⁸⁸, T. Golling¹⁷⁷, D. Golubkov¹²⁹, A. Gomes^{125a,125b,125d},
 L.S. Gomez Fajardo⁴², R. Gonçalo^{125a}, J. Goncalves Pinto Firmino Da Costa¹³⁷,
 L. Gonella²¹, S. González de la Hoz¹⁶⁸, G. Gonzalez Parra¹², S. Gonzalez-Sevilla⁴⁹,
 L. Goossens³⁰, P.A. Gorbounov⁹⁶, H.A. Gordon²⁵, I. Gorelov¹⁰⁴, B. Gorini³⁰,
 E. Gorini^{72a,72b}, A. Gorišek⁷⁴, E. Gornicki³⁹, A.T. Goshaw⁶, C. Gössling⁴³,
 M.I. Gostkin⁶⁴, M. Goughri^{136a}, D. Goujdami^{136c}, M.P. Goulette⁴⁹, A.G. Goussiou¹³⁹,
 C. Goy⁵, S. Gozpinar²³, H.M.X. Grabas¹³⁷, L. Graber⁵⁴, I. Grabowska-Bold^{38a},
 P. Grafström^{20a,20b}, K.-J. Grahn⁴², J. Gramling⁴⁹, E. Gramstad¹¹⁸, S. Grancagnolo¹⁶,
 V. Grassi¹⁴⁹, V. Gratchev¹²², H.M. Gray³⁰, E. Graziani^{135a}, O.G. Grebenyuk¹²²,
 Z.D. Greenwood^{78,m}, K. Gregersen⁷⁷, I.M. Gregor⁴², P. Grenier¹⁴⁴, J. Griffiths⁸,
 A.A. Grillo¹³⁸, K. Grimm⁷¹, S. Grinstein^{12,n}, Ph. Gris³⁴, Y.V. Grishkevich⁹⁸,
 J.-F. Grivaz¹¹⁶, J.P. Grohs⁴⁴, A. Grohsjean⁴², E. Gross¹⁷³, J. Grosse-Knetter⁵⁴,
 G.C. Grossi^{134a,134b}, J. Groth-Jensen¹⁷³, Z.J. Grout¹⁵⁰, L. Guan^{33b}, F. Guescini⁴⁹,
 D. Guest¹⁷⁷, O. Gueta¹⁵⁴, C. Guicheney³⁴, E. Guido^{50a,50b}, T. Guillemin¹¹⁶, S. Guindon²,
 U. Gul⁵³, C. Gumpert⁴⁴, J. Gunther¹²⁷, J. Guo³⁵, S. Gupta¹¹⁹, P. Gutierrez¹¹²,
 N.G. Gutierrez Ortiz⁵³, C. Gutsche⁷⁷, N. Guttman¹⁵⁴, C. Guyot¹³⁷, C. Gwenlan¹¹⁹,
 C.B. Gwilliam⁷³, A. Haas¹⁰⁹, C. Haber¹⁵, H.K. Hadavand⁸, N. Haddad^{136e}, P. Haefner²¹,
 S. Hageböck²¹, Z. Hajduk³⁹, H. Hakobyan¹⁷⁸, M. Haleem⁴², D. Hall¹¹⁹, G. Halladjian⁸⁹,
 K. Hamacher¹⁷⁶, P. Hamal¹¹⁴, K. Hamano¹⁷⁰, M. Hamer⁵⁴, A. Hamilton^{146a},
 S. Hamilton¹⁶², G.N. Hamity^{146c}, P.G. Hamnett⁴², L. Han^{33b}, K. Hanagaki¹¹⁷,
 K. Hanawa¹⁵⁶, M. Hance¹⁵, P. Hanke^{58a}, R. Hanna¹³⁷, J.B. Hansen³⁶, J.D. Hansen³⁶,
 P.H. Hansen³⁶, K. Hara¹⁶¹, A.S. Hard¹⁷⁴, T. Harenberg¹⁷⁶, F. Hariri¹¹⁶, S. Harkusha⁹¹,
 D. Harper⁸⁸, R.D. Harrington⁴⁶, O.M. Harris¹³⁹, P.F. Harrison¹⁷¹, F. Hartjes¹⁰⁶,
 M. Hasegawa⁶⁶, S. Hasegawa¹⁰², Y. Hasegawa¹⁴¹, A. Hasib¹¹², S. Hassani¹³⁷, S. Haug¹⁷,
 M. Hauschild³⁰, R. Hauser⁸⁹, M. Havranek¹²⁶, C.M. Hawkes¹⁸, R.J. Hawkings³⁰,
 A.D. Hawkins⁸⁰, T. Hayashi¹⁶¹, D. Hayden⁸⁹, C.P. Hays¹¹⁹, H.S. Hayward⁷³,
 S.J. Haywood¹³⁰, S.J. Head¹⁸, T. Heck⁸², V. Hedberg⁸⁰, L. Heelan⁸, S. Heim¹²¹,
 T. Heim¹⁷⁶, B. Heinemann¹⁵, L. Heinrich¹⁰⁹, J. Hejbal¹²⁶, L. Helary²², I.R. Helgadottir⁸⁰,
 C. Heller⁹⁹, M. Heller³⁰, S. Hellman^{147a,147b}, D. Hellmich²¹, C. Helsen³⁰,
 J. Henderson¹¹⁹, R.C.W. Henderson⁷¹, Y. Heng¹⁷⁴, C. Hengler⁴², A. Henrichs¹⁷⁷,
 A.M. Henriques Correia³⁰, S. Henrot-Versille¹¹⁶, C. Hensel⁵⁴, G.H. Herbert¹⁶,
 Y. Hernández Jiménez¹⁶⁸, R. Herrberg-Schubert¹⁶, G. Herten⁴⁸, R. Hertenberger⁹⁹,
 L. Hervas³⁰, G.G. Hesketh⁷⁷, N.P. Hessey¹⁰⁶, R. Hickling⁷⁵, E. Higón-Rodriguez¹⁶⁸,
 E. Hill¹⁷⁰, J.C. Hill²⁸, K.H. Hiller⁴², S. Hillert²¹, S.J. Hillier¹⁸, I. Hinchliffe¹⁵, E. Hines¹²¹,
 M. Hirose¹⁵⁸, D. Hirschbuehl¹⁷⁶, J. Hobbs¹⁴⁹, N. Hod¹⁰⁶, M.C. Hodgkinson¹⁴⁰,
 P. Hodgson¹⁴⁰, A. Hoecker³⁰, M.R. Hoferkamp¹⁰⁴, F. Hoenig⁹⁹, J. Hoffman⁴⁰,
 D. Hoffmann⁸⁴, J.I. Hofmann^{58a}, M. Hohlfeld⁸², T.R. Holmes¹⁵, T.M. Hong¹²¹,
 L. Hooft van Huysduynen¹⁰⁹, Y. Horii¹⁰², J.-Y. Hostachy⁵⁵, S. Hou¹⁵², A. Hoummada^{136a},

J. Howard¹¹⁹, J. Howarth⁴², M. Hrabovsky¹¹⁴, I. Hristova¹⁶, J. Hrivnac¹¹⁶, T. Hryn'ova⁵,
 C. Hsu^{146c}, P.J. Hsu⁸², S.-C. Hsu¹³⁹, D. Hu³⁵, X. Hu²⁵, Y. Huang⁴², Z. Hubacek³⁰,
 F. Hubaut⁸⁴, F. Huegging²¹, T.B. Huffman¹¹⁹, E.W. Hughes³⁵, G. Hughes⁷¹,
 M. Huhtinen³⁰, T.A. Hülsing⁸², M. Hurwitz¹⁵, N. Huseynov^{64,b}, J. Huston⁸⁹, J. Huth⁵⁷,
 G. Iacobucci⁴⁹, G. Iakovidis¹⁰, I. Ibragimov¹⁴², L. Iconomidou-Fayard¹¹⁶, E. Ideal¹⁷⁷,
 P. Iengo^{103a}, O. Igonkina¹⁰⁶, T. Iizawa¹⁷², Y. Ikegami⁶⁵, K. Ikematsu¹⁴², M. Ikeno⁶⁵,
 Y. Ilchenko^{31,o}, D. Iliadis¹⁵⁵, N. Ilic¹⁵⁹, Y. Inamaru⁶⁶, T. Ince¹⁰⁰, P. Ioannou⁹,
 M. Iodice^{135a}, K. Iordanidou⁹, V. Ippolito⁵⁷, A. Irles Quiles¹⁶⁸, C. Isaksson¹⁶⁷,
 M. Ishino⁶⁷, M. Ishitsuka¹⁵⁸, R. Ishmukhametov¹¹⁰, C. Issever¹¹⁹, S. Istin^{19a},
 J.M. Iturbe Ponce⁸³, R. Iuppa^{134a,134b}, J. Ivarsson⁸⁰, W. Iwanski³⁹, H. Iwasaki⁶⁵,
 J.M. Izen⁴¹, V. Izzo^{103a}, B. Jackson¹²¹, M. Jackson⁷³, P. Jackson¹, M.R. Jaekel³⁰,
 V. Jain², K. Jakobs⁴⁸, S. Jakobsen³⁰, T. Jakoubek¹²⁶, J. Jakubek¹²⁷, D.O. Jamin¹⁵²,
 D.K. Jana⁷⁸, E. Jansen⁷⁷, H. Jansen³⁰, J. Janssen²¹, M. Janus¹⁷¹, G. Jarlskog⁸⁰,
 N. Javadov^{64,b}, T. Javůrek⁴⁸, L. Jeanty¹⁵, J. Jejelava^{51a,p}, G.-Y. Jeng¹⁵¹, D. Jennens⁸⁷,
 P. Jenni^{48,q}, J. Jentzsch⁴³, C. Jeske¹⁷¹, S. Jézéquel⁵, H. Ji¹⁷⁴, J. Jia¹⁴⁹, Y. Jiang^{33b},
 M. Jimenez Belenguer⁴², S. Jin^{33a}, A. Jinaru^{26a}, O. Jinnouchi¹⁵⁸, M.D. Joergensen³⁶,
 K.E. Johansson^{147a,147b}, P. Johansson¹⁴⁰, K.A. Johns⁷, K. Jon-And^{147a,147b}, G. Jones¹⁷¹,
 R.W.L. Jones⁷¹, T.J. Jones⁷³, J. Jongmanns^{58a}, P.M. Jorge^{125a,125b}, K.D. Joshi⁸³,
 J. Jovicevic¹⁴⁸, X. Ju¹⁷⁴, C.A. Jung⁴³, R.M. Jungst³⁰, P. Jussel⁶¹, A. Juste Rozas^{12,n},
 M. Kaci¹⁶⁸, A. Kaczmarzka³⁹, M. Kado¹¹⁶, H. Kagan¹¹⁰, M. Kagan¹⁴⁴, E. Kajomovitz⁴⁵,
 C.W. Kalderon¹¹⁹, S. Kama⁴⁰, A. Kamenshchikov¹²⁹, N. Kanaya¹⁵⁶, M. Kaneda³⁰,
 S. Kaneti²⁸, V.A. Kantserov⁹⁷, J. Kanzaki⁶⁵, B. Kaplan¹⁰⁹, A. Kapliy³¹, D. Kar⁵³,
 K. Karakostas¹⁰, N. Karastathis¹⁰, M. Karnevskiy⁸², S.N. Karpov⁶⁴, Z.M. Karpova⁶⁴,
 K. Karthik¹⁰⁹, V. Kartvelishvili⁷¹, A.N. Karyukhin¹²⁹, L. Kashif¹⁷⁴, G. Kasieczka^{58b},
 R.D. Kass¹¹⁰, A. Kastanas¹⁴, Y. Kataoka¹⁵⁶, A. Katre⁴⁹, J. Katzy⁴², V. Kaushik⁷,
 K. Kawagoe⁶⁹, T. Kawamoto¹⁵⁶, G. Kawamura⁵⁴, S. Kazama¹⁵⁶, V.F. Kazanin¹⁰⁸,
 M.Y. Kazarinov⁶⁴, R. Keeler¹⁷⁰, R. Kehoe⁴⁰, M. Keil⁵⁴, J.S. Keller⁴², J.J. Kempster⁷⁶,
 H. Keoshkerian⁵, O. Kepka¹²⁶, B.P. Kerševan⁷⁴, S. Kersten¹⁷⁶, K. Kessoku¹⁵⁶,
 J. Keung¹⁵⁹, F. Khalil-zada¹¹, H. Khandanyan^{147a,147b}, A. Khanov¹¹³, A. Khodinov⁹⁷,
 A. Khomich^{58a}, T.J. Khoo²⁸, G. Khoriauli²¹, A. Khoroshilov¹⁷⁶, V. Khovanskiy⁹⁶,
 E. Khramov⁶⁴, J. Khubua^{51b}, H.Y. Kim⁸, H. Kim^{147a,147b}, S.H. Kim¹⁶¹, N. Kimura¹⁷²,
 O. Kind¹⁶, B.T. King⁷³, M. King¹⁶⁸, R.S.B. King¹¹⁹, S.B. King¹⁶⁹, J. Kirk¹³⁰,
 A.E. Kiryunin¹⁰⁰, T. Kishimoto⁶⁶, D. Kisielevska^{38a}, F. Kiss⁴⁸, T. Kittelmann¹²⁴,
 K. Kiuchi¹⁶¹, E. Kladiva^{145b}, M. Klein⁷³, U. Klein⁷³, K. Kleinknecht⁸², P. Klimek^{147a,147b},
 A. Klimentov²⁵, R. Klingenberg⁴³, J.A. Klinger⁸³, T. Klioutchnikova³⁰, P.F. Klok¹⁰⁵,
 E.-E. Kluge^{58a}, P. Kluit¹⁰⁶, S. Kluth¹⁰⁰, E. Kneringer⁶¹, E.B.F.G. Knoop⁸⁴, A. Knue⁵³,
 D. Kobayashi¹⁵⁸, T. Kobayashi¹⁵⁶, M. Kobel⁴⁴, M. Kocian¹⁴⁴, P. Kodys¹²⁸,
 P. Koesesarki²¹, T. Koffas²⁹, E. Koffeman¹⁰⁶, L.A. Kogan¹¹⁹, S. Kohlmann¹⁷⁶,
 Z. Kohout¹²⁷, T. Kohriki⁶⁵, T. Koi¹⁴⁴, H. Kolanoski¹⁶, I. Koletsou⁵, J. Koll⁸⁹,
 A.A. Komar^{95,*}, Y. Komori¹⁵⁶, T. Kondo⁶⁵, N. Kondrashova⁴², K. Köneke⁴⁸,
 A.C. König¹⁰⁵, S. König⁸², T. Kono^{65,r}, R. Konoplich^{109,s}, N. Konstantinidis⁷⁷,
 R. Kopeliainsky¹⁵³, S. Koperny^{38a}, L. Köpke⁸², A.K. Kopp⁴⁸, K. Korcyl³⁹, K. Kordas¹⁵⁵,
 A. Korn⁷⁷, A.A. Korol^{108,t}, I. Korolkov¹², E.V. Korolkova¹⁴⁰, V.A. Korotkov¹²⁹,

O. Kortner¹⁰⁰, S. Kortner¹⁰⁰, V.V. Kostyukhin²¹, V.M. Kotov⁶⁴, A. Kotwal⁴⁵,
 C. Kourkoumelis⁹, V. Kouskoura¹⁵⁵, A. Koutsman^{160a}, R. Kowalewski¹⁷⁰,
 T.Z. Kowalski^{38a}, W. Kozanecki¹³⁷, A.S. Kozhin¹²⁹, V. Kral¹²⁷, V.A. Kramarenko⁹⁸,
 G. Kramberger⁷⁴, D. Krasnopevtsev⁹⁷, M.W. Krasny⁷⁹, A. Krasznahorkay³⁰,
 J.K. Kraus²¹, A. Kravchenko²⁵, S. Kreiss¹⁰⁹, M. Kretz^{58c}, J. Kretzschmar⁷³,
 K. Kreutzfeldt⁵², P. Krieger¹⁵⁹, K. Kroeninger⁵⁴, H. Kroha¹⁰⁰, J. Kroll¹²¹, J. Kroseberg²¹,
 J. Krstic^{13a}, U. Kruchonak⁶⁴, H. Krüger²¹, T. Kruker¹⁷, N. Krumnack⁶³,
 Z.V. Krumshteyn⁶⁴, A. Kruse¹⁷⁴, M.C. Kruse⁴⁵, M. Kruskal²², T. Kubota⁸⁷, S. Kuday^{4a},
 S. Kuehn⁴⁸, A. Kugel^{58c}, A. Kuhl¹³⁸, T. Kuhl⁴², V. Kukhtin⁶⁴, Y. Kulchitsky⁹¹,
 S. Kuleshov^{32b}, M. Kuna^{133a,133b}, J. Kunkle¹²¹, A. Kupco¹²⁶, H. Kurashige⁶⁶,
 Y.A. Kurochkin⁹¹, R. Kurumida⁶⁶, V. Kus¹²⁶, E.S. Kuwertz¹⁴⁸, M. Kuze¹⁵⁸, J. Kvita¹¹⁴,
 A. La Rosa⁴⁹, L. La Rotonda^{37a,37b}, C. Lacasta¹⁶⁸, F. Lacava^{133a,133b}, J. Lacey²⁹,
 H. Lacker¹⁶, D. Lacour⁷⁹, V.R. Lacuesta¹⁶⁸, E. Ladygin⁶⁴, R. Lafaye⁵, B. Laforge⁷⁹,
 T. Lagouri¹⁷⁷, S. Lai⁴⁸, H. Laier^{58a}, L. Lambourne⁷⁷, S. Lammers⁶⁰, C.L. Lampen⁷,
 W. Lampl⁷, E. Lançon¹³⁷, U. Landgraf⁴⁸, M.P.J. Landon⁷⁵, V.S. Lang^{58a},
 A.J. Lankford¹⁶⁴, F. Lanni²⁵, K. Lantzsck³⁰, S. Laplace⁷⁹, C. Lapoire²¹, J.F. Laporte¹³⁷,
 T. Lari^{90a}, M. Lassnig³⁰, P. Laurelli⁴⁷, W. Lavrijsen¹⁵, A.T. Law¹³⁸, P. Laycock⁷³,
 O. Le Dortz⁷⁹, E. Le Guirriec⁸⁴, E. Le Menedeu¹², T. LeCompte⁶, F. Ledroit-Guillon⁵⁵,
 C.A. Lee¹⁵², H. Lee¹⁰⁶, J.S.H. Lee¹¹⁷, S.C. Lee¹⁵², L. Lee¹, G. Lefebvre⁷⁹, M. Lefebvre¹⁷⁰,
 F. Legger⁹⁹, C. Leggett¹⁵, A. Lehan⁷³, M. Lehmacher²¹, G. Lehmann Miotto³⁰, X. Lei⁷,
 W.A. Leight²⁹, A. Leisos¹⁵⁵, A.G. Leister¹⁷⁷, M.A.L. Leite^{24d}, R. Leitner¹²⁸,
 D. Lellouch¹⁷³, B. Lemmer⁵⁴, K.J.C. Leney⁷⁷, T. Lenz²¹, G. Lenzen¹⁷⁶, B. Lenzi³⁰,
 R. Leone⁷, S. Leone^{123a,123b}, K. Leonhardt⁴⁴, C. Leonidopoulos⁴⁶, S. Leontsinis¹⁰,
 C. Leroy⁹⁴, C.G. Lester²⁸, C.M. Lester¹²¹, M. Levchenko¹²², J. Levêque⁵, D. Levin⁸⁸,
 L.J. Levinson¹⁷³, M. Levy¹⁸, A. Lewis¹¹⁹, G.H. Lewis¹⁰⁹, A.M. Leyko²¹, M. Leyton⁴¹,
 B. Li^{33b,u}, B. Li⁸⁴, H. Li¹⁴⁹, H.L. Li³¹, L. Li⁴⁵, L. Li^{33e}, S. Li⁴⁵, Y. Li^{33c,v}, Z. Liang¹³⁸,
 H. Liao³⁴, B. Liberti^{134a}, P. Lichard³⁰, K. Lie¹⁶⁶, J. Liebal²¹, W. Liebig¹⁴, C. Limbach²¹,
 A. Limosani⁸⁷, S.C. Lin^{152,w}, T.H. Lin⁸², F. Linde¹⁰⁶, B.E. Lindquist¹⁴⁹,
 J.T. Linnemann⁸⁹, E. Lipeles¹²¹, A. Lipniacka¹⁴, M. Lisovyi⁴², T.M. Liss¹⁶⁶,
 D. Lissauer²⁵, A. Lister¹⁶⁹, A.M. Litke¹³⁸, B. Liu¹⁵², D. Liu¹⁵², J.B. Liu^{33b}, K. Liu^{33b,x},
 L. Liu⁸⁸, M. Liu⁴⁵, M. Liu^{33b}, Y. Liu^{33b}, M. Livan^{120a,120b}, S.S.A. Livermore¹¹⁹,
 A. Lleres⁵⁵, J. Llorente Merino⁸¹, S.L. Lloyd⁷⁵, F. Lo Sterzo¹⁵², E. Lobodzinska⁴²,
 P. Loch⁷, W.S. Lockman¹³⁸, T. Loddenkoetter²¹, F.K. Loebinger⁸³,
 A.E. Loevschall-Jensen³⁶, A. Loginov¹⁷⁷, T. Lohse¹⁶, K. Lohwasser⁴², M. Lokajicek¹²⁶,
 V.P. Lombardo⁵, B.A. Long²², J.D. Long⁸⁸, R.E. Long⁷¹, L. Lopes^{125a},
 D. Lopez Mateos⁵⁷, B. Lopez Paredes¹⁴⁰, I. Lopez Paz¹², J. Lorenz⁹⁹,
 N. Lorenzo Martinez⁶⁰, M. Losada¹⁶³, P. Loscutoff¹⁵, X. Lou⁴¹, A. Lounis¹¹⁶, J. Love⁶,
 P.A. Love⁷¹, A.J. Lowe^{144,e}, F. Lu^{33a}, N. Lu⁸⁸, H.J. Lubatti¹³⁹, C. Luci^{133a,133b},
 A. Lucotte⁵⁵, F. Luehring⁶⁰, W. Lukas⁶¹, L. Luminari^{133a}, O. Lundberg^{147a,147b},
 B. Lund-Jensen¹⁴⁸, M. Lungwitz⁸², D. Lynn²⁵, R. Lysak¹²⁶, E. Lytken⁸⁰, H. Ma²⁵,
 L.L. Ma^{33d}, G. Maccarrone⁴⁷, A. Macchiolo¹⁰⁰, J. Machado Miguens^{125a,125b}, D. Macina³⁰,
 D. Madaffari⁸⁴, R. Madar⁴⁸, H.J. Maddocks⁷¹, W.F. Mader⁴⁴, A. Madsen¹⁶⁷, M. Maeno⁸,
 T. Maeno²⁵, E. Magradze⁵⁴, K. Mahboubi⁴⁸, J. Mahlstedt¹⁰⁶, S. Mahmoud⁷³,

C. Maiani¹³⁷, C. Maidantchik^{24a}, A.A. Maier¹⁰⁰, A. Maio^{125a,125b,125d}, S. Majewski¹¹⁵,
 Y. Makida⁶⁵, N. Makovec¹¹⁶, P. Mal^{137,y}, B. Malaescu⁷⁹, Pa. Malecki³⁹, V.P. Maleev¹²²,
 F. Malek⁵⁵, U. Mallik⁶², D. Malon⁶, C. Malone¹⁴⁴, S. Maltezos¹⁰, V.M. Malyshev¹⁰⁸,
 S. Malyukov³⁰, J. Mamuzic^{13b}, B. Mandelli³⁰, L. Mandelli^{90a}, I. Mandić⁷⁴,
 R. Mandrysch⁶², J. Maneira^{125a,125b}, A. Manfredini¹⁰⁰, L. Manhaes de Andrade Filho^{24b},
 J.A. Manjarres Ramos^{160b}, A. Mann⁹⁹, P.M. Manning¹³⁸, A. Manousakis-Katsikakis⁹,
 B. Mansoulie¹³⁷, R. Mantifel⁸⁶, L. Mapelli³⁰, L. March¹⁶⁸, J.F. Marchand²⁹,
 G. Marchiori⁷⁹, M. Marcisovsky¹²⁶, C.P. Marino¹⁷⁰, M. Marjanovic^{13a}, C.N. Marques^{125a},
 F. Marroquin^{24a}, S.P. Marsden⁸³, Z. Marshall¹⁵, L.F. Marti¹⁷, S. Marti-Garcia¹⁶⁸,
 B. Martin³⁰, B. Martin⁸⁹, T.A. Martin¹⁷¹, V.J. Martin⁴⁶, B. Martin dit Latour¹⁴,
 H. Martinez¹³⁷, M. Martinez^{12,n}, S. Martin-Haugh¹³⁰, A.C. Martyniuk⁷⁷, M. Marx¹³⁹,
 F. Marzano^{133a}, A. Marzin³⁰, L. Masetti⁸², T. Mashimo¹⁵⁶, R. Mashinistov⁹⁵, J. Masik⁸³,
 A.L. Maslennikov¹⁰⁸, I. Massa^{20a,20b}, L. Massa^{20a,20b}, N. Massol⁵, P. Mastrandrea¹⁴⁹,
 A. Mastroberardino^{37a,37b}, T. Masubuchi¹⁵⁶, P. Mättig¹⁷⁶, J. Mattmann⁸², J. Maurer^{26a},
 S.J. Maxfield⁷³, D.A. Maximov^{108,t}, R. Mazini¹⁵², L. Mazzaferro^{134a,134b},
 G. Mc Goldrick¹⁵⁹, S.P. Mc Kee⁸⁸, A. McCarn⁸⁸, R.L. McCarthy¹⁴⁹, T.G. McCarthy²⁹,
 N.A. McCubbin¹³⁰, K.W. McFarlane^{56,*}, J.A. Mcfayden⁷⁷, G. Mchedlidze⁵⁴,
 S.J. McMahon¹³⁰, R.A. McPherson^{170,i}, A. Meade⁸⁵, J. Mechnich¹⁰⁶, M. Medinnis⁴²,
 S. Meehan³¹, S. Mehlhase⁹⁹, A. Mehta⁷³, K. Meier^{58a}, C. Meineck⁹⁹, B. Meirose⁸⁰,
 C. Melachrinou³¹, B.R. Mellado Garcia^{146c}, F. Meloni¹⁷, A. Mengarelli^{20a,20b},
 S. Menke¹⁰⁰, E. Meoni¹⁶², K.M. Mercurio⁵⁷, S. Mergelmeyer²¹, N. Meric¹³⁷, P. Mermod⁴⁹,
 L. Merola^{103a,103b}, C. Meroni^{90a}, F.S. Merritt³¹, H. Merritt¹¹⁰, A. Messina^{30,z},
 J. Metcalfe²⁵, A.S. Mete¹⁶⁴, C. Meyer⁸², C. Meyer¹²¹, J-P. Meyer¹³⁷, J. Meyer³⁰,
 R.P. Middleton¹³⁰, S. Migas⁷³, L. Mijović²¹, G. Mikenberg¹⁷³, M. Mikestikova¹²⁶,
 M. Mikuž⁷⁴, A. Milic³⁰, D.W. Miller³¹, C. Mills⁴⁶, A. Milov¹⁷³, D.A. Milstead^{147a,147b},
 D. Milstein¹⁷³, A.A. Minaenko¹²⁹, I.A. Minashvili⁶⁴, A.I. Mincer¹⁰⁹, B. Mindur^{38a},
 M. Mineev⁶⁴, Y. Ming¹⁷⁴, L.M. Mir¹², G. Mirabelli^{133a}, T. Mitani¹⁷², J. Mitrevski⁹⁹,
 V.A. Mitsou¹⁶⁸, S. Mitsui⁶⁵, A. Miucci⁴⁹, P.S. Miyagawa¹⁴⁰, J.U. Mjörnmark⁸⁰,
 T. Moe^{147a,147b}, K. Mochizuki⁸⁴, S. Mohapatra³⁵, W. Mohr⁴⁸, S. Molander^{147a,147b},
 R. Moles-Valls¹⁶⁸, K. Mönig⁴², C. Monini⁵⁵, J. Monk³⁶, E. Monnier⁸⁴,
 J. Montejo Berlingen¹², F. Monticelli⁷⁰, S. Monzani^{133a,133b}, R.W. Moore³, N. Morange⁶²,
 D. Moreno⁸², M. Moreno Llácer⁵⁴, P. Morettini^{50a}, M. Morgenstern⁴⁴, M. Morii⁵⁷,
 S. Moritz⁸², A.K. Morley¹⁴⁸, G. Mornacchi³⁰, J.D. Morris⁷⁵, L. Morvaj¹⁰², H.G. Moser¹⁰⁰,
 M. Mosidze^{51b}, J. Moss¹¹⁰, K. Motohashi¹⁵⁸, R. Mount¹⁴⁴, E. Mountricha²⁵,
 S.V. Mouraviev^{95,*}, E.J.W. Moyses⁸⁵, S. Muanza⁸⁴, R.D. Mudd¹⁸, F. Mueller^{58a},
 J. Mueller¹²⁴, K. Mueller²¹, T. Mueller²⁸, T. Mueller⁸², D. Muenstermann⁴⁹,
 Y. Munwes¹⁵⁴, J.A. Murillo Quijada¹⁸, W.J. Murray^{171,130}, H. Musheghyan⁵⁴,
 E. Musto¹⁵³, A.G. Myagkov^{129,aa}, M. Myska¹²⁷, O. Nackenhorst⁵⁴, J. Nadal⁵⁴,
 K. Nagai⁶¹, R. Nagai¹⁵⁸, Y. Nagai⁸⁴, K. Nagano⁶⁵, A. Nagarkar¹¹⁰, Y. Nagasaka⁵⁹,
 M. Nagel¹⁰⁰, A.M. Nairz³⁰, Y. Nakahama³⁰, K. Nakamura⁶⁵, T. Nakamura¹⁵⁶,
 I. Nakano¹¹¹, H. Namasivayam⁴¹, G. Nanava²¹, R. Narayan^{58b}, T. Nattermann²¹,
 T. Naumann⁴², G. Navarro¹⁶³, R. Nayyar⁷, H.A. Neal⁸⁸, P.Yu. Nechaeva⁹⁵, T.J. Neep⁸³,
 P.D. Nef¹⁴⁴, A. Negri^{120a,120b}, G. Negri³⁰, M. Negrini^{20a}, S. Nektarijevic⁴⁹, A. Nelson¹⁶⁴,

T.K. Nelson¹⁴⁴, S. Nemecek¹²⁶, P. Nemethy¹⁰⁹, A.A. Nepomuceno^{24a}, M. Nessi^{30,ab},
 M.S. Neubauer¹⁶⁶, M. Neumann¹⁷⁶, R.M. Neves¹⁰⁹, P. Nevski²⁵, P.R. Newman¹⁸,
 D.H. Nguyen⁶, R.B. Nickerson¹¹⁹, R. Nicolaidou¹³⁷, B. Nicquevert³⁰, J. Nielsen¹³⁸,
 N. Nikiforou³⁵, A. Nikiforov¹⁶, V. Nikolaenko^{129,aa}, I. Nikolic-Audit⁷⁹, K. Nikolics⁴⁹,
 K. Nikolopoulos¹⁸, P. Nilsson⁸, Y. Ninomiya¹⁵⁶, A. Nisati^{133a}, R. Nisius¹⁰⁰, T. Nobe¹⁵⁸,
 L. Nodulman⁶, M. Nomachi¹¹⁷, I. Nomidis²⁹, S. Norberg¹¹², M. Nordberg³⁰,
 O. Novgorodova⁴⁴, S. Nowak¹⁰⁰, M. Nozaki⁶⁵, L. Nozka¹¹⁴, K. Ntekas¹⁰,
 G. Nunes Hanninger⁸⁷, T. Nunnemann⁹⁹, E. Nurse⁷⁷, F. Nuti⁸⁷, B.J. O'Brien⁴⁶,
 F. O'grady⁷, D.C. O'Neil¹⁴³, V. O'Shea⁵³, F.G. Oakham^{29,d}, H. Oberlack¹⁰⁰,
 T. Obermann²¹, J. Ocariz⁷⁹, A. Ochi⁶⁶, M.I. Ochoa⁷⁷, S. Oda⁶⁹, S. Odaka⁶⁵, H. Ogren⁶⁰,
 A. Oh⁸³, S.H. Oh⁴⁵, C.C. Ohm¹⁵, H. Ohman¹⁶⁷, W. Okamura¹¹⁷, H. Okawa²⁵,
 Y. Okumura³¹, T. Okuyama¹⁵⁶, A. Olariu^{26a}, A.G. Olchevski⁶⁴, S.A. Olivares Pino⁴⁶,
 D. Oliveira Damazio²⁵, E. Oliver Garcia¹⁶⁸, A. Olszewski³⁹, J. Olszowska³⁹,
 A. Onofre^{125a,125e}, P.U.E. Onyisi^{31,o}, C.J. Oram^{160a}, M.J. Oreglia³¹, Y. Oren¹⁵⁴,
 D. Orestano^{135a,135b}, N. Orlando^{72a,72b}, C. Oropeza Barrera⁵³, R.S. Orr¹⁵⁹,
 B. Osculati^{50a,50b}, R. Ospanov¹²¹, G. Otero y Garzon²⁷, H. Otono⁶⁹, M. Ouchrif^{136d},
 E.A. Ouellette¹⁷⁰, F. Ould-Saada¹¹⁸, A. Ouraou¹³⁷, K.P. Oussoren¹⁰⁶, Q. Ouyang^{33a},
 A. Ovcharova¹⁵, M. Owen⁸³, V.E. Ozcan^{19a}, N. Ozturk⁸, K. Pachal¹¹⁹,
 A. Pacheco Pages¹², C. Padilla Aranda¹², M. Pagáčová⁴⁸, S. Pagan Griso¹⁵,
 E. Paganis¹⁴⁰, C. Pahl¹⁰⁰, F. Paige²⁵, P. Pais⁸⁵, K. Pajchel¹¹⁸, G. Palacino^{160b},
 S. Palestini³⁰, M. Palka^{38b}, D. Pallin³⁴, A. Palma^{125a,125b}, J.D. Palmer¹⁸, Y.B. Pan¹⁷⁴,
 E. Panagiotopoulou¹⁰, J.G. Panduro Vazquez⁷⁶, P. Pani¹⁰⁶, N. Panikashvili⁸⁸,
 S. Panitkin²⁵, D. Pantea^{26a}, L. Paolozzi^{134a,134b}, Th.D. Papadopoulou¹⁰,
 K. Papageorgiou^{155,l}, A. Paramonov⁶, D. Paredes Hernandez³⁴, M.A. Parker²⁸,
 F. Parodi^{50a,50b}, J.A. Parsons³⁵, U. Parzefall⁴⁸, E. Pasqualucci^{133a}, S. Passaggio^{50a},
 A. Passeri^{135a}, F. Pastore^{135a,135b,*}, Fr. Pastore⁷⁶, G. Pásztor²⁹, S. Pataraiia¹⁷⁶,
 N.D. Patel¹⁵¹, J.R. Pater⁸³, S. Patricelli^{103a,103b}, T. Pauly³⁰, J. Pearce¹⁷⁰,
 L.E. Pedersen³⁶, M. Pedersen¹¹⁸, S. Pedraza Lopez¹⁶⁸, R. Pedro^{125a,125b},
 S.V. Peleganchuk¹⁰⁸, D. Pelikan¹⁶⁷, H. Peng^{33b}, B. Penning³¹, J. Penwell⁶⁰,
 D.V. Perepelitsa²⁵, E. Perez Codina^{160a}, M.T. Pérez García-Estañ¹⁶⁸, V. Perez Reale³⁵,
 L. Perini^{90a,90b}, H. Pernegger³⁰, R. Perrino^{72a}, R. Peschke⁴², V.D. Peshekhonov⁶⁴,
 K. Peters³⁰, R.F.Y. Peters⁸³, B.A. Petersen³⁰, T.C. Petersen³⁶, E. Petit⁴²,
 A. Petridis^{147a,147b}, C. Petridou¹⁵⁵, E. Petrolo^{133a}, F. Petrucci^{135a,135b},
 N.E. Pettersson¹⁵⁸, R. Pezoa^{32b}, P.W. Phillips¹³⁰, G. Piacquadio¹⁴⁴, E. Pianori¹⁷¹,
 A. Picazio⁴⁹, E. Piccaro⁷⁵, M. Piccinini^{20a,20b}, R. Piegai²⁷, D.T. Pignotti¹¹⁰,
 J.E. Pilcher³¹, A.D. Pilkington⁷⁷, J. Pina^{125a,125b,125d}, M. Pinamonti^{165a,165c,ac},
 A. Pinder¹¹⁹, J.L. Pinfold³, A. Pingel³⁶, B. Pinto^{125a}, S. Pires⁷⁹, M. Pitt¹⁷³,
 C. Pizio^{90a,90b}, L. Plazak^{145a}, M.-A. Pleier²⁵, V. Pleskot¹²⁸, E. Plotnikova⁶⁴,
 P. Plucinski^{147a,147b}, S. Poddar^{58a}, F. Podlyski³⁴, R. Poettgen⁸², L. Poggioli¹¹⁶,
 D. Pohl²¹, M. Pohl⁴⁹, G. Polesello^{120a}, A. Policicchio^{37a,37b}, R. Polifka¹⁵⁹, A. Polini^{20a},
 C.S. Pollard⁴⁵, V. Polychronakos²⁵, K. Pommès³⁰, L. Pontecorvo^{133a}, B.G. Pope⁸⁹,
 G.A. Popeneciu^{26b}, D.S. Popovic^{13a}, A. Poppleton³⁰, X. Portell Bueso¹², S. Pospisil¹²⁷,
 K. Potamianos¹⁵, I.N. Potrap⁶⁴, C.J. Potter¹⁵⁰, C.T. Potter¹¹⁵, G. Poulard³⁰,

J. Poveda⁶⁰, V. Pozdnyakov⁶⁴, P. Pralavorio⁸⁴, A. Pranko¹⁵, S. Prasad³⁰, R. Pravahan⁸,
 S. Prell⁶³, D. Price⁸³, J. Price⁷³, L.E. Price⁶, D. Prieur¹²⁴, M. Primavera^{72a}, M. Proissl⁴⁶,
 K. Prokofiev⁴⁷, F. Prokoshin^{32b}, E. Protopapadaki¹³⁷, S. Protopopescu²⁵, J. Proudfoot⁶,
 M. Przybycien^{38a}, H. Przysieszniak⁵, E. Ptacek¹¹⁵, D. Puddu^{135a,135b}, E. Pueschel⁸⁵,
 D. Puldon¹⁴⁹, M. Purohit^{25,ad}, P. Puzo¹¹⁶, J. Qian⁸⁸, G. Qin⁵³, Y. Qin⁸³, A. Quadt⁵⁴,
 D.R. Quarrie¹⁵, W.B. Quayle^{165a,165b}, M. Queitsch-Maitland⁸³, D. Quilty⁵³,
 A. Qureshi^{160b}, V. Radeka²⁵, V. Radescu⁴², S.K. Radhakrishnan¹⁴⁹, P. Radloff¹¹⁵,
 P. Rados⁸⁷, F. Ragusa^{90a,90b}, G. Rahal¹⁷⁹, S. Rajagopalan²⁵, M. Rammensee³⁰,
 A.S. Randle-Conde⁴⁰, C. Rangel-Smith¹⁶⁷, K. Rao¹⁶⁴, F. Rauscher⁹⁹, T.C. Rave⁴⁸,
 T. Ravenscroft⁵³, M. Raymond³⁰, A.L. Read¹¹⁸, N.P. Readioff⁷³, D.M. Rebuffi^{120a,120b},
 A. Redelbach¹⁷⁵, G. Redlinger²⁵, R. Reece¹³⁸, K. Reeves⁴¹, L. Rehnisch¹⁶, H. Reisin²⁷,
 M. Relich¹⁶⁴, C. Rembser³⁰, H. Ren^{33a}, Z.L. Ren¹⁵², A. Renaud¹¹⁶, M. Rescigno^{133a},
 S. Resconi^{90a}, O.L. Rezanova^{108,t}, P. Reznicek¹²⁸, R. Rezvani⁹⁴, R. Richter¹⁰⁰,
 M. Ridel⁷⁹, P. Rieck¹⁶, J. Rieger⁵⁴, M. Rijssenbeek¹⁴⁹, A. Rimoldi^{120a,120b}, L. Rinaldi^{20a},
 E. Ritsch⁶¹, I. Riu¹², F. Rizatdinova¹¹³, E. Rizvi⁷⁵, S.H. Robertson^{86,i},
 A. Robichaud-Veronneau⁸⁶, D. Robinson²⁸, J.E.M. Robinson⁸³, A. Robson⁵³,
 C. Roda^{123a,123b}, L. Rodrigues³⁰, S. Roe³⁰, O. Røhne¹¹⁸, S. Rolli¹⁶², A. Romaniouk⁹⁷,
 M. Romano^{20a,20b}, E. Romero Adam¹⁶⁸, N. Rompotis¹³⁹, M. Ronzani⁴⁸, L. Roos⁷⁹,
 E. Ros¹⁶⁸, S. Rosati^{133a}, K. Rosbach⁴⁹, M. Rose⁷⁶, P. Rose¹³⁸, P.L. Rosendahl¹⁴,
 O. Rosenthal¹⁴², V. Rossetti^{147a,147b}, E. Rossi^{103a,103b}, L.P. Rossi^{50a}, R. Rosten¹³⁹,
 M. Rotaru^{26a}, I. Roth¹⁷³, J. Rothberg¹³⁹, D. Rousseau¹¹⁶, C.R. Royon¹³⁷, A. Rozanov⁸⁴,
 Y. Rozen¹⁵³, X. Ruan^{146c}, F. Rubbo¹², I. Rubinskiy⁴², V.I. Rud⁹⁸, C. Rudolph⁴⁴,
 M.S. Rudolph¹⁵⁹, F. Rühr⁴⁸, A. Ruiz-Martinez³⁰, Z. Rurikova⁴⁸, N.A. Rusakovich⁶⁴,
 A. Ruschke⁹⁹, J.P. Rutherford⁷, N. Ruthmann⁴⁸, Y.F. Ryabov¹²², M. Rybar¹²⁸,
 G. Rybkin¹¹⁶, N.C. Ryder¹¹⁹, A.F. Saavedra¹⁵¹, S. Sacerdoti²⁷, A. Saddique³, I. Sadeh¹⁵⁴,
 H.F.W. Sadrozinski¹³⁸, R. Sadykov⁶⁴, F. Safai Tehrani^{133a}, H. Sakamoto¹⁵⁶,
 Y. Sakurai¹⁷², G. Salamanna^{135a,135b}, A. Salamon^{134a}, M. Saleem¹¹², D. Salek¹⁰⁶,
 P.H. Sales De Bruin¹³⁹, D. Salihagic¹⁰⁰, A. Salnikov¹⁴⁴, J. Salt¹⁶⁸, D. Salvatore^{37a,37b},
 F. Salvatore¹⁵⁰, A. Salvucci¹⁰⁵, A. Salzburger³⁰, D. Sampsonidis¹⁵⁵, A. Sanchez^{103a,103b},
 J. Sánchez¹⁶⁸, V. Sanchez Martinez¹⁶⁸, H. Sandaker¹⁴, R.L. Sandbach⁷⁵, H.G. Sander⁸²,
 M.P. Sanders⁹⁹, M. Sandhoff¹⁷⁶, T. Sandoval²⁸, C. Sandoval¹⁶³, R. Sandstroem¹⁰⁰,
 D.P.C. Sankey¹³⁰, A. Sansoni⁴⁷, C. Santoni³⁴, R. Santonico^{134a,134b}, H. Santos^{125a},
 I. Santoyo Castillo¹⁵⁰, K. Sapp¹²⁴, A. Saponov⁶⁴, J.G. Saraiva^{125a,125d}, B. Sarrazin²¹,
 G. Sartiso¹⁷⁶, O. Sasaki⁶⁵, Y. Sasaki¹⁵⁶, G. Sauvage^{5,*}, E. Sauvan⁵, P. Savard^{159,d},
 D.O. Savu³⁰, C. Sawyer¹¹⁹, L. Sawyer^{78,m}, D.H. Saxon⁵³, J. Saxon¹²¹, C. Sbarra^{20a},
 A. Sbrizzi³, T. Scanlon⁷⁷, D.A. Scannicchio¹⁶⁴, M. Scarcella¹⁵¹, V. Scarfone^{37a,37b},
 J. Schaarschmidt¹⁷³, P. Schacht¹⁰⁰, D. Schaefer³⁰, R. Schaefer⁴², S. Schaepe²¹,
 S. Schaetzel^{58b}, U. Schäfer⁸², A.C. Schaffer¹¹⁶, D. Schaile⁹⁹, R.D. Schamberger¹⁴⁹,
 V. Scharf^{58a}, V.A. Schegelsky¹²², D. Scheirich¹²⁸, M. Schernau¹⁶⁴, M.I. Scherzer³⁵,
 C. Schiavi^{50a,50b}, J. Schieck⁹⁹, C. Schillo⁴⁸, M. Schioppa^{37a,37b}, S. Schlenker³⁰,
 E. Schmidt⁴⁸, K. Schmieden³⁰, C. Schmitt⁸², S. Schmitt^{58b}, B. Schneider¹⁷,
 Y.J. Schnellbach⁷³, U. Schnoor⁴⁴, L. Schoeffel¹³⁷, A. Schoening^{58b}, B.D. Schoenrock⁸⁹,
 A.L.S. Schorlemmer⁵⁴, M. Schott⁸², D. Schouten^{160a}, J. Schovancova²⁵, S. Schramm¹⁵⁹,

M. Schreyer¹⁷⁵, C. Schroeder⁸², N. Schuh⁸², M.J. Schultens²¹, H.-C. Schultz-Coulon^{58a},
 H. Schulz¹⁶, M. Schumacher⁴⁸, B.A. Schumm¹³⁸, Ph. Schune¹³⁷, C. Schwanenberger⁸³,
 A. Schwartzman¹⁴⁴, Ph. Schwegler¹⁰⁰, Ph. Schwemling¹³⁷, R. Schwienhorst⁸⁹,
 J. Schwindling¹³⁷, T. Schwindt²¹, M. Schwoerer⁵, F.G. Sciacca¹⁷, E. Scifo¹¹⁶, G. Sciolla²³,
 W.G. Scott¹³⁰, F. Scuri^{123a,123b}, F. Scutti²¹, J. Searcy⁸⁸, G. Sedov⁴², E. Sedykh¹²²,
 S.C. Seidel¹⁰⁴, A. Seiden¹³⁸, F. Seifert¹²⁷, J.M. Seixas^{24a}, G. Sekhniaidze^{103a},
 S.J. Sekula⁴⁰, K.E. Selbach⁴⁶, D.M. Seliverstov^{122,*}, G. Sellers⁷³,
 N. Semprini-Cesari^{20a,20b}, C. Serfon³⁰, L. Serin¹¹⁶, L. Serkin⁵⁴, T. Serre⁸⁴, R. Seuster^{160a},
 H. Severini¹¹², T. Sfiligoi⁷⁴, F. Sforza¹⁰⁰, A. Sfyrla³⁰, E. Shabalina⁵⁴, M. Shamim¹¹⁵,
 L.Y. Shan^{33a}, R. Shang¹⁶⁶, J.T. Shank²², M. Shapiro¹⁵, P.B. Shatalov⁹⁶, K. Shaw^{165a,165b},
 C.Y. Shehu¹⁵⁰, P. Sherwood⁷⁷, L. Shi^{152,ae}, S. Shimizu⁶⁶, C.O. Shimmin¹⁶⁴,
 M. Shimojima¹⁰¹, M. Shiyakova⁶⁴, A. Shmeleva⁹⁵, M.J. Shochet³¹, D. Short¹¹⁹,
 S. Shrestha⁶³, E. Shulga⁹⁷, M.A. Shupe⁷, S. Shushkevich⁴², P. Sicho¹²⁶,
 O. Sidiropoulou¹⁵⁵, D. Sidorov¹¹³, A. Sidoti^{133a}, F. Siegert⁴⁴, Dj. Sijacki^{13a},
 J. Silva^{125a,125d}, Y. Silver¹⁵⁴, D. Silverstein¹⁴⁴, S.B. Silverstein^{147a}, V. Simak¹²⁷,
 O. Simard⁵, Lj. Simic^{13a}, S. Simion¹¹⁶, E. Simioni⁸², B. Simmons⁷⁷, R. Simoniello^{90a,90b},
 M. Simonyan³⁶, P. Sinervo¹⁵⁹, N.B. Sinev¹¹⁵, V. Sipica¹⁴², G. Siragusa¹⁷⁵, A. Sircar⁷⁸,
 A.N. Sisakyan^{64,*}, S.Yu. Sivoklov⁹⁸, J. Sjölín^{147a,147b}, T.B. Sjursen¹⁴, H.P. Skottowe⁵⁷,
 K.Yu. Skovpen¹⁰⁸, P. Skubic¹¹², M. Slater¹⁸, T. Slavicek¹²⁷, K. Sliwa¹⁶², V. Smakhtin¹⁷³,
 B.H. Smart⁴⁶, L. Smestad¹⁴, S.Yu. Smirnov⁹⁷, Y. Smirnov⁹⁷, L.N. Smirnova^{98,af},
 O. Smirnova⁸⁰, K.M. Smith⁵³, M. Smizanska⁷¹, K. Smolek¹²⁷, A.A. Snesev⁹⁵,
 G. Snidero⁷⁵, S. Snyder²⁵, R. Sobie^{170,i}, F. Socher⁴⁴, A. Soffer¹⁵⁴, D.A. Soh^{152,ae},
 C.A. Solans³⁰, M. Solar¹²⁷, J. Solc¹²⁷, E.Yu. Soldatov⁹⁷, U. Soldevila¹⁶⁸,
 A.A. Solodkov¹²⁹, A. Soloshenko⁶⁴, O.V. Solovyanov¹²⁹, V. Solovyev¹²², P. Sommer⁴⁸,
 H.Y. Song^{33b}, N. Soni¹, A. Sood¹⁵, A. Sopczak¹²⁷, B. Sopko¹²⁷, V. Sopko¹²⁷, V. Sorin¹²,
 M. Sosebee⁸, R. Soualah^{165a,165c}, P. Soueid⁹⁴, A.M. Soukharev¹⁰⁸, D. South⁴²,
 S. Spagnolo^{72a,72b}, F. Spanò⁷⁶, W.R. Spearman⁵⁷, F. Spettel¹⁰⁰, R. Spighi^{20a}, G. Spigo³⁰,
 L.A. Spiller⁸⁷, M. Spousta¹²⁸, T. Spreitzer¹⁵⁹, B. Spurlock⁸, R.D. St. Denis^{53,*},
 S. Staerz⁴⁴, J. Stahlman¹²¹, R. Stamen^{58a}, S. Stamm¹⁶, E. Stanecka³⁹, R.W. Stanek⁶,
 C. Stanescu^{135a}, M. Stanescu-Bellu⁴², M.M. Stanitzki⁴², S. Stapnes¹¹⁸,
 E.A. Starchenko¹²⁹, J. Stark⁵⁵, P. Staroba¹²⁶, P. Starovoitov⁴², R. Staszewski³⁹,
 P. Stavina^{145a,*}, P. Steinberg²⁵, B. Stelzer¹⁴³, H.J. Stelzer³⁰, O. Stelzer-Chilton^{160a},
 H. Stenzel⁵², S. Stern¹⁰⁰, G.A. Stewart⁵³, J.A. Stillings²¹, M.C. Stockton⁸⁶, M. Stoebe⁸⁶,
 G. Stoicea^{26a}, P. Stolte⁵⁴, S. Stonjek¹⁰⁰, A.R. Stradling⁸, A. Straessner⁴⁴,
 M.E. Stramaglia¹⁷, J. Strandberg¹⁴⁸, S. Strandberg^{147a,147b}, A. Strandlie¹¹⁸,
 E. Strauss¹⁴⁴, M. Strauss¹¹², P. Strizenec^{145b}, R. Ströhmer¹⁷⁵, D.M. Strom¹¹⁵,
 R. Stroynowski⁴⁰, A. Struebig¹⁰⁵, S.A. Stucci¹⁷, B. Stugu¹⁴, N.A. Styles⁴², D. Su¹⁴⁴,
 J. Su¹²⁴, R. Subramaniam⁷⁸, A. Succurro¹², Y. Sugaya¹¹⁷, C. Suhr¹⁰⁷, M. Suk¹²⁷,
 V.V. Sulin⁹⁵, S. Sultansoy^{4c}, T. Sumida⁶⁷, S. Sun⁵⁷, X. Sun^{33a}, J.E. Sundermann⁴⁸,
 K. Suruliz¹⁴⁰, G. Susinno^{37a,37b}, M.R. Sutton¹⁵⁰, Y. Suzuki⁶⁵, M. Svatos¹²⁶,
 S. Swedish¹⁶⁹, M. Swiatlowski¹⁴⁴, I. Sykora^{145a}, T. Sykora¹²⁸, D. Ta⁸⁹, C. Taccini^{135a,135b},
 K. Tackmann⁴², J. Taenzer¹⁵⁹, A. Taffard¹⁶⁴, R. Tafirout^{160a}, N. Taiblum¹⁵⁴, H. Takai²⁵,
 R. Takashima⁶⁸, H. Takeda⁶⁶, T. Takeshita¹⁴¹, Y. Takubo⁶⁵, M. Talby⁸⁴,

A.A. Talyshev^{108,t}, J.Y.C. Tam¹⁷⁵, K.G. Tan⁸⁷, J. Tanaka¹⁵⁶, R. Tanaka¹¹⁶, S. Tanaka¹³²,
 S. Tanaka⁶⁵, A.J. Tanasijczuk¹⁴³, B.B. Tannenwald¹¹⁰, N. Tannoury²¹, S. Tapprogge⁸²,
 S. Tarem¹⁵³, F. Tarrade²⁹, G.F. Tartarelli^{90a}, P. Tas¹²⁸, M. Tasevsky¹²⁶, T. Tashiro⁶⁷,
 E. Tassi^{37a,37b}, A. Tavares Delgado^{125a,125b}, Y. Tayalati^{136d}, F.E. Taylor⁹³, G.N. Taylor⁸⁷,
 W. Taylor^{160b}, F.A. Teischinger³⁰, M. Teixeira Dias Castanheira⁷⁵, P. Teixeira-Dias⁷⁶,
 K.K. Temming⁴⁸, H. Ten Kate³⁰, P.K. Teng¹⁵², J.J. Teoh¹¹⁷, S. Terada⁶⁵, K. Terashi¹⁵⁶,
 J. Terron⁸¹, S. Terzo¹⁰⁰, M. Testa⁴⁷, R.J. Teuscher^{159,i}, J. Therhaag²¹,
 T. Theveneaux-Pelzer³⁴, J.P. Thomas¹⁸, J. Thomas-Wilsker⁷⁶, E.N. Thompson³⁵,
 P.D. Thompson¹⁸, P.D. Thompson¹⁵⁹, R.J. Thompson⁸³, A.S. Thompson⁵³,
 L.A. Thomsen³⁶, E. Thomson¹²¹, M. Thomson²⁸, W.M. Thong⁸⁷, R.P. Thun^{88,*},
 F. Tian³⁵, M.J. Tibbetts¹⁵, V.O. Tikhomirov^{95,ag}, Yu.A. Tikhonov^{108,t}, S. Timoshenko⁹⁷,
 E. Tiouchichine⁸⁴, P. Tipton¹⁷⁷, S. Tisserant⁸⁴, T. Todorov⁵, S. Todorova-Nova¹²⁸,
 B. Toggerson⁷, J. Tojo⁶⁹, S. Tokár^{145a}, K. Tokushuku⁶⁵, K. Tollefson⁸⁹, L. Tomlinson⁸³,
 M. Tomoto¹⁰², L. Tompkins³¹, K. Toms¹⁰⁴, N.D. Topilin⁶⁴, E. Torrence¹¹⁵, H. Torres¹⁴³,
 E. Torró Pastor¹⁶⁸, J. Toth^{84,ah}, F. Touchard⁸⁴, D.R. Tovey¹⁴⁰, H.L. Tran¹¹⁶,
 T. Trefzger¹⁷⁵, L. Tremblet³⁰, A. Tricoli³⁰, I.M. Trigger^{160a}, S. Trincaz-Duvoid⁷⁹,
 M.F. Tripiana¹², W. Trischuk¹⁵⁹, B. Trocmé⁵⁵, C. Troncon^{90a}, M. Trottier-McDonald¹⁴³,
 M. Trovatelli^{135a,135b}, P. True⁸⁹, M. Trzebinski³⁹, A. Trzupek³⁹, C. Tsarouchas³⁰,
 J.C-L. Tseng¹¹⁹, P.V. Tsiareshka⁹¹, D. Tsionou¹³⁷, G. Tsipolitis¹⁰, N. Tsirintanis⁹,
 S. Tsiskaridze¹², V. Tsiskaridze⁴⁸, E.G. Tskhadadze^{51a}, I.I. Tsukerman⁹⁶, V. Tsulaia¹⁵,
 S. Tsuno⁶⁵, D. Tsybychev¹⁴⁹, A. Tudorache^{26a}, V. Tudorache^{26a}, A.N. Tuna¹²¹,
 S.A. Tupputi^{20a,20b}, S. Turchikhin^{98,af}, D. Turecek¹²⁷, I. Turk Cakir^{4d}, R. Turra^{90a,90b},
 P.M. Tuts³⁵, A. Tykhonov⁴⁹, M. Tylmad^{147a,147b}, M. Tyndel¹³⁰, K. Uchida²¹, I. Ueda¹⁵⁶,
 R. Ueno²⁹, M. Ughetto⁸⁴, M. Ugland¹⁴, M. Uhlenbrock²¹, F. Ukegawa¹⁶¹, G. Unal³⁰,
 A. Undrus²⁵, G. Unel¹⁶⁴, F.C. Ungaro⁴⁸, Y. Unno⁶⁵, C. Unverdorben⁹⁹, D. Urbaniec³⁵,
 P. Urquijo⁸⁷, G. Usai⁸, A. Usanova⁶¹, L. Vacavant⁸⁴, V. Vacek¹²⁷, B. Vachon⁸⁶,
 N. Valencic¹⁰⁶, S. Valentinetti^{20a,20b}, A. Valero¹⁶⁸, L. Valery³⁴, S. Valkar¹²⁸,
 E. Valladolid Gallego¹⁶⁸, S. Vallecorsa⁴⁹, J.A. Valls Ferrer¹⁶⁸, W. Van Den Wollenberg¹⁰⁶,
 P.C. Van Der Deijl¹⁰⁶, R. van der Geer¹⁰⁶, H. van der Graaf¹⁰⁶, R. Van Der Leeuw¹⁰⁶,
 D. van der Ster³⁰, N. van Eldik³⁰, P. van Gemmeren⁶, J. Van Nieuwkoop¹⁴³,
 I. van Vulpen¹⁰⁶, M.C. van Woerden³⁰, M. Vanadia^{133a,133b}, W. Vandelli³⁰, R. Vanguri¹²¹,
 A. Vaniachine⁶, P. Vankov⁴², F. Vannucci⁷⁹, G. Vardanyan¹⁷⁸, R. Vari^{133a}, E.W. Varnes⁷,
 T. Varol⁸⁵, D. Varouchas⁷⁹, A. Vartapetian⁸, K.E. Varvell¹⁵¹, F. Vazeille³⁴,
 T. Vazquez Schroeder⁵⁴, J. Veatch⁷, F. Veloso^{125a,125c}, S. Veneziano^{133a},
 A. Ventura^{72a,72b}, D. Ventura⁸⁵, M. Venturi¹⁷⁰, N. Venturi¹⁵⁹, A. Venturini²³,
 V. Vercesi^{120a}, M. Verducci^{133a,133b}, W. Verkerke¹⁰⁶, J.C. Vermeulen¹⁰⁶, A. Vest⁴⁴,
 M.C. Vetterli^{143,d}, O. Viazlo⁸⁰, I. Vichou¹⁶⁶, T. Vickey^{146c,ai}, O.E. Vickey Boeriu^{146c},
 G.H.A. Viehhauser¹¹⁹, S. Viel¹⁶⁹, R. Vigne³⁰, M. Villa^{20a,20b}, M. Villaplana Perez^{90a,90b},
 E. Vilucchi⁴⁷, M.G. Vincter²⁹, V.B. Vinogradov⁶⁴, J. Virzi¹⁵, I. Vivarelli¹⁵⁰,
 F. Vives Vaque³, S. Vlachos¹⁰, D. Vladoiu⁹⁹, M. Vlasak¹²⁷, A. Vogel²¹, M. Vogel^{32a},
 P. Vokac¹²⁷, G. Volpi^{123a,123b}, M. Volpi⁸⁷, H. von der Schmitt¹⁰⁰, H. von Radziewski⁴⁸,
 E. von Toerne²¹, V. Vorobel¹²⁸, K. Vorobev⁹⁷, M. Vos¹⁶⁸, R. Voss³⁰, J.H. Vosseveld⁷³,
 N. Vranjes¹³⁷, M. Vranjes Milosavljevic^{13a}, V. Vrba¹²⁶, M. Vreeswijk¹⁰⁶, T. Vu Anh⁴⁸,

R. Vuillermet³⁰, I. Vukotic³¹, Z. Vykydal¹²⁷, P. Wagner²¹, W. Wagner¹⁷⁶, H. Wahlberg⁷⁰, S. Wahrmund⁴⁴, J. Wakabayashi¹⁰², J. Walder⁷¹, R. Walker⁹⁹, W. Walkowiak¹⁴², R. Wall¹⁷⁷, P. Waller⁷³, B. Walsh¹⁷⁷, C. Wang^{152,aj}, C. Wang⁴⁵, F. Wang¹⁷⁴, H. Wang¹⁵, H. Wang⁴⁰, J. Wang⁴², J. Wang^{33a}, K. Wang⁸⁶, R. Wang¹⁰⁴, S.M. Wang¹⁵², T. Wang²¹, X. Wang¹⁷⁷, C. Wanotayaroj¹¹⁵, A. Warburton⁸⁶, C.P. Ward²⁸, D.R. Wardrope⁷⁷, M. Warsinsky⁴⁸, A. Washbrook⁴⁶, C. Wasicki⁴², P.M. Watkins¹⁸, A.T. Watson¹⁸, I.J. Watson¹⁵¹, M.F. Watson¹⁸, G. Watts¹³⁹, S. Watts⁸³, B.M. Waugh⁷⁷, S. Webb⁸³, M.S. Weber¹⁷, S.W. Weber¹⁷⁵, J.S. Webster³¹, A.R. Weidberg¹¹⁹, P. Weigell¹⁰⁰, B. Weinert⁶⁰, J. Weingarten⁵⁴, C. Weiser⁴⁸, H. Weits¹⁰⁶, P.S. Wells³⁰, T. Wenaus²⁵, D. Wendland¹⁶, Z. Weng^{152,ae}, T. Wengler³⁰, S. Wenig³⁰, N. Vermes²¹, M. Werner⁴⁸, P. Werner³⁰, M. Wessels^{58a}, J. Wetter¹⁶², K. Whalen²⁹, A. White⁸, M.J. White¹, R. White^{32b}, S. White^{123a,123b}, D. Whiteson¹⁶⁴, D. Wicke¹⁷⁶, F.J. Wickens¹³⁰, W. Wiedenmann¹⁷⁴, M. Wielers¹³⁰, P. Wienemann²¹, C. Wigglesworth³⁶, L.A.M. Wiik-Fuchs²¹, P.A. Wijeratne⁷⁷, A. Wildauer¹⁰⁰, M.A. Wildt^{42,ak}, H.G. Wilkens³⁰, J.Z. Will⁹⁹, H.H. Williams¹²¹, S. Williams²⁸, C. Willis⁸⁹, S. Willocq⁸⁵, A. Wilson⁸⁸, J.A. Wilson¹⁸, I. Wingerter-Seez⁵, F. Winklmeier¹¹⁵, B.T. Winter²¹, M. Wittgen¹⁴⁴, T. Wittig⁴³, J. Wittkowski⁹⁹, S.J. Wollstadt⁸², M.W. Wolter³⁹, H. Wolters^{125a,125c}, B.K. Wosiek³⁹, J. Wotschack³⁰, M.J. Woudstra⁸³, K.W. Wozniak³⁹, M. Wright⁵³, M. Wu⁵⁵, S.L. Wu¹⁷⁴, X. Wu⁴⁹, Y. Wu⁸⁸, E. Wulf³⁵, T.R. Wyatt⁸³, B.M. Wynne⁴⁶, S. Xella³⁶, M. Xiao¹³⁷, D. Xu^{33a}, L. Xu^{33b,al}, B. Yabsley¹⁵¹, S. Yacoub^{146b,am}, R. Yakabe⁶⁶, M. Yamada⁶⁵, H. Yamaguchi¹⁵⁶, Y. Yamaguchi¹¹⁷, A. Yamamoto⁶⁵, K. Yamamoto⁶³, S. Yamamoto¹⁵⁶, T. Yamamura¹⁵⁶, T. Yamanaka¹⁵⁶, K. Yamauchi¹⁰², Y. Yamazaki⁶⁶, Z. Yan²², H. Yang^{33e}, H. Yang¹⁷⁴, U.K. Yang⁸³, Y. Yang¹¹⁰, S. Yanush⁹², L. Yao^{33a}, W-M. Yao¹⁵, Y. Yasu⁶⁵, E. Yatsenko⁴², K.H. Yau Wong²¹, J. Ye⁴⁰, S. Ye²⁵, I. Yeletsikh⁶⁴, A.L. Yen⁵⁷, E. Yildirim⁴², M. Yilmaz^{4b}, R. Yoosoofmiya¹²⁴, K. Yorita¹⁷², R. Yoshida⁶, K. Yoshihara¹⁵⁶, C. Young¹⁴⁴, C.J.S. Young³⁰, S. Youssef²², D.R. Yu¹⁵, J. Yu⁸, J.M. Yu⁸⁸, J. Yu¹¹³, L. Yuan⁶⁶, A. Yurkewicz¹⁰⁷, I. Yusuf^{28,an}, B. Zabinski³⁹, R. Zaidan⁶², A.M. Zaitsev^{129,aa}, A. Zaman¹⁴⁹, S. Zambito²³, L. Zanello^{133a,133b}, D. Zanzi¹⁰⁰, C. Zeitnitz¹⁷⁶, M. Zeman¹²⁷, A. Zemla^{38a}, K. Zengel²³, O. Zenin¹²⁹, T. Ženiš^{145a}, D. Zerwas¹¹⁶, G. Zevi della Porta⁵⁷, D. Zhang⁸⁸, F. Zhang¹⁷⁴, H. Zhang⁸⁹, J. Zhang⁶, L. Zhang¹⁵², X. Zhang^{33d}, Z. Zhang¹¹⁶, Z. Zhao^{33b}, A. Zhemchugov⁶⁴, J. Zhong¹¹⁹, B. Zhou⁸⁸, L. Zhou³⁵, N. Zhou¹⁶⁴, C.G. Zhu^{33d}, H. Zhu^{33a}, J. Zhu⁸⁸, Y. Zhu^{33b}, X. Zhuang^{33a}, K. Zhukov⁹⁵, A. Zibell¹⁷⁵, D. Zieminska⁶⁰, N.I. Zimine⁶⁴, C. Zimmermann⁸², R. Zimmermann²¹, S. Zimmermann²¹, S. Zimmermann⁴⁸, Z. Zinonos⁵⁴, M. Ziolkowski¹⁴², G. Zobernig¹⁷⁴, A. Zoccoli^{20a,20b}, M. zur Nedden¹⁶, G. Zurzolo^{103a,103b}, V. Zutshi¹⁰⁷, L. Zwalinski³⁰.

¹ Department of Physics, University of Adelaide, Adelaide, Australia

² Physics Department, SUNY Albany, Albany NY, United States of America

³ Department of Physics, University of Alberta, Edmonton AB, Canada

⁴ (a) Department of Physics, Ankara University, Ankara; (b) Department of Physics, Gazi University, Ankara; (c) Division of Physics, TOBB University of Economics and Technology, Ankara; (d) Turkish Atomic Energy Authority, Ankara, Turkey

- ⁵ LAPP, CNRS/IN2P3 and Université de Savoie, Annecy-le-Vieux, France
- ⁶ High Energy Physics Division, Argonne National Laboratory, Argonne IL, United States of America
- ⁷ Department of Physics, University of Arizona, Tucson AZ, United States of America
- ⁸ Department of Physics, The University of Texas at Arlington, Arlington TX, United States of America
- ⁹ Physics Department, University of Athens, Athens, Greece
- ¹⁰ Physics Department, National Technical University of Athens, Zografou, Greece
- ¹¹ Institute of Physics, Azerbaijan Academy of Sciences, Baku, Azerbaijan
- ¹² Institut de Física d'Altes Energies and Departament de Física de la Universitat Autònoma de Barcelona, Barcelona, Spain
- ¹³ ^(a) Institute of Physics, University of Belgrade, Belgrade; ^(b) Vinca Institute of Nuclear Sciences, University of Belgrade, Belgrade, Serbia
- ¹⁴ Department for Physics and Technology, University of Bergen, Bergen, Norway
- ¹⁵ Physics Division, Lawrence Berkeley National Laboratory and University of California, Berkeley CA, United States of America
- ¹⁶ Department of Physics, Humboldt University, Berlin, Germany
- ¹⁷ Albert Einstein Center for Fundamental Physics and Laboratory for High Energy Physics, University of Bern, Bern, Switzerland
- ¹⁸ School of Physics and Astronomy, University of Birmingham, Birmingham, United Kingdom
- ¹⁹ ^(a) Department of Physics, Bogazici University, Istanbul; ^(b) Department of Physics, Dogus University, Istanbul; ^(c) Department of Physics Engineering, Gaziantep University, Gaziantep, Turkey
- ²⁰ ^(a) INFN Sezione di Bologna; ^(b) Dipartimento di Fisica e Astronomia, Università di Bologna, Bologna, Italy
- ²¹ Physikalisches Institut, University of Bonn, Bonn, Germany
- ²² Department of Physics, Boston University, Boston MA, United States of America
- ²³ Department of Physics, Brandeis University, Waltham MA, United States of America
- ²⁴ ^(a) Universidade Federal do Rio De Janeiro COPPE/EE/IF, Rio de Janeiro; ^(b) Federal University of Juiz de Fora (UFJF), Juiz de Fora; ^(c) Federal University of Sao Joao del Rei (UFSJ), Sao Joao del Rei; ^(d) Instituto de Fisica, Universidade de Sao Paulo, Sao Paulo, Brazil
- ²⁵ Physics Department, Brookhaven National Laboratory, Upton NY, United States of America
- ²⁶ ^(a) National Institute of Physics and Nuclear Engineering, Bucharest; ^(b) National Institute for Research and Development of Isotopic and Molecular Technologies, Physics Department, Cluj Napoca; ^(c) University Politehnica Bucharest, Bucharest; ^(d) West University in Timisoara, Timisoara, Romania
- ²⁷ Departamento de Física, Universidad de Buenos Aires, Buenos Aires, Argentina
- ²⁸ Cavendish Laboratory, University of Cambridge, Cambridge, United Kingdom
- ²⁹ Department of Physics, Carleton University, Ottawa ON, Canada
- ³⁰ CERN, Geneva, Switzerland

- ³¹ Enrico Fermi Institute, University of Chicago, Chicago IL, United States of America
- ³² (a) Departamento de Física, Pontificia Universidad Católica de Chile, Santiago; (b) Departamento de Física, Universidad Técnica Federico Santa María, Valparaíso, Chile
- ³³ (a) Institute of High Energy Physics, Chinese Academy of Sciences, Beijing; (b) Department of Modern Physics, University of Science and Technology of China, Anhui; (c) Department of Physics, Nanjing University, Jiangsu; (d) School of Physics, Shandong University, Shandong; (e) Physics Department, Shanghai Jiao Tong University, Shanghai, China
- ³⁴ Laboratoire de Physique Corpusculaire, Clermont Université and Université Blaise Pascal and CNRS/IN2P3, Clermont-Ferrand, France
- ³⁵ Nevis Laboratory, Columbia University, Irvington NY, United States of America
- ³⁶ Niels Bohr Institute, University of Copenhagen, Kobenhavn, Denmark
- ³⁷ (a) INFN Gruppo Collegato di Cosenza, Laboratori Nazionali di Frascati; (b) Dipartimento di Fisica, Università della Calabria, Rende, Italy
- ³⁸ (a) AGH University of Science and Technology, Faculty of Physics and Applied Computer Science, Krakow; (b) Marian Smoluchowski Institute of Physics, Jagiellonian University, Krakow, Poland
- ³⁹ The Henryk Niewodniczanski Institute of Nuclear Physics, Polish Academy of Sciences, Krakow, Poland
- ⁴⁰ Physics Department, Southern Methodist University, Dallas TX, United States of America
- ⁴¹ Physics Department, University of Texas at Dallas, Richardson TX, United States of America
- ⁴² DESY, Hamburg and Zeuthen, Germany
- ⁴³ Institut für Experimentelle Physik IV, Technische Universität Dortmund, Dortmund, Germany
- ⁴⁴ Institut für Kern- und Teilchenphysik, Technische Universität Dresden, Dresden, Germany
- ⁴⁵ Department of Physics, Duke University, Durham NC, United States of America
- ⁴⁶ SUPA - School of Physics and Astronomy, University of Edinburgh, Edinburgh, United Kingdom
- ⁴⁷ INFN Laboratori Nazionali di Frascati, Frascati, Italy
- ⁴⁸ Fakultät für Mathematik und Physik, Albert-Ludwigs-Universität, Freiburg, Germany
- ⁴⁹ Section de Physique, Université de Genève, Geneva, Switzerland
- ⁵⁰ (a) INFN Sezione di Genova; (b) Dipartimento di Fisica, Università di Genova, Genova, Italy
- ⁵¹ (a) E. Andronikashvili Institute of Physics, Iv. Javakhishvili Tbilisi State University, Tbilisi; (b) High Energy Physics Institute, Tbilisi State University, Tbilisi, Georgia
- ⁵² II Physikalisches Institut, Justus-Liebig-Universität Giessen, Giessen, Germany
- ⁵³ SUPA - School of Physics and Astronomy, University of Glasgow, Glasgow, United Kingdom
- ⁵⁴ II Physikalisches Institut, Georg-August-Universität, Göttingen, Germany
- ⁵⁵ Laboratoire de Physique Subatomique et de Cosmologie, Université Grenoble-Alpes,

CNRS/IN2P3, Grenoble, France

⁵⁶ Department of Physics, Hampton University, Hampton VA, United States of America

⁵⁷ Laboratory for Particle Physics and Cosmology, Harvard University, Cambridge MA, United States of America

⁵⁸ ^(a) Kirchhoff-Institut für Physik, Ruprecht-Karls-Universität Heidelberg, Heidelberg;

^(b) Physikalisches Institut, Ruprecht-Karls-Universität Heidelberg, Heidelberg; ^(c) ZITI Institut für technische Informatik, Ruprecht-Karls-Universität Heidelberg, Mannheim, Germany

⁵⁹ Faculty of Applied Information Science, Hiroshima Institute of Technology, Hiroshima, Japan

⁶⁰ Department of Physics, Indiana University, Bloomington IN, United States of America

⁶¹ Institut für Astro- und Teilchenphysik, Leopold-Franzens-Universität, Innsbruck, Austria

⁶² University of Iowa, Iowa City IA, United States of America

⁶³ Department of Physics and Astronomy, Iowa State University, Ames IA, United States of America

⁶⁴ Joint Institute for Nuclear Research, JINR Dubna, Dubna, Russia

⁶⁵ KEK, High Energy Accelerator Research Organization, Tsukuba, Japan

⁶⁶ Graduate School of Science, Kobe University, Kobe, Japan

⁶⁷ Faculty of Science, Kyoto University, Kyoto, Japan

⁶⁸ Kyoto University of Education, Kyoto, Japan

⁶⁹ Department of Physics, Kyushu University, Fukuoka, Japan

⁷⁰ Instituto de Física La Plata, Universidad Nacional de La Plata and CONICET, La Plata, Argentina

⁷¹ Physics Department, Lancaster University, Lancaster, United Kingdom

⁷² ^(a) INFN Sezione di Lecce; ^(b) Dipartimento di Matematica e Fisica, Università del Salento, Lecce, Italy

⁷³ Oliver Lodge Laboratory, University of Liverpool, Liverpool, United Kingdom

⁷⁴ Department of Physics, Jožef Stefan Institute and University of Ljubljana, Ljubljana, Slovenia

⁷⁵ School of Physics and Astronomy, Queen Mary University of London, London, United Kingdom

⁷⁶ Department of Physics, Royal Holloway University of London, Surrey, United Kingdom

⁷⁷ Department of Physics and Astronomy, University College London, London, United Kingdom

⁷⁸ Louisiana Tech University, Ruston LA, United States of America

⁷⁹ Laboratoire de Physique Nucléaire et de Hautes Energies, UPMC and Université Paris-Diderot and CNRS/IN2P3, Paris, France

⁸⁰ Fysiska institutionen, Lunds universitet, Lund, Sweden

⁸¹ Departamento de Física Teórica C-15, Universidad Autónoma de Madrid, Madrid, Spain

⁸² Institut für Physik, Universität Mainz, Mainz, Germany

⁸³ School of Physics and Astronomy, University of Manchester, Manchester, United

Kingdom

⁸⁴ CPPM, Aix-Marseille Université and CNRS/IN2P3, Marseille, France

⁸⁵ Department of Physics, University of Massachusetts, Amherst MA, United States of America

⁸⁶ Department of Physics, McGill University, Montreal QC, Canada

⁸⁷ School of Physics, University of Melbourne, Victoria, Australia

⁸⁸ Department of Physics, The University of Michigan, Ann Arbor MI, United States of America

⁸⁹ Department of Physics and Astronomy, Michigan State University, East Lansing MI, United States of America

⁹⁰ ^(a) INFN Sezione di Milano; ^(b) Dipartimento di Fisica, Università di Milano, Milano, Italy

⁹¹ B.I. Stepanov Institute of Physics, National Academy of Sciences of Belarus, Minsk, Republic of Belarus

⁹² National Scientific and Educational Centre for Particle and High Energy Physics, Minsk, Republic of Belarus

⁹³ Department of Physics, Massachusetts Institute of Technology, Cambridge MA, United States of America

⁹⁴ Group of Particle Physics, University of Montreal, Montreal QC, Canada

⁹⁵ P.N. Lebedev Institute of Physics, Academy of Sciences, Moscow, Russia

⁹⁶ Institute for Theoretical and Experimental Physics (ITEP), Moscow, Russia

⁹⁷ Moscow Engineering and Physics Institute (MEPhI), Moscow, Russia

⁹⁸ D.V.Skobel'tsyn Institute of Nuclear Physics, M.V.Lomonosov Moscow State University, Moscow, Russia

⁹⁹ Fakultät für Physik, Ludwig-Maximilians-Universität München, München, Germany

¹⁰⁰ Max-Planck-Institut für Physik (Werner-Heisenberg-Institut), München, Germany

¹⁰¹ Nagasaki Institute of Applied Science, Nagasaki, Japan

¹⁰² Graduate School of Science and Kobayashi-Maskawa Institute, Nagoya University, Nagoya, Japan

¹⁰³ ^(a) INFN Sezione di Napoli; ^(b) Dipartimento di Fisica, Università di Napoli, Napoli, Italy

¹⁰⁴ Department of Physics and Astronomy, University of New Mexico, Albuquerque NM, United States of America

¹⁰⁵ Institute for Mathematics, Astrophysics and Particle Physics, Radboud University Nijmegen/Nikhef, Nijmegen, Netherlands

¹⁰⁶ Nikhef National Institute for Subatomic Physics and University of Amsterdam, Amsterdam, Netherlands

¹⁰⁷ Department of Physics, Northern Illinois University, DeKalb IL, United States of America

¹⁰⁸ Budker Institute of Nuclear Physics, SB RAS, Novosibirsk, Russia

¹⁰⁹ Department of Physics, New York University, New York NY, United States of America

¹¹⁰ Ohio State University, Columbus OH, United States of America

¹¹¹ Faculty of Science, Okayama University, Okayama, Japan

- ¹¹² Homer L. Dodge Department of Physics and Astronomy, University of Oklahoma, Norman OK, United States of America
- ¹¹³ Department of Physics, Oklahoma State University, Stillwater OK, United States of America
- ¹¹⁴ Palacký University, RCPTM, Olomouc, Czech Republic
- ¹¹⁵ Center for High Energy Physics, University of Oregon, Eugene OR, United States of America
- ¹¹⁶ LAL, Université Paris-Sud and CNRS/IN2P3, Orsay, France
- ¹¹⁷ Graduate School of Science, Osaka University, Osaka, Japan
- ¹¹⁸ Department of Physics, University of Oslo, Oslo, Norway
- ¹¹⁹ Department of Physics, Oxford University, Oxford, United Kingdom
- ¹²⁰ ^(a) INFN Sezione di Pavia; ^(b) Dipartimento di Fisica, Università di Pavia, Pavia, Italy
- ¹²¹ Department of Physics, University of Pennsylvania, Philadelphia PA, United States of America
- ¹²² Petersburg Nuclear Physics Institute, Gatchina, Russia
- ¹²³ ^(a) INFN Sezione di Pisa; ^(b) Dipartimento di Fisica E. Fermi, Università di Pisa, Pisa, Italy
- ¹²⁴ Department of Physics and Astronomy, University of Pittsburgh, Pittsburgh PA, United States of America
- ¹²⁵ ^(a) Laboratório de Instrumentação e Física Experimental de Partículas - LIP, Lisboa; ^(b) Faculdade de Ciências, Universidade de Lisboa, Lisboa; ^(c) Department of Physics, University of Coimbra, Coimbra; ^(d) Centro de Física Nuclear da Universidade de Lisboa, Lisboa; ^(e) Departamento de Física, Universidade do Minho, Braga; ^(f) Departamento de Física Teórica y del Cosmos and CAFPE, Universidad de Granada, Granada (Spain); ^(g) Dep Física and CEFITEC of Faculdade de Ciências e Tecnologia, Universidade Nova de Lisboa, Caparica, Portugal
- ¹²⁶ Institute of Physics, Academy of Sciences of the Czech Republic, Praha, Czech Republic
- ¹²⁷ Czech Technical University in Prague, Praha, Czech Republic
- ¹²⁸ Faculty of Mathematics and Physics, Charles University in Prague, Praha, Czech Republic
- ¹²⁹ State Research Center Institute for High Energy Physics, Protvino, Russia
- ¹³⁰ Particle Physics Department, Rutherford Appleton Laboratory, Didcot, United Kingdom
- ¹³¹ Physics Department, University of Regina, Regina SK, Canada
- ¹³² Ritsumeikan University, Kusatsu, Shiga, Japan
- ¹³³ ^(a) INFN Sezione di Roma; ^(b) Dipartimento di Fisica, Sapienza Università di Roma, Roma, Italy
- ¹³⁴ ^(a) INFN Sezione di Roma Tor Vergata; ^(b) Dipartimento di Fisica, Università di Roma Tor Vergata, Roma, Italy
- ¹³⁵ ^(a) INFN Sezione di Roma Tre; ^(b) Dipartimento di Matematica e Fisica, Università Roma Tre, Roma, Italy
- ¹³⁶ ^(a) Faculté des Sciences Ain Chock, Réseau Universitaire de Physique des Hautes

- Energies - Université Hassan II, Casablanca; ^(b) Centre National de l'Energie des Sciences Techniques Nucleaires, Rabat; ^(c) Faculté des Sciences Semlalia, Université Cadi Ayyad, LPHEA-Marrakech; ^(d) Faculté des Sciences, Université Mohamed Premier and LPTPM, Oujda; ^(e) Faculté des sciences, Université Mohammed V-Agdal, Rabat, Morocco
- ¹³⁷ DSM/IRFU (Institut de Recherches sur les Lois Fondamentales de l'Univers), CEA Saclay (Commissariat à l'Energie Atomique et aux Energies Alternatives), Gif-sur-Yvette, France
- ¹³⁸ Santa Cruz Institute for Particle Physics, University of California Santa Cruz, Santa Cruz CA, United States of America
- ¹³⁹ Department of Physics, University of Washington, Seattle WA, United States of America
- ¹⁴⁰ Department of Physics and Astronomy, University of Sheffield, Sheffield, United Kingdom
- ¹⁴¹ Department of Physics, Shinshu University, Nagano, Japan
- ¹⁴² Fachbereich Physik, Universität Siegen, Siegen, Germany
- ¹⁴³ Department of Physics, Simon Fraser University, Burnaby BC, Canada
- ¹⁴⁴ SLAC National Accelerator Laboratory, Stanford CA, United States of America
- ¹⁴⁵ ^(a) Faculty of Mathematics, Physics & Informatics, Comenius University, Bratislava; ^(b) Department of Subnuclear Physics, Institute of Experimental Physics of the Slovak Academy of Sciences, Kosice, Slovak Republic
- ¹⁴⁶ ^(a) Department of Physics, University of Cape Town, Cape Town; ^(b) Department of Physics, University of Johannesburg, Johannesburg; ^(c) School of Physics, University of the Witwatersrand, Johannesburg, South Africa
- ¹⁴⁷ ^(a) Department of Physics, Stockholm University; ^(b) The Oskar Klein Centre, Stockholm, Sweden
- ¹⁴⁸ Physics Department, Royal Institute of Technology, Stockholm, Sweden
- ¹⁴⁹ Departments of Physics & Astronomy and Chemistry, Stony Brook University, Stony Brook NY, United States of America
- ¹⁵⁰ Department of Physics and Astronomy, University of Sussex, Brighton, United Kingdom
- ¹⁵¹ School of Physics, University of Sydney, Sydney, Australia
- ¹⁵² Institute of Physics, Academia Sinica, Taipei, Taiwan
- ¹⁵³ Department of Physics, Technion: Israel Institute of Technology, Haifa, Israel
- ¹⁵⁴ Raymond and Beverly Sackler School of Physics and Astronomy, Tel Aviv University, Tel Aviv, Israel
- ¹⁵⁵ Department of Physics, Aristotle University of Thessaloniki, Thessaloniki, Greece
- ¹⁵⁶ International Center for Elementary Particle Physics and Department of Physics, The University of Tokyo, Tokyo, Japan
- ¹⁵⁷ Graduate School of Science and Technology, Tokyo Metropolitan University, Tokyo, Japan
- ¹⁵⁸ Department of Physics, Tokyo Institute of Technology, Tokyo, Japan
- ¹⁵⁹ Department of Physics, University of Toronto, Toronto ON, Canada
- ¹⁶⁰ ^(a) TRIUMF, Vancouver BC; ^(b) Department of Physics and Astronomy, York

University, Toronto ON, Canada

¹⁶¹ Faculty of Pure and Applied Sciences, University of Tsukuba, Tsukuba, Japan

¹⁶² Department of Physics and Astronomy, Tufts University, Medford MA, United States of America

¹⁶³ Centro de Investigaciones, Universidad Antonio Narino, Bogota, Colombia

¹⁶⁴ Department of Physics and Astronomy, University of California Irvine, Irvine CA, United States of America

¹⁶⁵ ^(a) INFN Gruppo Collegato di Udine, Sezione di Trieste, Udine; ^(b) ICTP, Trieste; ^(c) Dipartimento di Chimica, Fisica e Ambiente, Università di Udine, Udine, Italy

¹⁶⁶ Department of Physics, University of Illinois, Urbana IL, United States of America

¹⁶⁷ Department of Physics and Astronomy, University of Uppsala, Uppsala, Sweden

¹⁶⁸ Instituto de Física Corpuscular (IFIC) and Departamento de Física Atómica, Molecular y Nuclear and Departamento de Ingeniería Electrónica and Instituto de Microelectrónica de Barcelona (IMB-CNM), University of Valencia and CSIC, Valencia, Spain

¹⁶⁹ Department of Physics, University of British Columbia, Vancouver BC, Canada

¹⁷⁰ Department of Physics and Astronomy, University of Victoria, Victoria BC, Canada

¹⁷¹ Department of Physics, University of Warwick, Coventry, United Kingdom

¹⁷² Waseda University, Tokyo, Japan

¹⁷³ Department of Particle Physics, The Weizmann Institute of Science, Rehovot, Israel

¹⁷⁴ Department of Physics, University of Wisconsin, Madison WI, United States of America

¹⁷⁵ Fakultät für Physik und Astronomie, Julius-Maximilians-Universität, Würzburg, Germany

¹⁷⁶ Fachbereich C Physik, Bergische Universität Wuppertal, Wuppertal, Germany

¹⁷⁷ Department of Physics, Yale University, New Haven CT, United States of America

¹⁷⁸ Yerevan Physics Institute, Yerevan, Armenia

¹⁷⁹ Centre de Calcul de l'Institut National de Physique Nucléaire et de Physique des Particules (IN2P3), Villeurbanne, France

^a Also at Department of Physics, King's College London, London, United Kingdom

^b Also at Institute of Physics, Azerbaijan Academy of Sciences, Baku, Azerbaijan

^c Also at Particle Physics Department, Rutherford Appleton Laboratory, Didcot, United Kingdom

^d Also at TRIUMF, Vancouver BC, Canada

^e Also at Department of Physics, California State University, Fresno CA, United States of America

^f Also at Tomsk State University, Tomsk, Russia

^g Also at CPPM, Aix-Marseille Université and CNRS/IN2P3, Marseille, France

^h Also at Università di Napoli Parthenope, Napoli, Italy

ⁱ Also at Institute of Particle Physics (IPP), Canada

^j Also at Department of Physics, St. Petersburg State Polytechnical University, St. Petersburg, Russia

^k Also at Chinese University of Hong Kong, China

- ^l Also at Department of Financial and Management Engineering, University of the Aegean, Chios, Greece
- ^m Also at Louisiana Tech University, Ruston LA, United States of America
- ⁿ Also at Institutio Catalana de Recerca i Estudis Avancats, ICREA, Barcelona, Spain
- ^o Also at Department of Physics, The University of Texas at Austin, Austin TX, United States of America
- ^p Also at Institute of Theoretical Physics, Iliia State University, Tbilisi, Georgia
- ^q Also at CERN, Geneva, Switzerland
- ^r Also at Ochadai Academic Production, Ochanomizu University, Tokyo, Japan
- ^s Also at Manhattan College, New York NY, United States of America
- ^t Also at Novosibirsk State University, Novosibirsk, Russia
- ^u Also at Institute of Physics, Academia Sinica, Taipei, Taiwan
- ^v Also at LAL, Université Paris-Sud and CNRS/IN2P3, Orsay, France
- ^w Also at Academia Sinica Grid Computing, Institute of Physics, Academia Sinica, Taipei, Taiwan
- ^x Also at Laboratoire de Physique Nucléaire et de Hautes Energies, UPMC and Université Paris-Diderot and CNRS/IN2P3, Paris, France
- ^y Also at School of Physical Sciences, National Institute of Science Education and Research, Bhubaneswar, India
- ^z Also at Dipartimento di Fisica, Sapienza Università di Roma, Roma, Italy
- ^{aa} Also at Moscow Institute of Physics and Technology State University, Dolgoprudny, Russia
- ^{ab} Also at Section de Physique, Université de Genève, Geneva, Switzerland
- ^{ac} Also at International School for Advanced Studies (SISSA), Trieste, Italy
- ^{ad} Also at Department of Physics and Astronomy, University of South Carolina, Columbia SC, United States of America
- ^{ae} Also at School of Physics and Engineering, Sun Yat-sen University, Guangzhou, China
- ^{af} Also at Faculty of Physics, M.V.Lomonosov Moscow State University, Moscow, Russia
- ^{ag} Also at Moscow Engineering and Physics Institute (MEPhI), Moscow, Russia
- ^{ah} Also at Institute for Particle and Nuclear Physics, Wigner Research Centre for Physics, Budapest, Hungary
- ^{ai} Also at Department of Physics, Oxford University, Oxford, United Kingdom
- ^{aj} Also at Department of Physics, Nanjing University, Jiangsu, China
- ^{ak} Also at Institut für Experimentalphysik, Universität Hamburg, Hamburg, Germany
- ^{al} Also at Department of Physics, The University of Michigan, Ann Arbor MI, United States of America
- ^{am} Also at Discipline of Physics, University of KwaZulu-Natal, Durban, South Africa
- ^{an} Also at University of Malaya, Department of Physics, Kuala Lumpur, Malaysia
- * Deceased